Optical coherent phase diversity systems

OPTICAL COHERENT PHASE DIVERSITY SYSTEMS

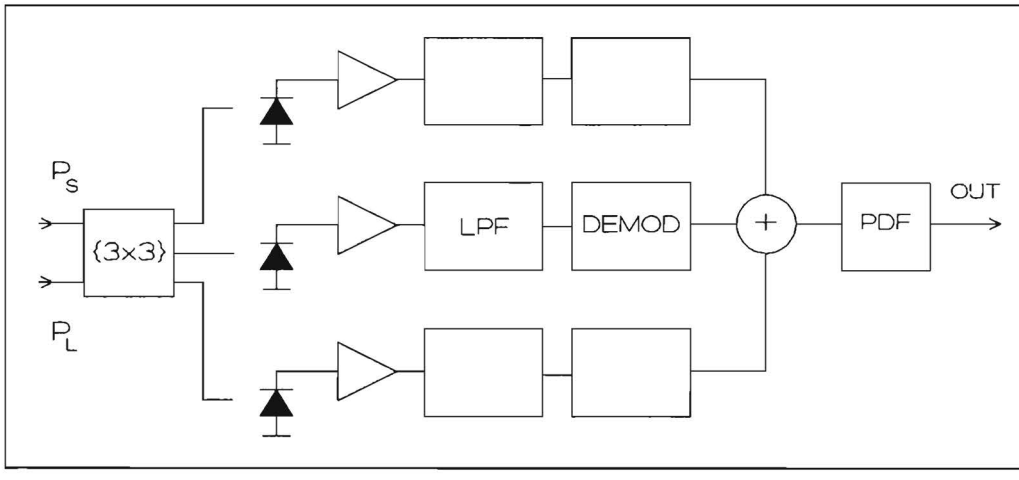

W.H.C. DE KROM

Optical Coherent Phase Diversity Systems

Optical Coherent Phase Diversity Systems

Proefschrift

ter verkrijging van de graad van doctor aan de Technische Universiteit Eindhoven, op gezag van de Rector Magnificus, prof. dr. J.H van Lint, voor een commissie aangewezen door het College van Dekanen in het openbaar te verdedigen op dinsdag 12 mei 1992 om 16.00 uur

door

Willibrordus Hubertus Cornelis de Krom

geboren te Tilburg

Dit proefschrift is goedgekeurd door

Promotor : prof. ir. G.D. Khoe

en

Copromotor : dr. ir. W.C. van Etten

CIP-GEGEVENS KONINKLIJKE BIBLIOTHEEK, DEN HAAG

Krom, Willibrordus Hubertus Cornelis de

Optical coherent phase diversity systems / Willibrordus Hubertus Cornelis de Krom. - [S.1. : s.n.]. - I11., fig., tab.
Proefschrift Eindhoven. - Met lit. opg., reg. - Met samenvatting in het Nederlands.
ISBN 90-9004897-9
NUGI 832
Trefw.: optische telecommunicatiesystemen / optische datatransmissiesystemen.

aan : mijn ouders,

Anne

en

Mariëlle.

CONTENTS

SUMMARY

This thesis deals with the calculation and specification of various system parameters and component tolerances required for the realization of optical coherent phase diversity ASK/DPSK receivers. To get more insight in this matter, we developed various theories, mathematical tools and models. If necessary existing theories were extended, in order to calculate the performance of the diversity receivers, and provide a model that is closer to the experimental systems. Based on these mathematical tools and models, the influence of various system impairments (e.g., phase noise, intensity noise, and system imperfections) is investigated.

The impact of laser phase noise on the performance of a coherent (3x3) phase and polarization diversity DPSK receiver is studied. Exact analytical equations are derived for the Bit Error Rate (BER) as a function of the Signal-to-Noise Ratio (SNR) and the FWHM laser linewidths. Special attention is paid to the polarization diversity concept in combination with phase diversity reception, to assure polarization insensitive operation. The influence of polarization overcoupling in the beamsplitters used is calculated and shown to be negligible for typical values.
The results obtained on laser phase noise for the (3x3) phase and polarization diversity receiver are compared with published work on optical coherent phase (and polarization) diversity ASK and CPFSK receivers.

The mathematical models and the accompanying computer programs are used to investigate the impact of local oscillator Relative Intensity Noise (RIN) on the performance of a (2x2) and (3x3) phase diversity ASK receiver. The analytical equations obtained are exact and show an optimum value for the local oscillator power (P_L) for which the sensitivity penalty is minimal. This optimum value of P_L is a function of the threshold level and the RIN. For values of P_L larger than this optimum, the (3x3) ASK receiver outperforms the (2x2) ASK receiver. The reverse is true for smaller values of P_L. Further it is shown, that in case of RIN the BER of the (2x2) phase diversity ASK receiver shows a time varying character with a frequency equal to twice the IF. This in contrary with the BER of the (3x3) phase diversity

ASK receiver, which for a given value of the SNR is constant. Comparison of the results obtained from literature reveal that a phase diversity DPSK receiver with comparable conditions is somewhat less sensitive to local oscillator intensity noise.

The developed mathematical models and computer programs are also applied to study the impact of IF gain imbalance and an aberration of the phase relations at the outputs of the optical hybrid. The sensitivity penalty for the (2x2) and (3x3) phase diversity ASK receiver due to these imperfections is calculated, and values for the component tolerances are obtained. For both phase diversity receivers, the BER is highly dependent on the threshold level, and shows a time varying character with a frequency equal to twice the IF.

A problem encountered in optical coherent ASK systems is the sensitivity degradation due to the use of an external amplitude modulator with a non-ideal Off/On (Extinction) Ratio. Exact analytical equations are derived for the BER, and the sensitivity penalty for a (2x2) and (3x3) phase diversity ASK receiver is calculated for various practical values of the Extinction Ratio (ER). The sensitivity penalty depends on the threshold level and therefore, optimization of this level is required for optimal performance. It is shown, that the sensitivity penalty for the (3x3) phase diversity ASK receiver for non-zero values of the ER is somewhat less than for the (2x2) phase diversity ASK receiver.
In case of ASK modulation of the optical carrier, the FWHM bandwidth of IF power spectrum is maximal for an ideal ER of zero. For nonzero values, the modulation index is smaller, which results in a smaller value of the FWHM bandwidth.

CHAPTER 1.

GENERAL INTRODUCTION

1.1 Introduction

Telecommunication services have always been important for mankind. In the last two decades an exponential growth of these services can be observed, and they play an even more important role than before. Telecommunication services are viewed by most developed nations as an important and essential activity, since they effectively reduce the size of our planet by reducing the time of information flow and capital transfer. Besides, these services provide an infrastructure for industrial development and research. For this reason, most developed nations are targeting the telecommunication services as an important basis of their economic growth.

The increasing demand for efficient high-speed broadband data links has set the stage for the introduction of optical fiber communication systems. Optical fiber transmission has several promising features in comparison with the more conventional transmission systems which use, for example, coaxial cables and twisted pairs as a transmission medium. These features are related to several typical properties of the optical fiber used. The optical fiber manufactured today has a huge bandwidth potential of approximately 20 THz and a propagation loss, for a wavelength of 1.5 μm, well below 0.3 dB/km, which is close to the theoretical limit [1.1]. Therefore, the optical fiber offers a combination of wide bandwidth and low loss which is unmatched by any other line transmission medium known.
The availability of **high bandwidth** makes the fiber attractive for high-capacity short-distance Local Area Network (LAN) applications. The extremely low propagation loss of the fiber is in this case a welcome advantage, but not a central consideration. In spite of a significant increase in the transmission capacity of operational optical fiber communication systems, even the most advanced of today's systems still access only a tiny fraction of the available bandwidth [1.2,1.3].

The **low-loss** property of the fiber in combination with the high bandwidth makes it very useful for application to long distance transmissions, for example in trunk or undersea systems, where it is not desirable to have many repeaters (active devices) along the path. By using optical fibers instead of copper cables, the repeater distance can be significantly increased.

In mainly the last decade, lightwave communication systems have moved towards technologies that allow for more effective use of the wide-bandwidth and low-loss properties of the optical fiber. Intensity-Modulation/Direct-Detection (IM/DD) systems were the first commercially available optical communication systems. In IM/DD systems, the information signal is impressed on the optical carrier by varying the optical power. At the receiving end, the information signal is recovered by detecting the power of the optical wave received. These systems effectively exploit mainly the low propagation loss of the fiber they only exploit the wide bandwidth in a modest way.
Multi-channel transmission can be accomplished by applying Wavelength Division Multiplexing (WDM) [1.4-1.6]. At the receiver, demultiplexing takes place by means of optical filtering. Since narrowband, tunable and small size optical filters are not easy to construct [1.7], the optical selectivity of a WDM IM/DD receiver is limited. The necessary channel spacing to prevent crosstalk from adjacent channels may be several orders higher than the bandwidth required by the data signal transmitted. Therefore, it is, given the present technology, difficult to effectively use the huge bandwidth potential of the fiber by means of IM/DD communication systems.

A lightwave communication system that promises to play an important role in next-generation systems uses optical coherent (pseudo) homodyne or heterodyne reception. Optical coherent reception provides a means of exploiting more effectively the attractive properties of the optical fiber. Besides, optical coherent systems offer a larger sensitivity (10-20 dB) and have significant better selectivity characteristics than IM/DD systems. In this context, the usage of the term "coherent" may differ from that in radio literature, where usually phase locking of the local oscillator laser and the signal received is assumed. Optical coherent reception and other for this thesis important definitions will be explained in Chapter 2.

In an optical coherent system, the information signal is impressed on the optical carrier at the transmitter by varying the amplitude, the frequency or the phase. At the receiving end of the communication link, the optical wave received is mixed with the light from a local oscillator laser. After detection of the combined wave by means of a photodiode, an Intermediate Frequency (IF) signal results. This contains the amplitude, the phase and the frequency information of the signal transmitted.
The higher sensitivity and selectivity of optical coherent reception are offset by various drawbacks. Firstly, the State-Of-Polarization (SOP) of the local oscillator laser and the optical wave received should be matched for optimal performance. Secondly, the lasers must have high spectral stabilities and small laser linewidths compared to the information bandwidth. Finally, the commercial viability of the coherent receiver for communication applications depends on the possibility of integrating the (total) receiver structure. The receiver complexity is still too involved for the today's optical integration technology, but progress is being made towards the solution [1.8-1.10]. Coherent systems are still in an experimental stage, but concluding from several publications, it may well turn out to be the next great advance in optical communications [1.11-1.18].
For multi-channel transmission the channels are wavelength multiplexed and a selection of one of the wavelength-multiplexed channels can be accomplished by using a tunable semiconductor local oscillator laser. The filtering takes place at a fixed IF by means of a simple electronic filter. Since electrical filtering can be much sharper than optical filtering, the selectivity is increased and a more efficient use of the optical spectrum is allowed. The sensitivity is increased due to the possibility of boosting the information carrying part of the received signal optical before detection by the photodiode, and the use of more efficient modulation formats. These features make the optical coherent receiver a promising competitor for the conventional IM/DD receiver.

The performance of (optical) communication systems is usually specified in terms of the number of photons/bit or the Signal-to-Noise Ratio (SNR) of the receiver, required to meet the desired sensitivity requirements. In general,

these sensitivity requirements are expressed as the number of photons/bit required to obtain a Bit Error Rate (BER) of usually 10^{-9}. The presentation of the BER as a function of, for example, the number of photons/bit gives more detailed information. For reasons of comparison with literature, the sensitivity is usually specified in relation to a BER of 10^{-9}, even though for practical reasons the measurement of receiver sensitivity may be carried out at other BER's. The calculation of the performance of optical coherent receivers substantially differs from that of IM/DD receivers and Radio Frequency (RF) coherent receivers. This is mainly due to the phase noise and the intensity noise introduced by both lasers. The latter will be thoroughly discussed in Chapter 3 and 4 of this thesis.

1.2 Framework of the research

As mentioned in the preceding section optical communications are very important and worldwide a lot of progress has already been made. For Dutch industry and research it is of vital importance to have the necessary know-how and sufficient suitably educated industrial researchers to take up these developments on an economically acceptable scale. In this framework a national project (IOP, Innovatief Onderzoek Programma) is founded in which TUD (Technische Universiteit Delft), UT (Universiteit Twente) and TUE (Technische Universiteit Eindhoven) participate, with support of Philips, the Dutch PTT and FEL/TNO. The aim of the project is to gain and exchange experience and beside that, to provide an infrastructure of know-how on a national scale. Based on the consideration that communication applications for optics are planned in the near future for IBCN's (Integrated Broadband Communication Networks), the subject matter of the project is chosen to be the development and implementation of an optical coherent phase diversity receiver, which in a final stage can be realized in a few Opto-Electronic Integrated Circuits (OEIC's).
This project is distributed over the participants in such a way that the experience and know-how acquired will be optimally used.

1.3 The subject of the thesis

This thesis is intended as a contribution to the development of optical coherent phase diversity receivers for broadband communications. The subject of the thesis is mainly focused on the calculation and specification of necessary system parameters and component tolerances for an optical coherent phase diversity receiver. By means of mathematical models, phase diversity receivers of interest have been analyzed in terms of the BER as a function of the SNR. This in contrast with reference [1.19] where various optical coherent receivers have been analyzed by means of computer simulations. The application of phase diversity techniques has several advantages which will be explained in Chapter 3. Special attention is paid to the influence and reduction of different system imperfections. In this thesis, we restrict ourselves to the following most promising digital modulation formats :

1. Amplitude Shift Keying (ASK),
2. Differential Phase Shift Keying (DPSK),
3. Frequency Shift Keying (FSK), and
4. Continuous Phase Frequency Shift Keying (CPFSK).

The research plan carried out included the following aspects :

- The development of mathematical tools and models, that enable the calculation of the BER as a function of the SNR.
- The application of these models to analyze the sensitivity degradation of different receivers due to different noise influences such as shot noise, thermal noise, phase noise and intensity noise.
- The extension of these models to enable the computation of the sensitivity penalty due to system imperfections and non-idealities such as an aberration of the phase relations of the outputs of the optical hybrid used, a gain imbalance in the pre-amplifiers at the IF stage, non-ideal polarization beamsplitters and non-ideal extinction ratios for {2x2} and {3x3} phase diversity ASK receivers.
- The calculation of IF power spectra for ASK phase diversity receivers for non-ideal extinction ratios.

- The development of receiver structures to minimize the influence of polarization fluctuations and intensity noise.
- The influence of the threshold level in ASK phase diversity receivers for system imperfections and intensity noise.

1.4 The outline of the thesis

This thesis is mainly focused on the calculation and specification of system parameters and component tolerances required for the optical coherent phase diversity receivers. To allow better control of the problems encountered, we distinguish a number of partial problems. Various new theories, mathematical tools and models have been developed. Some existing theories have been reviewed and, if necessary, extended. Most of the work presented in the Chapters 3 to 5, has already been published in the IEEE/OSA Journal of Lightwave Technology.

Chapter 2

Chapter 2 gives a review of the basic relations and principles concerning optical coherent reception, and describes the general configuration of a standard optical coherent communication system. The results have been compared with the conventional Intensity-Modulation/Direct-Detection scheme, and the most important differences discussed.

Chapter 3

Chapter 3 describes the impact of laser phase noise on the performance of an optical {3x3} phase diversity DPSK receiver [1.20]. Special attention is paid to the polarization insensitive reception by using polarization diversity techniques. Besides, the influence of non-ideal polarizing beamsplitters is discussed. The results obtained have been compared with published work on optical coherent ASK, DPSK and CPFSK receivers.

Chapter 4

Chapter 4 is devoted to the modeling and description of laser intensity noise in a {2x2} and {3x3} phase diversity ASK receiver [1.21]. The results

have been compared with published results on a {3x3} phase diversity DPSK receiver. Receiver structures for reducing the influence of intensity noise are discussed and compared.

Chapter 5

Chapter 5 describes the modeling of the gain imbalance and non-ideal phase relations of the optical hybrid in a {2x2} and {3x3} phase diversity ASK receiver [1.22]. The sensitivity degradation due to these imperfections is computed, and values for the component tolerances have been derived.

Chapter 6

The topic of chapter 6 is the modeling of non-ideal Extinction Ratios (ER's) of an external amplitude modulator, used in a {2x2} and {3x3} phase diversity ASK receiver. The sensitivity degradation introduced has been computed for various practical values. The influence of non-ideal ER's on the shape of the IF spectrum has been investigated and compared with measured results.

Chapter 7

Finally, in chapter 7 the main results of this thesis are summarized and conclusions drawn.

References

[1.1] J. Gowar, "Optical Communication Systems",
Prentice Hall, New York, 1984.

[1.2] R.S. Vodhanel, M.Z. Iqbal, J.L. Gimlett, and R.E. Wagner, "10 Gbit/s 48.5 km DPSK transmission experiment with direct modulation of a 1530 nm DFB laser and 1310 nm optimized fiber",
Part 1, Tech. Dig. ECOC 1990 (Amsterdam The Netherlands), pp. 41-44.

[1.3] T. Imal, Y. Ichihashi, N. Ohkawa, T. Sugle, Y. Hayashi and T. Itho, "A Field experiment in 2.5 Gbit/s optical coherent transmission through installed submarine trunklines",
Part 1, Tech. Dig. ECOC 1990 (Amsterdam The Netherlands), pp. 323-326.

[1.4] O.E. DeLange, "Wide-band optical communication systems : Part II frequency-division multiplexing",
Proc. IEEE, vol. 58, pp. 1683-1690, Oct. 1970.

[1.5] W. van Etten and J. van der Plaats, "Fundamentals of Optical Fiber Communications",
Prentice Hall, New York, 1991.

[1.6] C.A. Bracket, "Dense WDM networks",
Part 1, Tech. Dig. ECOC 1988 (Brighton England), pp. 533-540.

[1.7] A.R. Vellekoop and M.K. Smit, "Four-channel integrated wavelength demultiplexer with weak polarization dependence",
J. Lightwave Technol., vol. 9, no. 3, pp. 310-314, March 1991.

[1.8] E.C.M. Pennings, "Bends in optical ridge waveguides",
PhD thesis, Delft University of Technology, June 1990,
ISBN 90-9003413-7.

[1.9] M.K. Smit, "Integrated optics",
PhD thesis, Delft University of Technology, June 1991,
ISBN 90-9004261-X.

[1.10] L.B. Soldano, M.K. Smit, A.H. de Vreede, J.W.M. van Uffelen, B.H. Verbeek, P. van Bennekom, W.H.C. de Krom and W. van Etten, "New all-passive 4x4 planar optical phase diversity network",
Post-deadline Papers ECOC 1991 (Paris France), pp. 96-99.

[1.11] T. Okoshi, "Heterodyne and coherent optical fiber communications : recent progress",
Trans. Microwave Theory Tech., vol. MTT-30, no. 8, pp. 1138-1149, Aug. 1982.

[1.12] R.A. Linke and A.H. Gnauck, "High-capacity coherent lightwave systems",
J. Lightwave Technol., vol. 6, no. 11, pp. 1750-1769, Nov. 1988.

[1.13] T. Okoshi, and K. Kikuchi, "Coherent Optical Fiber Communications",
Kluwer Academic Publishers, Dordrecht, 1988.

[1.14] M.C. Brain et al., "Progress toward the field deployment of coherent optical fiber systems",
J. Lightwave Technol., vol. 8, no. 3, pp. 423-437, March 1990.

[1.15] S. Saito, T. Imai and T. Itho, "An over 2200 km coherent transmission experiment at 2.5 Gb/s using Erbium-doped-fiber in-line amplifiers",
J. Lightwave Technol., vol. 9, no. 2, pp. 161-169, Febr. 1991.

[1.16] T. Chikama, T. Naito, T. Klyonaga, G. Ishikawa and H. Kuwahara, "Optical heterodyne continuous phase FSK transmission experiment up to 4 Gb/s",
Part 1, Tech. Dig. ECOC 1990 (Amsterdam The Netherlands), pp. 65-68.

[1.17] T. Imai, Y. Ichihashi, N. Ohkawa, T. Sugle, Y. Hayashi and T. Itho, "A field experiment in 2.5 Gbit/s optical coherent transmission through installed submarine trunklines",
Part 1, Tech. Dig. ECOC 1990 (Amsterdam The Netherlands), pp. 323-326.

[1.18] Y. Hayashi, N. Ohkawa, H. Fushimi, D. Yanai, "A fully-engineered coherent optical trunk transmission system",
Part 1, Tech. Dig. ECOC 1991 (Paris France), pp. 393-396.

[1.19] F. Libbrecht, "Studie en systeemsimulatie van optische informatie-transmissie",
PhD Thesis, Rijksuniversiteit Gent, 1991.

[1.20] W.H.C. de Krom, "Impact of laser phase noise on the performance of a (3x3) phase and polarization diversity optical homodyne DPSK receiver",
J. Lightwave Technol., vol. 8, no. 11, pp. 1709-1716, Nov. 1990.

[1.21] W.H.C. de Krom, "Impact of local oscillator intensity noise and the threshold level on the performance of a {2x2} and {3x3} phase-diversity ASK receiver",
J. Lightwave Technol., vol. 9, no. 5, pp. 641-649, May 1991.

[1.22] W.H.C. de Krom, "Sensitivity degradation of an optical {2x2} and a {3x3} phase diversity ASK receiver due to gain imbalance and nonideal phase relations of the optical hybrid",
J. Lightwave Technol., vol. 9, no. 11, pp. 1593-1601, Nov. 1991.

CHAPTER 2.

OPTICAL COHERENT SYSTEMS, A GENERAL APPROACH

2.1 Defining the key terms

There is unclearity about a uniform definition of the term "coherent" if the use of this term is compared with that in radio technique, in fiber optics, and in lightwave communication systems.

In general fiber optics, "coherent" means that the phase of a lightwave is fixed or at least predictable in time and place between points on the lightwave. If two lightwaves are concerned, "coherent" means that the phase relation of the two lightwaves is constant [2.1,2.2].

In radio technique, "coherent detection" has the same meaning as synchronous detection, which implies a phase locking of the signal received with the local oscillator [2.3].

In lightwave communication systems the term "coherent reception" is usually defined according to the following definition which is also used in this thesis [2.4].

> **Optical coherent reception** : the process of optical reception which is characterized by the use of a local oscillator laser for boosting the information carrying part of the optical signal received before detection by means of a photodiode. At the receiver, the incoming signal at an optical frequency f_S, is combined with a locally generated optical wave at a frequency f_L. The composite wave is detected by a photodiode, whose output is an electrical signal centered at $f_S - f_L$, the intermediate frequency. This electrical signal is an exact replica of the incoming optical signal, translated down in frequency from the optical to the electrical domain, where further processing can be done by conventional radio techniques.

Primary based on the IF value, the set of "optical coherent systems" may be divided into subsets. In this thesis we distinguish the following three

subsets :

1. **Optical heterodyne reception** : at the receiver, the incoming signal wave is combined with a local oscillator wave of different frequency, which after detection by means of a photodiode results in an **IF** which is **the frequency difference** (also called beat frequency) of the two optical waves. This technique requires a stable IF which can be obtained by means of a frequency-locked loop [2.1].

2. **Optical homodyne reception** : at the receiver, the incoming signal wave is combined with the local oscillator wave at the original carrier frequency. This carrier frequency is phase locked to the incoming signal and after detection by means of a photodiode, an **IF of 0 Hz** is obtained.

3. **Optical pseudo homodyne reception** : at the **phase diversity** receiver, the incoming signal wave is combined with the local oscillator wave at a slightly different frequency. This results in a near zero value for the **IF (IF << bit rate)**. Since no phase locking is required for phase diversity reception, real optical homodyne reception as defined above is not possible.

In lightwave communication systems, a specified quality of performance is required to define the receiver sensitivity by means of a single quantity. In general, the receiver sensitivity is defined as :

> **Sensitivity** : the minimum optical signal power (in dBm or in W) or photons/bit required by an optical receiver to achieve a specified Bit Error Rate (BER) of usually 10^{-9} [2.1].

In this thesis the definition of receiver sensitivity in terms of the ratio photons/bit is preferred, since this is both independent of the wavelength and the bit time.

In multi-channel lightwave systems, a measure for the minimum allowable channel spacing in the optical frequency domain is the receiver selectivity. In this thesis, receiver selectivity is defined as :

> **Selectivity** : the ability to receive an optical frequency band, while rejecting the others. The closer the allowable distance in the optical frequency domain between the passband and the stopband, the higher the selectivity [2.1].

2.2 Transmission and coherent reception of optical signals

2.2.1 The transmission medium

As mentioned in the introduction, the optical fiber of today has several advantages over the more conventional copper transmission media such as e.g., twisted pair, coax and waveguides. As shown in Figure 2.1, an optical fiber offers a combination of a large bandwidth potential and a low loss property, unmatched by any other line transmission medium known.

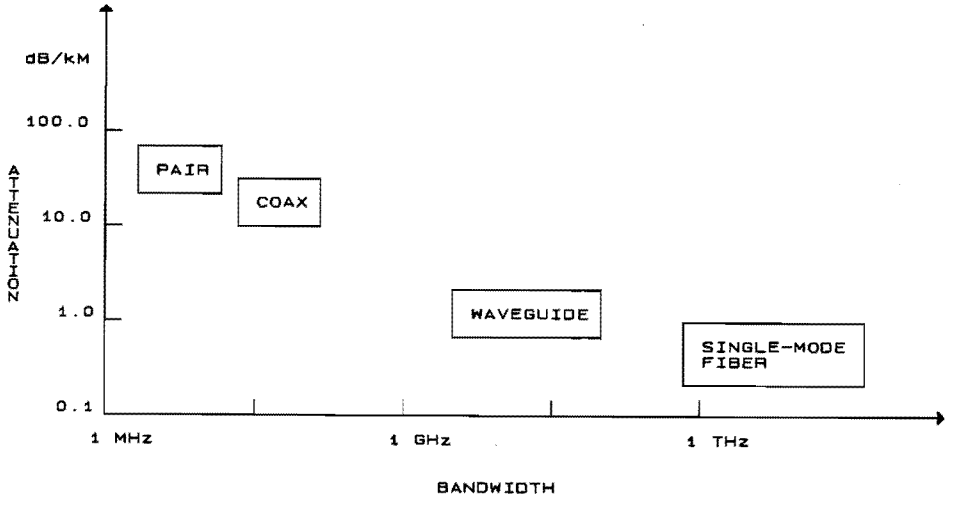

Figure 2.1 *Loss and bandwidth of various transmission media.*

The simplest single-mode fiber design consists of a doped silica core which is surrounded by a pure or doped silica cladding. The overall diameter of the single-mode fiber is approximately 125 μm. The refractive index of the core is a few tenths of a percentage larger than the refractive index of the cladding. This index difference provides the light-guiding mechanism of the fiber. The typical attenuation characteristic of a standard single-mode fiber is depicted in Figure 2.2 (reproduced from [2.4]).

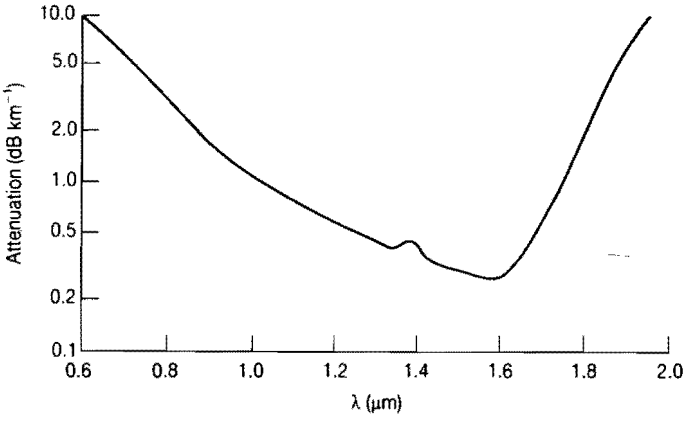

Figure 2.2 *Attenuation of a single-mode fiber as function of the wavelength.*

From Figure 2.2, it can be concluded that a low-loss region exists between 1450-1600 nm where the fiber attenuation is about 0.3 dB/km. For 1550 nm the attenuation is minimal, and therefore, this wavelength is usually preferred for coherent transmissions. This wavelength region of 1450-1600 nm corresponds to an optical transmission bandwidth of approximately 20 THz.

Inherent to a single-mode fiber is the pulse broadening due to chromatic dispersion. In the wavelength region around 1550 nm, the dispersion of a standard single-mode fiber is less than 20 ps/km.nm [2.4]. The lasers in coherent transmission systems are monomode, have small linewidths, and besides, the maximum frequency deviation of the optical carrier is of the same order as the modulation bandwidth, which for the systems of today, is of the order of several GHz. For two optical signals having a frequency difference of 2.5 GHz, which corresponds to $\Delta\lambda$ = 0.02 nm for a wavelength of

1550 nm, the delay is 0.4 ps/km. Since the un-repeated transmission distance is usually less than 100 km, the maximal delay time is about 40 ps. Besides, by application of dispersion-flattened fiber with a dispersion of less than 6 ps/km.nm, the delay time introduced can even further be reduced [2.4]. Therefore, the influence of chromatic dispersion on the performance of present optical coherent communication systems is rather small and can usually be neglected.

One of the drawbacks of coherent receivers mentioned in the introduction is the polarization dependence of the performance. For an optimal receiver performance, the polarization state of both the local oscillator wave and the optical wave received should be carefully matched. For this reason the ideal optical fiber for coherent transmission would maintain one single (preferable linear) polarization state independent of the time. However, in practice the fiber contains random irregularities which produce anisotropic effects. The resulting birefringence leads to a difference in propagation velocity of the two possible orthogonal polarization states as they propagate along the fiber. Other important (time-dependent) parameters that affect the birefringence of the fiber are mechanical vibrations, tension changes, and temperature fluctuations. This implies that the State-Of-Polarization (SOP) of the light at the output of the fiber is not constant, but changes randomly in time over periods of minutes or hours [2.5-2.7].

2.2.2 Coherent reception of optical signals

In comparison with the conventional Intensity-Modulation/Direct-Detection (IM/DD) receivers, an optical coherent receiver is characterized by the use of a local oscillator laser. A block-diagram of an optical coherent system is depicted in Figure 2.3.

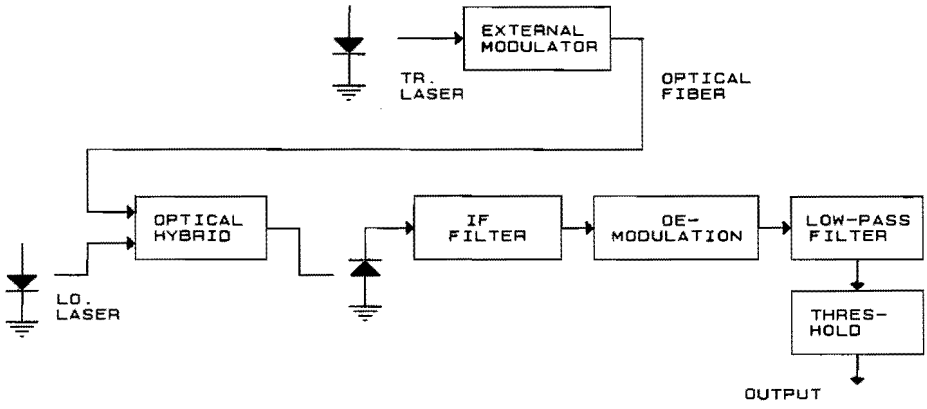

Figure 2.3 *Block-diagram of an optical coherent communication system.*

The local oscillator laser generates a continuous optical wave at or close to the carrier frequency of the optical wave received. At the receiving end, the optical wave received and the local oscillator wave are combined by means of a beamsplitter or an optical hybrid, before sending the composite wave to the photodiode. After the opto-electronic conversion, a photocurrent is produced at an Intermediate Frequency (IF), which contains the amplitude, phase and frequency information of the signal transmitted (a conventional and well-known technique in radio reception). Depending on the value of the IF, it is called optical coherent homodyne reception if the IF = 0 Hz and the local oscillator laser is **phase locked** with the optical wave received or optical coherent heterodyne reception for nonzero IF and **frequency locking** of both waves. Optical homodyne reception is not an easy technique to implement for two reasons. Firstly, it requires an optical phase-locked loop with a large bandwidth to phase synchronize the local oscillator with the transmitting laser. With the present day semiconductor lasers, an optical phase-locked loop is still hard to realize. Secondly, wavefront distortion should be prevented and an accurate matching of the wavefronts is necessary. Since optical homodyne reception is very vulnerable to a relaxation of the phase relation of the local oscillator and the optical wave received. For general optical heterodyne reception, the demands are less stringent and frequency locking of both lasers, a less involved technique, is sufficient.

Basic equations

The optical signal wave received can be described as the following complex electromagnetic field $E_S(t)$

$$E_S(t) \propto \sqrt{P_S}.\exp\ (j(\omega_S t + \vartheta_S(t))) \ , \tag{2.1}$$

where P_S is the optical power received, ω_S is the optical radial frequency, and $\vartheta_S(t)$ represents the phase noise of the transmitting laser. The electromagnetic wave generated by the local oscillator laser can be described as

$$E_L(t) \propto \sqrt{P_L}.\exp\ (j(\omega_L t + \vartheta_L(t))) \ , \tag{2.2}$$

where P_L is the optical power of the local oscillator laser, ω_L the optical radial frequency, and $\vartheta_L(t)$ is the phase noise of the local oscillator. At the receiving end, both waves are combined and the resulting composite wave

$$E(t) = E_S(t) + E_L(t) \ , \tag{2.3}$$

is sent to the photodiode. The photocurrent generated by the photodiode is proportional to the optical power received, and therefore, proportional to the product of the composite wave (Equation (2.3)) with its complex conjugate. The photocurrent can then be written as

$$i(t) = RP(t) \propto R\{E(t).E(t)^*\} \ . \tag{2.4}$$

In Equation (2.4), P(t) is the optical power of the composite wave, and R is the responsivity of the photodiode in A/W. The responsivity is given by

$$R = \frac{e\eta}{h\nu} \ , \tag{2.5}$$

where e is the electron charge, η the quantum efficiency of the photodiode, h is Plank's constant, and ν represents the optical frequency. If the SOP of both the local oscillator wave and the signal wave received are optimally matched, the photocurrent is then given by

$$I(t) = RP_L + RP_S + 2R\sqrt{P_L P_S}.\cos(\omega_{IF}t + \phi(t)) \ , \qquad (2.6)$$

where $\omega_{IF} = \omega_L - \omega_S$ is the Intermediate Frequency (IF) in radials per second and $\phi(t) = \vartheta_S(t) - \vartheta_L(t)$, the combined phase noise of the transmitting and the local oscillator laser. The third term of Equation (2.6) is the most interesting one, since it contains all the information of the signal received (i.e., amplitude, frequency and phase). Therefore, the first two terms may be filtered out, for an IF much larger than the information bandwidth, by proper low-pass filtering. In optical detection, in this case an opto-electronic signal conversion by means of a photodiode, an inevitable noise component arises due to the fact that light may be considered to consist of photons. The detection of these photons produces a flow of electrons and the statistics of the generation of electrons is Poisson distributed. However, if the average number of photons received is large, the noise introduced can conveniently be assumed to be Gaussian distributed with zero mean. The noise introduced by the photodiode is called shot noise. Shot noise is usually assumed to have a flat power spectrum. In case of coherent reception, the shot noise is proportional to the sum of the optical power received (P_S) and the local oscillator power (P_L). However, for a properly designed optical coherent receiver, the local oscillator power is several orders of magnitude larger than the power received. Therefore, it is reasonable to assume that the shot noise introduced by the local oscillator is dominant. The double-sided spectral noise density due to shot noise can then be written as

$$N_s = eRP_L \ . \qquad (2.7)$$

The total noise contribution N_T at the IF stage, after IF filtering with a filter matched to the signal, having a noise bandwidth B, which is defined to cover both negative and positive frequency bands (double-sided), is given by

$$N_T B = eRP_L B + NB + N_{th} B \ , \qquad (2.8)$$

where N (A^2/Hz) is the double-sided spectral noise density due to the dark and background current, which is independent of the signal. The thermal noise spectrum is assumed to be flat (white) over a wide frequency range with a double-sided spectral noise density of N_{th} A^2/Hz.

The SNR of an optical coherent receiver can then defined to be [2.4]

$$SNR \triangleq \frac{\langle S_r \rangle}{N_T B} = \frac{2R^2 P_L P_S}{2(eRP_L + N + N_{th})B} = \frac{R^2 P_S^2}{(eRP_S + P_S/P_L(N + N_{th}))B} \quad (2.9)$$

This expression is valid for the heterodyne case. For the optical homodyne receiver, the cosine in Equation (2.6) equals one, and the IF average mean square current of the signal part of the photocurrent $\langle S_r \rangle$ (Equation 2.6) is doubled. From Equation (2.9) it becomes apparent that the sensitivity of a coherent receiver is improved significantly over that of an IM/DD receiver, by comparing it with the relation for the SNR of an IM/DD receiver [2.4]

$$SNR \triangleq \frac{\langle S_r \rangle}{N_T B} = \frac{R^2 \langle P_S^2 \rangle}{(eRP_S + N + N_{th})B} . \quad (2.10)$$

The comparison of Equation (2.9) with (2.10) reveals that for a properly designed coherent receiver the receiver noise terms (i.e., N, and N_{th}) are reduced by a factor of P_S/P_L. By boosting the local oscillator power, the influences of the noise terms that are not correlated to the signal are reduced. Therefore, in theory, an optical coherent receiver can approach the shot noise limit very closely. However, in the considerations above, several influences have been simplified (e.g., a pure and stable optical frequency).

In summary, the advantages of coherent reception in comparison with IM/DD reception are :

1. **Higher selectivity**. Mixing the optical wave received with the light of the (in frequency closely spaced) local oscillator laser results in a signal that can be processed and selectively filtered electronically. For

IM/DD receivers the latter is performed by optical filtering which is more difficult to realize and less selective. For this reason, a coherent receiver allows a closer channel spacing in the frequency band.

2. **Increased sensitivity**. By mixing the optical wave received with the light of a much stronger local oscillator laser, the information carrying part of the signal received is amplified before detection. In this way, the thermal noise and the noise due to the dark and background current become less significant. In comparison with IM/DD systems, it is obvious that a coherent receiver can approach the shot noise limit very closely.

In comparison with conventional IM/DD systems, coherent systems have various drawbacks. Firstly, the introduction of a local oscillator laser and more sophisticated modulation schemes results in an increase of the system complexity and cost. Secondly, the signal processing required has become more critical and involved than in case of an IM/DD scheme. Finally, due to the severe requirements for the coherence of the optical waves, the optical sources used should have high spectral purity and stability. These aspects will be discussed in the following chapters.

2.3 The transmitter

2.3.1 The optical source

The first part of the optical coherent system depicted in Figure 2.3 is the optical transmitter. The source of optical radiation is usually chosen to be a semiconductor DFB (Distributed FeedBack) or DBR (Distributed Bragg Reflector) laser. The small size, long lifetime and high efficiency of the semiconductor laser has made this device a nearly ideal light source for optical communications. However, for optimal coherent reception even more severe demands are imposed to the spectrum of the semiconductor laser. The laser spectrum should possess a high spectral purity and stability. Any relaxation of these requirements will result in a sensitivity degradation of the optical coherent system. In order to meet these requirements, a stabilization of

the bias current and the temperature of the semiconductor laser is absolutely necessary. A small deviation in temperature (T) ($df/dT \cong 11$ to 12 GHz/K) and in the laser bias current (I) ($df/dI \cong -0.05$ to -3 GHz/mA) results in a major change of the laser frequency.
The frequency spectrum of an ideal monomode semiconductor laser is characterized by one sharp line at the carrier frequency. However, in practice the spectrum is broadened due to laser phase noise and has a Lorentzian shape instead of one sharp line. Further important impairments of the spectrum are due to intensity noise and reflections in the optical circuitry. In the following sections the influence of phase noise, intensity noise and reflections in the optical circuitry will be discussed in more detail.

Intensity noise

Beside coherent light due to the stimulated recombination of Electron Hole Pairs (EHP's) in the laser cavity, a semiconductor laser also emits so-called incoherent light generated by the spontaneous recombination of EHP's in the laser cavity. For semiconductor lasers, the spontaneous emission of photons in the laser cavity gives onset to noise problems. This spontaneous emission is the main cause for excess noise terms such as intensity noise and phase noise. Due to the small device size, the optical energy storage in the cavity is small, and therefore, the sensitivity to the perturbations of spontaneous emission in semiconductor lasers is usually significant. The influence of the spontaneous emission could be reduced by increasing the size of the laser cavity. The latter can be accomplished by using external cavities [2.8]. Intensity noise manifests itself as a random fluctuation of the optical power, and is especially pronounced near the threshold and diminishes as the laser bias current is increased. Statistically, intensity noise behaves like shot noise, after detection by a photodiode which implies that it is also Gaussian distributed and has a flat power spectrum (white noise) over a wide frequency range. Intensity noise is usually characterized by the so-called Relative Intensity Noise (RIN). The RIN spectral density is defined as the variance of the optical power fluctuations, divided by the mean optical power squared in 1 Hz bandwidth (dB/Hz). The degradation in receiver sensitivity for coherent receivers due to the local oscillator

laser intensity noise can be quite significant for small signal values (Equation (2.6)) [2.9-2.11]. However, by means of balanced receiver structures the impact can be significantly reduced [2.9,2.10]. This in trade for bandwidth, since the input capacity of a balanced receiver is usually larger than for an unbalanced receiver.

Phase noise

In addition to causing intensity noise, spontaneous emission also generates phase fluctuations in the laser output. Phase noise decreases the coherence time of the laser light. Limited coherence time manifests itself as a broadening of the laser spectrum. The laser spectrum, which under ideal conditions consists of one sharp line, can be shown to have a Lorentzian line shape due to the presence of phase noise (Figure 2.4).

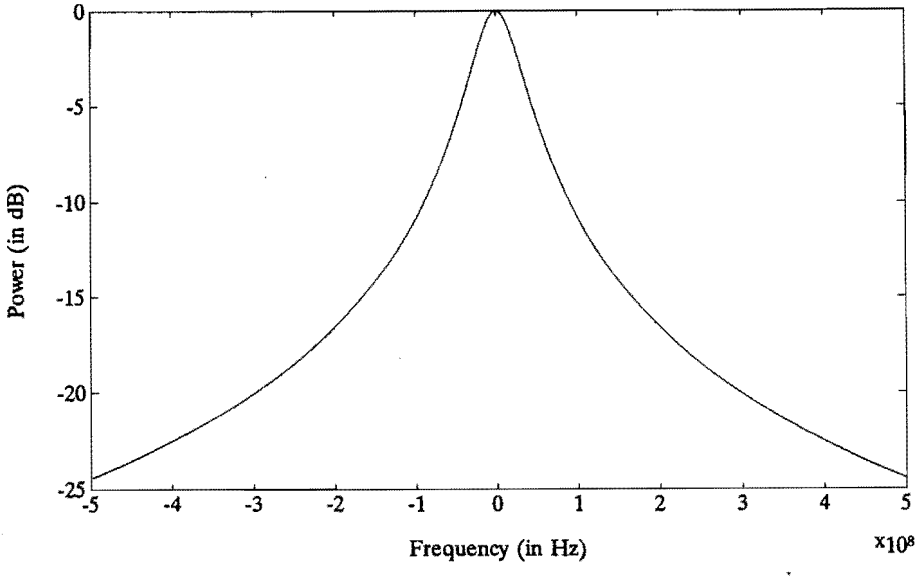

Figure 2.4 *Example of an equivalent baseband laser spectrum due to laser phase noise.*

The laser spectrum is given by the following equation [2.14-2.16]

$$S_L(\nu) = \frac{\Delta\nu}{2\pi[(\Delta\nu/2)^2 + (\nu-\nu_0)^2]}, \qquad (2.11)$$

where ν_0 is the resonant frequency of the laser cavity and $\Delta\nu$ is the laser linewidth, which is defined as the 3.0 dB linewidth, also called the Full-Width-Half-Maximum (FWHM) laser linewidth. Statistically, the phase difference $\phi(t) - \phi(t-\tau)$ ($\phi(t)$ as in Equation (2.6)) may be considered to be Gaussian distributed, since the phase changes are introduced by a large number of independent noise events [2.6].

It is obvious that laser phase noise is a nonnegligible impairment in phase modulated communication systems. However, even coherent systems employing amplitude modulation suffer from sensitivity degradation due to the laser phase noise. This has to do with the unavoidable filtering of the IF signal received. Filtering of phase noise can lead to a conversion of laser phase noise into amplitude noise, which for amplitude modulation is an important impairment [2.17]. Laser phase noise also causes a broadening of the IF spectrum, and therefore, the bandwidth of the IF filter should be increased in order to accommodate the necessary signal power. The latter implies that the noise bandwidth is extended and the impact of the shot and thermal noise is increased at the expense of receiver sensitivity [2.18].

Reflections

Optical feedback in the laser cavity should be avoided, since it can destroy the coherence of the laser. Semiconductor DFB/DBR lasers are inherently very vulnerable to reflections back into the laser cavity. Reflections can cause serious degradation of the performance of coherent systems through two different mechanisms : (1) reflection of optical power back into the laser cavity, contributing to laser phase noise leading to linewidth broadening, and (2) conversion of laser phase noise into excess intensity noise by reflections between single-mode fiber components, acting like a Fabry-Perot interferometer [2.19]. These so-called interferometers in an optical transmission system can be formed by two reflecting surfaces, that originate from non-ideal connectors, fiber splices or fiber endfaces in the transmitter and

detector modules. Reflections caused by the first mechanism can be eliminated by optically isolating the lasers from reflections. The deterioration through the second mechanism is much harder to combat, since this conversion takes place outside the laser module. Therefore, even when the lasers are optimally isolated from reflections back into the cavity, reflections can still cause serious problems via the second mechanism.
Reflections in a coherent system can occur both in the path of the signal light as well as in the path of the local oscillator light. However, the signal path is long with respect to the local oscillator path. For this reason, possible reflections in the signal path will be more effectively attenuated than the reflections in the local oscillator path. Therefore, especially the local oscillator laser should be carefully optically isolated from optical feedback. Moreover, special care should be given to preventing large discontinuities of the refractive index in the path of the local oscillator light.

2.3.2 Modulation

One (or more) of the basic parameters of the transmitting laser, amplitude, frequency, phase or polarization state, can be digitally modulated between two states related to the information signal. Modulation of the optical wave transmitted can be direct by impressing the information signal on the laser bias current or indirect by using an external modulator [2.20-2.22]. Direct modulation is only suitable for frequency modulation, since a small modulation of the laser bias current results in a large frequency modulation of 0.5-3 GHz/mA [2.23], while the average output power remains almost the same. Therefore, an external modulator is needed to modulate the amplitude of the optical wave transmitted in order to avoid "chirping" of the laser frequency. Phase and polarization modulation can also be accomplished by means of an external (waveguide) modulator. One principle of operation of an external waveguide modulator is to change the refractive index of the waveguide structure under the influence of a transverse electric field, applied via electrodes on either side of the waveguide. The transverse electric field is then modulated by the information signal.

2.4 The modulation format

In principle, the same modulation techniques as in radio communication can be used in optical communication systems. We distinguish two principles of modulation : (1) analog, and (2) digital modulation. Digital modulation formats have various well-known advantages over analog modulation formats such as a good performance with minimum equipment complexity and a good degree of immunity to certain channel impairments. In optical communication systems the emphasis is placed on digital modulation formats. However, according to reference [2.24] there has been a growing recognition that the original proposal for a fiber-based Broadband Integrated Service Digital Network (BISDN), which provides voice, data and video services, will not be cost-competitive for the short term. The bottlenecks are the high costs of electronic multiplexing and demultiplexing of digitized video channels for each subscriber and the required decoding of digitized video at each TV set. For the time being, subcarrier multiplexed broadband service networks could be a good compromise for two reasons. The initial installation costs are low, and affordable graceful migration to digital video and BISDN can be achieved. However, in the long term digital modulation formats will be the final solution [2.24].

The study of suitable modulation formats is very important, since the ultimate receiver sensitivity as well as the performance requirements imposed on the transmitter and receiver components, especially the spectral stability and spectral purity of the semiconductor lasers, critically depend on the modulation format used. The typical digital modulation formats used in optical coherent communication systems are :

1. ASK (Amplitude Shift Keying), the amplitude of the carrier is switched between two levels, e.g. A_1 for a space, and A_2 for a mark. However, in optical communications On-Off Keying (OOK) is typical which implies that A_1 is usually chosen to be zero.
2. (CP)FSK ((Continuous Phase) Frequency Shift Keying), the frequency of the carrier is (continuously) switched between two frequencies, e.g. f_1 for a space, and f_2 for a mark.

3. MSK (Minimum Shift Keying), a special case of CPFSK with a modulation index 1/2.
4. PSK (Phase Shift Keying), the phase of the carrier is switched between two states, e.g. 0 for a space and π for a mark.
5. DPSK (Differential Phase Shift Keying), the phase of the carrier remains the same for a space and changes with π for a mark.
6. POLSK (Polarization Shift Keying), the state of polarization of the transmitting laser is switched between two orthogonal states.
7. DIPS (Data-Induced Polarization Switching). Polarization switching is combined with FSK modulation. The signal is launched at 45° to the principal axes of a birefringent medium. The frequency separation is chosen so, that the polarization states for a mark and a space at the output are orthogonal.

2.5 The coherent receiver structure

2.5.1 The local oscillator laser

The performance required of the local oscillator laser is in principle the same as for the transmitting laser, except for the difference that it must generate a continuous instead of a modulated wave. In order to approach the shot noise limit, and render the thermal noise sources in the receiver IF section negligible, sufficient local oscillator power is required. For coherent multi-channel distribution systems however, it is also desirable that the frequency of the local oscillator laser is tunable.

2.5.2 The combining and mixing

At the receiving end of a coherent system, the optical signal wave received is superimposed on the local oscillator wave by means of an optical hybrid. Until now, the latter is usually chosen to be a fused fiber coupler consisting of two or three standard single-mode fibers, which are aligned, fused and tapered until an equal output power distribution is obtained. For loss-

less devices, this also defines the phase relations between the different photocurrents, 180° for a (2x2) (two branch) fused fiber coupler, and 120° for a (3x3) (three branch) fused fiber coupler, respectively [2.25]. For future applications, much effort is devoted to the realization of passive planar waveguide couplers which are suited for opto-electronic integration [2.26-2.28]. The subsequent mixing of the composite wave is accomplished by a photodiode according to the principle discussed in section 2.2.2.
An optical coherent receiver, which operates according to the heterodyne principle, requires a stable IF for proper operation. The requirement for homodyne reception is even more severe, since a stable phase difference is required. In order to meet the requirement for optical coherent heterodyne reception, measurement and active control of the IF is necessary. In [2.29] a new Frequency-Locked Loop (FLL) for coherent reception is presented for locking the frequency of the local oscillator laser with the optical signal received. The heart of the FLL is a micro-controller, which makes it fast and flexible. The operation of the FLL is independent of the modulation format or the spectral linewidths of the lasers.

2.5.3 IF filtering

The primary function of the IF filter is to pass all the signal power, while rejecting the noise power outside the modulation bandwidth, and besides, to suppress the intersymbol interference. The ideal IF filter is a rectangular Low-Pass (LP) or BandPass (BP) filter, depending on the IF value.
In case of significant laser phase noise, the bandwidth of the IF filter should be large enough to prevent conversion from laser phase noise into amplitude noise [2.17]. The sensitivity degradation caused by an IF bandwidth exceeding the optimum value, can partly be compensated by the use of a post-detection filter. In Figure 2.3 a low-pass filter at the input of the threshold comparator is used as a post-detection filter [2.30-2.32].

2.5.4 Demodulation and threshold detection

The demodulation format depends on the modulation scheme. In principle all demodulation schemes used in radio communication can be applied in optical communication systems. For ideal conditions, implying optimally matched polarization states of the local oscillator and the signal received, and absence of laser phase noise, the performances of optical and Radio Frequency (RF) coherent communication systems are identical. For substantial phase noise, the ultimate performance of the optical coherent receiver highly depends on the modulation scheme used. The influence of laser phase noise can partially be reduced by using more phase noise tolerant (de)modulation schemes such as FSK or ASK. For ASK and FSK, the information signal is impressed on the amplitude and frequency of the optical carrier, respectively. The phase noise induces changes in amplitude and angle of the optical carrier. In case the frequency of these changes is small in comparison to the bit rate, the performance degradation will be moderate. For (D)PSK modulation, it is obvious that little can be done to reduce the influence of laser phase noise, since the information signal is impressed on the phase. In this case, elimination of the phase fluctuations also affects the information signal. For this reason, the spectral purity required of the lasers used in coherent optical (D)PSK systems, is very stringent. For a maximum allowable sensitivity penalty of 1.0 dB at a BER of 10^{-9}, the laser linewidths should be less than approximately 0.5% of the bit rate [2.33-2.35]. For coherent optical FSK and ASK systems, laser linewidths should be within 20% of the bit rate for negligible performance degradation [2.36, 2.37]. For optimal matching of the IF and post-detection filter and ASK/FSK (de)modulation, laser linewidths of the same order as the bit rate only result in a sensitivity penalty varying from 1.0 to 2.0 dB [2.38,2.39].

2.6 Phase diversity reception

A general diagram of a {3x3} optical coherent phase diversity receiver is depicted in Figure 2.5, consisting of three identical branches.

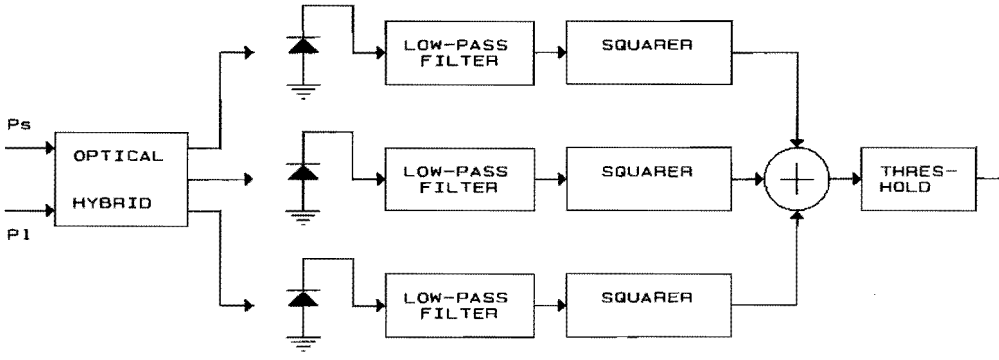

Figure 2.5 *General block-diagram of a {3x3} optical coherent phase receiver with low-pass filters and square-law detectors.*

For the optical hybrid a {3x3} fused fiber coupler can be used. When each output signal is detected by a photodiode, the resulting signal components of the three photocurrents have a 120° phase difference between them, provided the coupler is lossless. In Figure 2.6a the three signal components in the system of Figure 2.5 are given [2.4]. In this figure the IF is taken to be much smaller than the bit rate.

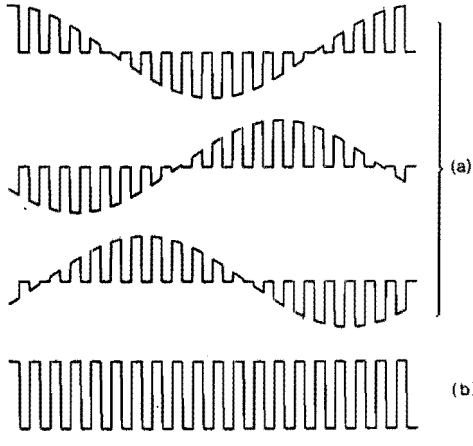

Figure 2.6 *(a) The signal components in a {3x3} phase diversity receiver, (b) The output signal when squarers are used as detectors. (reproduced from [2.4])*

A bit pattern consisting of an alternating sequence of 1's and 0's is assumed. From this figure it becomes clear that when in a certain branch the signal is lost, due to a zero crossing of the IF signal, the other branches still show a significant signal contribution. After demodulation, in this case of ASK by means of square-law detectors, and adding the squared current terms, the double-frequency terms are canceled out and a constant output value results (Figure 2.6b). Therefore, the phase diversity receiver is in principle insensitive to changes of the phase difference between the signal and the local oscillator ($\phi(t)$ in Equation (2.6)).
For the {2x2} optical coherent phase diversity receiver a phase difference between both photocurrents of 90° is required for proper operation. This can not be realized by means of one {2x2} fused fiber coupler and a more complex optical hybrid is required [2.40,2.41]. The {2x2} and {3x3} optical coherent phase diversity receiver will be thoroughly discussed in the following chapters.

2.7 Polarization handling

In order to make the interference of the local oscillator wave and the received signal wave more efficient, the SOP of both waves must coincide. As already discussed in section 2.7, random vibration of the fiber and temperature changes result in mechanical strain in the fiber. This strain introduces a birefringence, which changes in time. This birefringence causes the SOP of the wave received also to change randomly. In literature, different methods can be found to overcome the problems caused by a polarization mismatch.

Polarization Maintaining Fiber (PMF)

The use of polarization maintaining fibers prevents changes of the output SOP to a great extent. This is achieved by providing the PMF with a consistently large birefringence, which is much larger than the birefringence in a standard single-mode fiber. The birefringence can be accomplished by introducing an elliptic core or by placing Stress-Applying-Parts (SAP's) in the

cladding (Figure 2.7, reproduced from [2.4]).

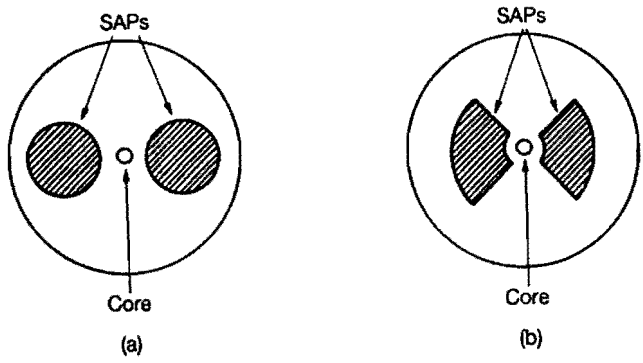

Figure 2.7 *Cross-section of polarization maintaining fibers.*
(a) PANDA fiber,
(b) Bow-tie fiber.

PMF's are only polarization maintaining when they are excited in one of their two principal axes, which requires proper alignment. Besides, PMF's exhibit a larger loss than the standard single-mode fiber, and they are also more expensive. Another problem is that a lot of standard single-mode fiber is already installed. Therefore, other solutions are desirable to make the coherent reception of optical signals polarization independent.
In optical coherent receivers PMF's are usually applied as interconnection between the local oscillator laser and the input of the optical hybrid.

Polarization state control

The principle of a polarization state controller is to change the state of polarization of the local oscillator laser in such a way that the IF signal power becomes maximal. This guarantees that the SOP of the signal wave received is optimally matched with the SOP of the local oscillator laser wave. The controlling of the SOP of the local oscillator laser can be accomplished by means of a set of piezo-electric or magnetic fiber squeezers (Figure 2.8) [2.42]. The applied transverse force produces a birefringence, which results in a phase difference between the two orthogonal polarization

components.

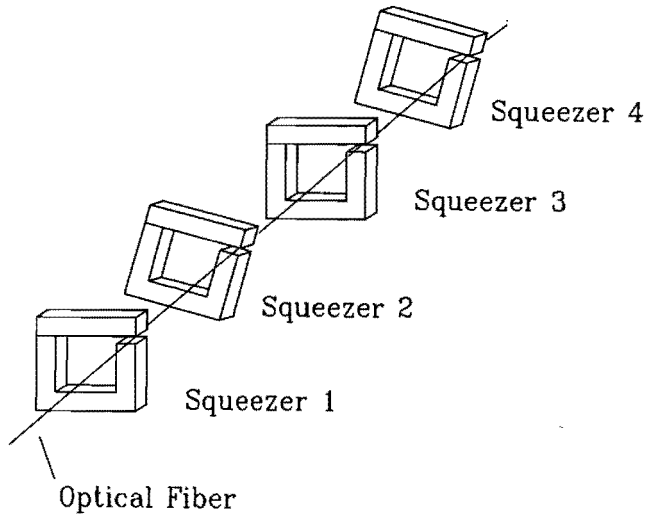

Figure 2.8 *A polarization controller using a set of squeezers.*

Another promising polarization controller uses a set of four nematic Liquid Crystals (LC's) instead of squeezers [2.43]. By applying a square wave voltage over the LC, the birefringence can be controlled.

Polarization scrambling

In this technique the SOP of the signal wave transmitted is changed in such a way, that over one bit period all possible polarization states are generated. The SOP of the local oscillator remains unchanged. It is obvious, that this polarization scrambling technique leads to a sensitivity degradation of at least 3.0 dB.

Polarization diversity receivers

The principle of polarization diversity is that the local oscillator wave and the optical wave received are split into two orthogonal polarization states. For proper operation, it is necessary that the power of the local

oscillator laser is equally divided between the two orthogonal polarization states. By means of a polarization beamsplitter, the signal wave received is also decomposed into two orthogonal polarization components, which are aligned to the polarization components of the local oscillator. The two paired orthogonal components are detected separately and demodulated by identical demodulation circuits. After demodulation the output signals are added and form the input signal of a threshold comparator. The result is that the total signal power received remains constant, independent of the input SOP. The polarization diversity principle will be thoroughly discussed in Chapter 3 for an optical coherent (3x3) phase and polarization diversity DPSK receiver.

Data-induced polarization switching

Data-Induced Polarization Switching (DIPS) is a simple yet powerful technique to solve the polarization matching problem in optical coherent FSK systems, which combines polarization switching with FSK data modulation. At the transmitter, a space is sent as f_s and a mark as f_m. The signal is then launched at 45° to the principal axes of a birefringent medium, for example a piece of PMF. The frequency-dependent time delay introduced between two orthogonal polarization components causes a phase difference. For a given birefringence, the frequency difference is chosen so that the polarization states at the output of the birefringent medium are orthogonal. The signal is transmitted through standard single-mode fiber to a standard optical coherent receiver. At the receiver, a signal with frequency f_s and polarization P_s, or a signal with frequency f_m and polarization P_m is received. Dual-filter FSK demodulation applied or delay-and-multiply can be applied to retrieve the original data signal [2.44-2.46]. This system, which combines wide-deviations FSK and data-induced polarization switching, is polarization insensitive, suffering a theoretical power penalty of 3 dB when compared with ideal optical coherent heterodyne reception with perfectly matched polarization states [2.44].

References

[2.1] R.A. Linke and P.S. Henry, "Coherent optical detection : A thousand calls on one circuit",
IEEE Spectrum Mag., pp. 52-57, Febr. 1987.

[2.2] IEEE Standard Dictionary of Electrical and Electronics Terms,
The Institute of Electrical and Electronics Engineers, Inc.,
New York, 1988.

[2.3] K.S. Shanmugam, "Digital and Analog Communication Systems",
John Wiley & Sons, New York, 1979.

[2.4] W. van Etten and J. van der Plaats, "Fundamentals of Optical Fiber Communications",
Prentice Hall, New York, 1991.

[2.5] L. Giehmann and M. Rocks, "Measurements of polarization fluctuations in installed single-mode optical fiber cables",
Opt. Quantum Electron., vol. 19, pp. 109-113, 1987.

[2.6] G. Nicholson, "Polarization fluctuation measurement on installed single-mode optical fiber cables",
J. Lightwave Technol., vol. 7, no. 8, pp. 1197-1200, Aug. 1988.

[2.7] T. Imai and T. Matsumoto, "Polarization fluctuations in single-mode optical fiber",
J. Lightwave Technol., vol. 6, no. 9, pp. 1366-1375, Sept. 1988.

[2.8] K. Petermann, "Laser Diode Modulation and Noise",
Kluwer Academic Publishers, Dordrecht, 1988.

[2.9] L.G. Kazovsky et al, "Impact of laser intensity noise on ASK two-port optical homodyne receivers",
Electron. Lett., vol. 23, no. 17, pp. 871-873, 1987.

[2.10] A.F. Elrefaie, D.A. Atlas, L.G. Kazovsky, R.E. Wagner, "Intensity noise in ASK coherent lightwave receivers",
Electron. Lett., vol. 24, no. 3, pp. 158-159, 1988.

[2.11] W.H.C. de Krom, "Impact of local oscillator intensity noise and the threshold level on the performance of a {2x2} and {3x3} phase-diversity ASK receiver",
J. Lightwave Technol., vol. 9, no. 5, May 1991.

[2.12] E. Patzak, R. Langenhorst, "Sensitivity degradation of conventional and balanced 3x3 port phase diversity DPSK receivers due to thermal and local oscillator intensity noise",
Electron. Lett., vol. 25, no. 8, pp. 545-547, 1989.

[2.13] G. L. Abbas, V.W.S. Chan and T.K. Yee, "A dual-detector optical heterodyne receiver for local oscillator noise suppression",
J. Lightwave Technol., vol. 3, no. 5, pp. 1110-1122, Oct. 1985.

[2.14] C.H. Henry, "Phase noise in semiconductor lasers",
J. Lightwave Technol., vol. 23, pp. 298-311, April 1986.

[2.15] S. Betti et al., "Effect of non-Lorentzian lineshape of a semiconductor laser on a PSK coherent heterodyne optical receiver",
Electron. Lett., vol. 23, no. 25, pp. 1366-1367, 1987.

[2.16] J. Franz, "Optische Übertragungssysteme mit Überlagerungsempfang",
Springer-Verlag, Berlin, 1988.

[2.17] G.J. Foschini and G. Vannucci, "Characterizing filtered lightwaves corrupted by phase noise",
Trans. on Information Theory, vol. 34, no. 6, Nov. 1988.

[2.18] L.G. Kazovsky, "Impact of laser phase noise on optical heterodyne communication systems",
J. of Optical Communications, vol. 7, no. 2, pp. 66-87, 1986.

[2.19] L.G. Kazovsky, "Impact of reflections on phase-diversity optical homodyne receivers",
Electron. Lett., vol. 24, no. 9, pp. 522-524, 1988.

[2.20] T. Wood, "Multiple quantum well (MQW) waveguide modulators,"
J. Lightwave Technol., vol. 6, no. 6, pp. 743-757, June 1988.

[2.21] S. Wang and S. Lin, "High speed III-V electro-optic waveguide modulators at λ = 1.3 μm",
J. Lightwave Technol., vol. 6, no. 6, pp. 758-771, June 1988.

[2.22] L. Thylén, "Integrated optics in $LiNbO_3$: recent developments in devices for telecommunications",
J. Lightwave Technol., vol. 6, no. 6, pp. 847-861, June 1988.

[2.23] T. Kimura, "Coherent optical fiber transmission",
J. Lightwave Technol., vol. 5, no. 4, pp. 414-428, June 1988.

[2.24] R. Olshansky, "Subcarrier multiplexed broadband service network: a migration path to BISDN",
Mag. Lightwave Telecommun. Syst., Vol. 1, no. 3, pp. 30-34, Aug. 1990.

[2.25] J. Siuzdak, "Optical couplers for coherent optical phase diversity systems",
EUT Report 88-E-190, March 1988, ISBN 90-6144-190-0.

[2.26] L.B. Soldano, F.B. Veerman, M.K. Smit, and B.H. Verbeek, "High-performance monomode planar couplers using a short multi-mode interference section",
Part 1, Tech. Dig. ECOC 1990 (Amsterdam The Netherlands), pp. 225-228.

[2.27] E.C.M. Pennings et al., "Ultra-compact, low loss directional coupler structures on InP for monolithic integration",
Part 2, Tech. Dig. ECOC 1990 (Amsterdam The Netherlands), pp. 405-408.

[2.28] L.B. Soldano, M.K. Smit, A.H. de Vreede, J.W.M. van Uffelen, B.H. Verbeek, P. van Bennekom, W.H.C. de Krom and W. van Etten, "New all-passive 4x4 planar optical phase diversity network",
Post-deadline Papers ECOC 1991 (Paris France), pp. 96-99.

[2.29] H.P.A. van den Boom, "A frequency-locked loop for a phase diversity optical homodyne receiver",
Part 1, Tech. Dig. ECOC 1990 (Amsterdam The Netherlands), pp. 377-380.

[2.30] G. Jacobsen and I. Garrett, "Theory for optical heterodyne DPSK receivers with post-detection filtering",
J. Lightwave Technol., vol. 5, no. 4, pp. 478-484, April 1987.

[2.31] G. Jacobsen and I. Garrett, "Theory for optical heterodyne ASK receivers using square-law detection and postdetection filtering",
IEE Proc., vol. 134, no. 5, pp. 303-312, Oct. 1987.

[2.32] J. Siuzdak and W. van Etten, "Heterodyne ASK multiport optical receivers using postdetection filtering",
J. Lightwave Technol., vol. 8, no. 1, pp. 71-77, Jan. 1990.

[2.33] G. Nicholson, "Probability of error for optical heterodyne DPSK system with quantum phase noise",
Electron. Lett., vol. 20, no. 24, 1984.

[2.34] L.G. Kazovsky, "Performance analysis and laser linewidth requirements for optical PSK heterodyne communication systems",
J. Lightwave Technol., vol. 4, no. 4, pp. 415-425, April 1986.

[2.35] W.H.C. de Krom, "Impact of laser phase noise on the performance of a (3x3) phase and polarization diversity optical homodyne DPSK receiver",
J. Lightwave Technol., vol. 8, no. 11, pp. 1709-1716, Nov. 1990.

[2.36] G. Jacobsen and I. Garrett, "Error-rate floor in optical ASK heterodyne systems caused by nonzero (semiconductor) laser linewidth",
Electron. Lett., vol. 21, no. 7, pp. 268-270, 1985.

[2.37] G. Jacobsen and I. Garrett, "Influence of (semiconductor) laser linewidth on the error-rate floor in dual-filter optical FSK receivers",
Electron. Lett., vol. 21, no. 7, pp. 280-282, 1985.

[2.38] L.G. Kazovsky, P. Meissner and E. Patzak, "ASK multiport optical homodyne receivers",
J. Lightwave Technol., vol. 5, no. 6, pp. 770-790, 1987.

[2.39] L.G. Kazovsky and O.K. Tonguz, "ASK and FSK coherent lightwave systems : a simplified approximate analysis",
J. Lightwave Technol., vol. 8, no. 3, pp. 338-352, March 1990.

[2.40] W.R. Leeb, "Realization of a 90° and 180° hybrids for optical frequencies",
Arch. Elek. Ubertragung, vol. 37, pp. 203-206, 1983.

[2.41] L.G. Kazovsky et al., "All-fiber 90° optical hybrid for coherent communications",
Appl. Opt., vol. 26, pp. 437-439, 1987.

[2.42] H.C. LeFevre, "Single-mode fiber fractional wave devices and polarisation controllers",
Electron. Lett., vol. 16, no. 20, pp. 778-780, 1980.

[2.43] S.R. Ascham, M.C.K. Wiltshire, S.J. Marsh and A.J. Gibbons, "A practical liquid crystal polarisation controller",
Part 1, Tech. Dig. ECOC 1990 (Amsterdam The Netherlands), pp. 393-396.

[2.44] L.J. Cimini et al., "Polarisation-insensitive coherent lightwave system using wide deviation FSK and data-induced polarisation switching",
Electron. Lett., vol. 24, no. 6, pp. 358-360, 1988.

[2.45] I.M.I. Habbab and L.J. Cimini, "Polarization-insensitive coherent lightwave system using wide-deviation FSK and data-induced polarization switching",
J. Lightwave Technol., vol. 6, no. 10, pp. 1537-1548, Oct. 1988.

[2.46] R. Noé, H. Rodler, A. Ebberg, G. Gaukel, B. Noll, J. Wittmann and F. Auracher, "Comparison of polarization handling methods in coherent systems",
J. Lightwave Technol., vol. 9, no. 10, pp. 1353-1366, Oct. 1991.

CHAPTER 3.

THE PHASE AND POLARIZATION DIVERSITY DPSK RECEIVER

3.1 Introduction

Optical coherent homodyne reception offers the best performance but requires an optical phase-locked loop to phase synchronize the local oscillator laser with the transmitting laser (Chapter 2). Since an optical phase-locked loop is not easy to realize, a solution for this problem can be found by using phase diversity reception techniques, where fading of the signal, caused by zero crossings of the IF signal, can be prevented by making use of an optical hybrid [3.1] and parallel detection of the phase shifted optical waves [3.2-3.5]. In this thesis such a receiver is called a pseudo homodyne phase diversity receiver, since no phase locking is required and the IF value is usually chosen to be near zero, even for high speed data transmissions. In comparison with an ideal homodyne receiver, phase diversity reception results in a minimum sensitivity penalty of 3.0 dB, and besides, it requires a precise optical hybrid and electrical signal processing. A second feature of phase diversity reception is that the photocurrents are already in baseband, and baseband circuitry, which is less expensive and easier to implement, is sufficient. A third feature of phase diversity reception is that the basic operation of the receiver is insensitive to changes in the phase difference between the local oscillator laser and the signal wave received (Chapter 2). These changes in the phase difference can be caused by phase noise. Therefore, phase diversity reception is able (depending on the modulation format) to tolerate relatively large laser linewidths without excessive performance degradation [3.6].

A lightwave propagating through a standard single-mode fiber has the inconvenience that its polarization state changes at random. Since the performance of an optical coherent receiver highly depends on the matching of the polarization states of both the optical wave received and the optical wave generated by the local oscillator laser, some kind of polarization

arrangement is necessary to prevent loss of information due to the random walk of the difference in polarization state of both optical waves. Various kinds of solutions have been found to overcome this problem. Examples are, adaptive polarization controllers, the use of polarization maintaining fibers, and the use of more complicated polarization insensitive receiver structures (Chapter 2), [3.7-3.9]. The latter can be realized by means of polarization diversity techniques in which the input light is decomposed into two orthogonal linear polarization states. The light in both polarization states is detected independently and processed electronically by identical demodulation schemes.

In this chapter, a {3x3} phase and polarization diversity receiver for the DPSK scheme and a conventional heterodyne DPSK receiver (Figure 3.1b) will be analyzed and their performances compared. For the heterodyne DPSK receiver, perfectly matched polarization states of both optical waves, and identical system parameters for the phase and polarization diversity receiver are assumed. The BER of both receivers will be expressed analytically, and the numerical results will be given for various laser linewidths as a function of the SNR. For reason of comparison, some results for the {3x3} phase diversity DPSK receiver and {2x2} phase and polarization diversity DPSK receiver have been quoted from the literature. The receivers have been analyzed under the assumption that the local oscillator power is large enough to neglect the noise introduced by the receiver (e.g. thermal noise). Therefore, the shot noise related to the local oscillator dominates all other noise sources. Further are assumed, abrupt phase transitions (intersymbol interference is absent), and in order to be able to neglect the Relative Intensity Noise (RIN), a high amplitude stability of both lasers (Chapter 4), [3.10]. A block-diagram of the phase diversity receiver analyzed is depicted in Figure 3.1a. It is a conventional {3x3} phase diversity receiver using the DPSK demodulation scheme and the signal is differentially encoded before modulation. In a DPSK scheme, a mark is transmitted by changing the phase 180° between two successive data bits. A space is transmitted by sending a pulse of which the carrier is in phase with its predecessor. Demodulation can then be achieved by comparing the carrier phase of two successive data bits. This can be accomplished by delaying the first data bit over one bit period and next multiplying the delayed data bit by its

successor.

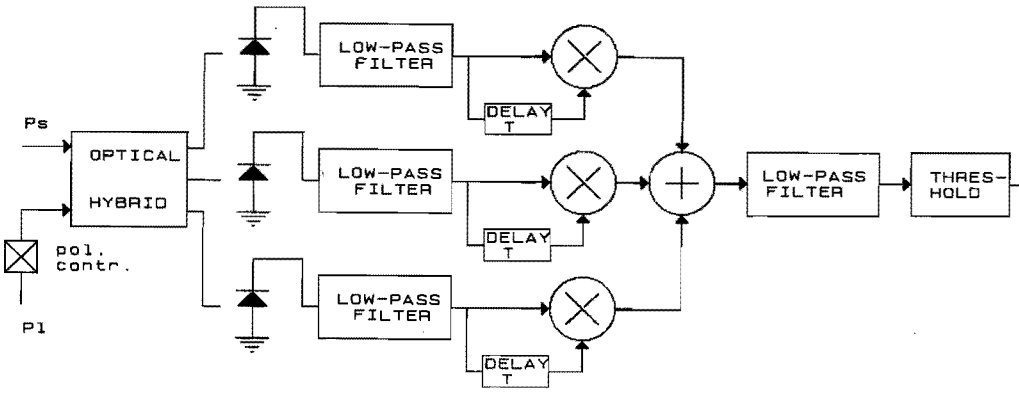

(a)

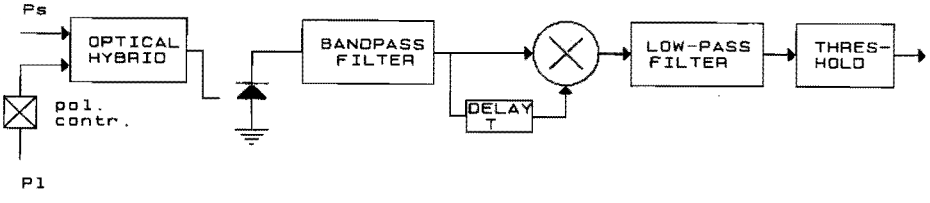

(b)

Figure 3.1 *(a) A (3x3) phase diversity DPSK receiver,*
(b) A heterodyne DPSK receiver.

3.2 The receiver structure

The model of the receiver analyzed is given in Figure 3.2 and consists of two polarization beamsplitters, two (3x3) DPSK phase diversity receivers as depicted in Figure 3.1a, with two exceptions. The polarization controller can be omitted as well as the threshold comparators. The latter are replaced by one single threshold comparator and the decision will be made after adding both demodulated data signals from both phase diversity receivers.

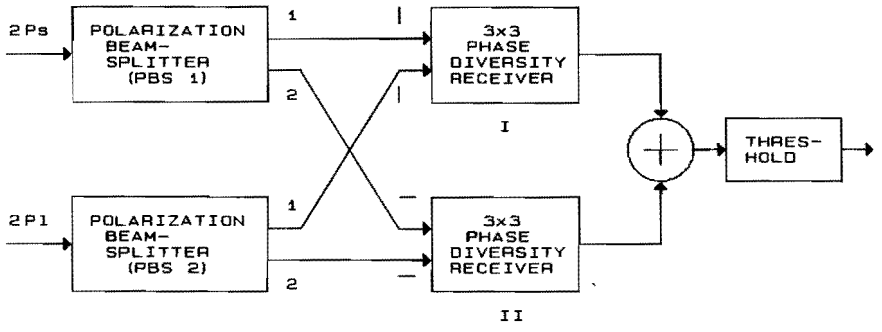

Figure 3.2 *The (3x3) phase and polarization diversity DPSK receiver.*

The light of both the local oscillator and the transmitting laser is supplied to the polarization beamsplitters, where it is split up into two orthogonal polarization states. Demodulation takes place for each polarization state separately, and since both processes are independent, the results can be added. This sum is compared by a threshold comparator (with reference level zero) to retrieve the final demodulated binary data signal. For proper operation it is desirable to split up the power of the local oscillator equally between the two orthogonal polarization states. These types of polarization independent or insensitive receiver structures were first introduced by Glance [3.7], Okoshi [3.11] and Kuwahara [3.12].

3.3 Mathematical representation of a (3x3) phase and polarization diversity DPSK receiver

It is assumed that the local oscillator laser is linearly polarized and has an optical power of $2P_L$ (the factor 2 is introduced here for mathematical convenience only), which is equally divided between the two orthogonal polarization states. The electromagnetic field of the local oscillator laser can then be given by

$$E_L(t) \propto \sqrt{2P_L}.\cos(\omega_L t + \theta_L(t)) \ , \tag{3.1}$$

where

ω_L is the local oscillator radial frequency, and

θ_L is the local oscillator phase noise.

The local oscillator power in each polarization state is received by three separate photodiodes, which implies that the three receiver branches carry statistically independent shot noise components. Under the restrictions mentioned earlier, this is the shot noise introduced by the local oscillator laser (Chapter 2). The shot noise in each receiver branch is assumed to have a zero mean Gaussian probability density function with variance $\sigma^2 = \frac{1}{3}eRP_L B$, where e is the electron charge, B is the double-sided receiver bandwidth, and R represents the responsivity of the photodiodes used, which in this case is assumed to be equal for all photodiodes. The responsivity is defined as follows

$$R = \frac{\eta e}{h\nu} \ , \tag{3.2}$$

where h is the Planck's constant, ν the frequency of the light, and η the quantum efficiency of the photodiodes used. The electromagnetic field of the local oscillator in both polarization states can be described as

$$E_{L_h}(t) \propto \sqrt{P_L}.\cos(\omega_L t + \theta_L(t) + \alpha_h) \ , \tag{3.3}$$

$$E_{L_v}(t) \propto \sqrt{P_L}.\cos(\omega_L t + \theta_L(t) + \alpha_v) \ , \tag{3.4}$$

where $\theta_L(t)$ is the local oscillator phase noise, and α_h and α_v the (fixed) phase shifts introduced by the difference in the optical path length in the beamsplitter for the vertical and horizontal polarized light. For the electromagnetic field of the optical signal received, we can give a similar equation, namely

$$E_S(t) \propto \sqrt{2P_S}.b(t).\cos(\omega_S t + \theta_S(t)) \ , \tag{3.5}$$

where

ω_S is the signal radial frequency,
$\theta_S(t)$ is the signal phase noise,
$2P_S$ the average signal power received of the transmitting laser, and
$b(t)$ the signaling waveform which is modeled as the digital baseband signal

$$b(t) = \sum_k b_k.\mathrm{rect}(t - kT_0) \ , \qquad k = 0,1,2... \tag{3.6}$$

where T_0 represents the bit time, and b_k is the symbol sequence, taking the value +1 or -1. The function rect(t) is equal to 1 for $t \in [0,T_0]$ and equal to 0 elsewhere.

Since the polarization state of the optical signal received is randomly changing, its power is randomly distributed between both polarization states. The amount by which the power is split up in the vertical or horizontal polarization states, is given by the factor β and $(1-\beta)$, respectively, with $0 \le \beta \le 1$. The electromagnetic field in both polarization states can be described as

$$E_{S_h}(t) \propto \sqrt{2P_S\beta}.b(t).\cos(\omega_S t + \theta_S(t) + \delta_h) \ , \tag{3.7}$$

$$E_{S_v}(t) \propto \sqrt{2P_S(1-\beta)}.b(t).\cos(\omega_S t + \theta_S(t) + \delta_v) \ , \tag{3.8}$$

where δ_h and δ_v are fixed phase shifts introduced by the difference in optical path length in the beamsplitters for the horizontal and vertical polarized light. It is well-known that DPSK is effective only when the linewidth of both the transmitting and local oscillator laser are substantially smaller than the bit rate $1/T_0$. Therefore, the low-pass filters which follow the photodiodes may be replaced by filters matched to the signal rect(t). The filtered photocurrents for the horizontal polarization state,

including phase noise and shot noise, are then given by

$$I_{h,k}(t) = \frac{2}{3}R\sqrt{2P_L P_S\beta}.b(t).\cos(\omega_{IF}t + \phi(t) + \rho + \frac{2}{3}\pi k) + n_k(t) \ , \qquad (3.9)$$

with k = 1,2,3 the number of optical hybrid outputs, and where ω_{IF} is the radial frequency offset between the transmitting and the local oscillator laser, $\phi(t) = \theta_L(t) - \theta_S(t)$, $\rho = \alpha_h - \delta_h$ and $n_k(t)$ stands for the shot noise current.

For the filtered photocurrents in the vertical polarization state, comprising phase noise and shot noise, can be written

$$I_{v,k}(t) = \frac{2}{3}R\sqrt{2P_L P_S(1-\beta)}.b(t).\cos(\omega_{IF}t + \phi(t) + \tau + \frac{2}{3}\pi k) + n_k'(t) \ , \qquad (3.10)$$

with k = 1, 2, 3, $\tau = \alpha_v - \delta_v$, and $n_k'(t)$ denotes the shot noise current.

If we define

$$S(t) \triangleq R\sqrt{2P_L P_S\beta}.b(t)$$

and (3.11)

$$S'(t) \triangleq R\sqrt{2P_L P_S(1-\beta)}.b(t) \ ,$$

the photocurrents in the horizontal polarization state read

$$I_{h_1}(t) = \frac{2}{3}S(t).\cos(\omega_{IF}t + \phi(t) + \rho) + n_1(t) \ , \qquad (3.12)$$

$$I_{h_2}(t) = \frac{2}{3}S(t).\cos(\omega_{IF}t + \phi(t) + \rho + \frac{2\pi}{3}) + n_2(t) \ , \qquad (3.13)$$

$$I_{h_3}(t) = \frac{2}{3}S(t).\cos(\omega_{IF}t + \phi(t) + \rho + \frac{4\pi}{3}) + n_3(t) \ . \qquad (3.14)$$

The photocurrents in the vertical polarization state comprising phase and shot noise, then read

$$I_{v_1}(t) = \frac{2}{3}S'(t).\cos(\omega_{IF}t + \phi(t) + \tau) + n_1'(t) , \tag{3.15}$$

$$I_{v_2}(t) = \frac{2}{3}S'(t).\cos(\omega_{IF}t + \phi(t) + \tau + \frac{2\pi}{3}) + n_2'(t) , \tag{3.16}$$

$$I_{v_3}(t) = \frac{2}{3}S'(t).\cos(\omega_{IF}t + \phi(t) + \tau + \frac{4\pi}{3}) + n_3'(t) . \tag{3.17}$$

The demodulated signal at the input of the threshold comparator can now simply be expressed by the following equation under the assumption of matched IF filtering

$$V_t(t) = c\sum_{n=1}^{3}\{I_{h_n}(t).I_{h_n}(t - T) + I_{v_n}(t).I_{v_n}(t - T)\} , \tag{3.18}$$

with T the delay time, which for DPSK modulation is equal to the bit time (T_0), c a constant, and n the number of receiver branches in both phase diversity receivers. By changing variables, $V_t(t)$ is expressed in two sums of squared variables. A conventional analysis is used [3.13], which for a similar purpose was introduced earlier by Cheng [3.14]. Twelve variables have been defined which are divided into two sets. These variables consist of linear combinations of the six photocurrents mentioned above.

Set 1. $(\bar{u} = (u_1, u_2, u_3, u_4, u_5, u_6))$

$$u_1 = I_{v_1}(t) + I_{v_1}(t - T) \qquad u_4 = I_{h_1}(t) + I_{h_1}(t - T)$$

$$u_2 = I_{v_2}(t) + I_{v_2}(t - T) \qquad u_5 = I_{h_2}(t) + I_{h_2}(t - T)$$

$$u_3 = I_{v_3}(t) + I_{v_3}(t - T) \qquad u_6 = I_{h_3}(t) + I_{h_3}(t - T) . \tag{3.19}$$

Set 2. $\bar{s} = ((s_1, s_2, s_3, s_4, s_5, s_6))$

$$s_1 = I_{v_1}(t) - I_{v_1}(t - T) \qquad s_4 = I_{h_1}(t) - I_{h_1}(t - T)$$

$$s_2 = I_{v_2}(t) - I_{v_2}(t - T) \qquad s_5 = I_{h_2}(t) - I_{h_2}(t - T)$$

$$s_3 = I_{v_3}(t) - I_{v_3}(t - T) \qquad s_6 = I_{h_3}(t) - I_{h_3}(t - T) \; . \tag{3.20}$$

Rewriting $V_t(t)$ in terms of these variables leads to the following equation

$$\begin{aligned} V_t(t) &= \frac{1}{4}c\Big[\big(u_1^2 + u_2^2 + u_3^2 + u_4^2 + u_5^2 + u_6^2\big) - \\ &\qquad \big(s_1^2 + s_2^2 + s_3^2 + s_4^2 + s_5^2 + s_6^2\big)\Big] \\ &= \frac{1}{4}c\Big[r_1^2 - r_2^2\Big] \; , \end{aligned} \tag{3.21}$$

where

$$r_1^2 = \big(u_1^2 + u_2^2 + u_3^2 + u_4^2 + u_5^2 + u_6^2\big) \; , \tag{3.22}$$

and

$$r_2^2 = \big(s_1^2 + s_2^2 + s_3^2 + s_4^2 + s_5^2 + s_6^2\big) \; . \tag{3.23}$$

The prior probability of sending a mark ($b_k = 1$) is assumed to be equal to that of sending a space ($b_k = -1$). The conditional bit error probability for receiving a space provided a mark was sent, $P(V_t(t) < 0 | b_k = 1)$, is in terms of r_1^2 and r_2^2 the probability $P(r_1^2 < r_2^2 | b_k = 1)$, implying that the threshold value $V_t(t) < 0$. This probability is equal to $P(r_1^2 > r_2^2 | b_k = -1)$ because of symmetry. These conditional error probabilities imply that the phase changes due to phase noise, are assumed to be negligible within one bit time. The total BER is then given by

$$BER = P(r_1^2 < r_2^2 | b_k = -1) = P(r_1 < r_2 | b_k = 1) \; . \tag{3.24}$$

If $f_1(r_1)$ represents the probability density function of r_1, and $f_2(r_2)$ the

probability density function of r_2, the total BER of the receiver, comprising shot noise only, reads

$$BER = \int_0^{\infty} f_1(r_1).\int_{r_1}^{\infty} f_2(r_2)\, dr_1.dr_2 \,. \tag{3.25}$$

The variables r_1 and r_2, respectively, can be regarded as the norm of the six dimensional vector $\bar{r} = (x_1,x_2,x_3,x_4,x_5,x_6)$, where all components are Gaussian distributed with equal variances and fixed mean values. By rotation of coordinates, it can be proved that under these conditions the probability density function is equal to that of a vector whose components have equal variances and mean values given by

$$\langle x_6 \rangle \triangleq A = \sqrt{\langle x_1^2 \rangle + \langle x_2^2 \rangle + \langle x_3^2 \rangle + \langle x_4^2 \rangle + \langle x_5^2 \rangle + \langle x_6^2 \rangle} \,,$$

and (3.26)

$$\langle x_1 \rangle = \langle x_2 \rangle = \langle x_3 \rangle = \langle x_4 \rangle = \langle x_5 \rangle = 0 \,,$$

where <.> denotes the mean value of the variable.
The probability density function can then be expressed by the six dimensional joint probability density function $\mathfrak{F}$ which reads

$$\mathfrak{F}(\bar{r}) = \frac{1}{(2\pi\sigma^2)^3}.\exp\left[-\frac{x_1^2 + x_2^2 + x_3^2 + x_4^2 + x_5^2 + (x_6 - A)^2}{2\sigma^2}\right] . \tag{3.27}$$

The Cartesian coordinates are transformed into the following six dimensional polar coordinates

$$\begin{aligned}
x &= r.\sin\theta_1\sin\theta_2\sin\theta_3\sin\theta_4\sin\theta_5 \,,\\
y &= r.\sin\theta_1\sin\theta_2\sin\theta_3\sin\theta_4\cos\theta_5 \,,\\
z &= r.\sin\theta_1\sin\theta_2\sin\theta_3\cos\theta_4 \,,\\
r &= r.\sin\theta_1\sin\theta_2\cos\theta_3 \,,\\
s &= r.\sin\theta_1\cos\theta_2 \,,\\
t &= r.\cos\theta_1 \,.
\end{aligned} \tag{3.28}$$

The Jacobian determinant (J) belonging to this coordinate transformation can be calculated to be

$$J = r^5.\sin^4\theta_1.\sin^3\theta_2.\sin^2\theta_3.\sin\theta_4 \ . \tag{3.29}$$

Substitution of Equation (3.28) and (3.29) in (3.27) results in Equation (3.30) after integration over θ_2, θ_3, θ_4, and θ_5, and equals the probability density function of the norm of a six dimensional vector.

$$\int_0^{\pi}\int_0^{\pi}\int_0^{\pi}\int_0^{\pi}\int_0^{2\pi} \Im \, d\theta_1.d\theta_2.d\theta_3.d\theta_4.d\theta_5$$

$$= \frac{1}{(2\pi\sigma^2)^3} \int_0^{\pi}\int_0^{\pi}\int_0^{\pi}\int_0^{\pi}\int_0^{2\pi} r^5.\sin^4\theta_1.\sin^3\theta_2.\sin^2\theta_3.\sin\theta_4 \times$$

$$\exp\left[-\frac{r^2+A^2-2rA\cos\theta_1}{2\sigma^2}\right] d\theta_1.d\theta_2.d\theta_3.d\theta_4.d\theta_5$$

$$= \frac{1}{(2\pi\sigma^2)^3} r^5.\exp\left[-\frac{r+A}{2\sigma^2}\right].\int_0^{\pi} \sin^4\theta_1.\exp\left[-\frac{2rA\cos\theta_1}{2\sigma^2}\right] d\theta_1 \times$$

$$\int_0^{\pi} \sin^3\theta_2 \, d\theta_2.\int_0^{\pi} \sin^2\theta_3 \, d\theta_3.\int_0^{\pi} \sin\theta_4 \, d\theta_4 \int_0^{2\pi} d\theta_5$$

$$= \frac{r^5}{(2\pi\sigma^2)^3}.\exp\left[-\frac{r^2+A^2}{2\sigma^2}\right].\int_0^{\pi} \sin^4\theta_1.\exp\left[-\frac{rA\cos\theta_1}{\sigma^2}\right] d\theta_1 \left(\frac{8}{3}\pi^2\right)$$

$$= \frac{r^5}{3\pi\sigma^6}.\exp\left[-\frac{r^2+A^2}{2\sigma^2}\right].\int_0^{\pi} \sin^4\theta_1.\exp\left[-\frac{rA\cos\theta_1}{\sigma^2}\right] d\theta_1 \ . \qquad (3.30)$$

Recalling the identity [3.15]

$$I_\nu(z) = \frac{(1/2.z)^\nu}{\pi^2\Gamma(\nu+1/2)} \int_0^{\pi} e^{\pm z.\cos\theta}.\sin^{2\nu}\theta \ d\theta \ , \qquad (3.31)$$

where $I_\nu(z)$ is the modified Bessel function of the first kind and order ν, and $\Gamma(\nu)$ is the Gamma function [3.15].

Substitution $\nu = 2$ in Equation (3.31) and comparing the result with Equation (3.30) shows that the integral can be replaced by a modified Bessel function of the first kind and order two. This results in the probability density function of the norm of a six dimensional vector, whose components have a Gaussian probability density function with equal variance and fixed mean values

$$\tilde{\vartheta} = \frac{r^3}{A^2\sigma^2}.I_2\left[\frac{Ar}{\sigma^2}\right].\exp\left[-\frac{r^2+A^2}{2\sigma^2}\right] \ . \qquad (3.32)$$

This result can be used to calculate the BER of the {3x3} phase and polarization diversity DPSK receiver. Since the equation for the BER of the diversity receiver is a double integral without taking into account the phase noise, we have two different six dimensional vectors each with its own noncentral parameter A_1 and A_2, respectively,

$$A_1 = \sqrt{\langle u_1^2\rangle + \langle u_2^2\rangle + \langle u_3^2\rangle + \langle u_4^2\rangle + \langle u_5^2\rangle + \langle u_6^2\rangle} \ ,$$

and $\qquad (3.33)$

$$A_2 = \sqrt{\langle s_1^2\rangle + \langle s_2^2\rangle + \langle s_3^2\rangle + \langle s_4^2\rangle + \langle s_5^2\rangle + \langle s_6^2\rangle} \ .$$

We can rewrite the photocurrents and their delayed version in terms of the phase difference $\Delta\Phi$, where $\Delta\Phi$ is defined according to the following equation

$$\Delta\Phi \triangleq \phi(t) - \phi(t-T) \ . \tag{3.34}$$

It is assumed that the phase difference $\Delta\Phi$ has a Gaussian distribution function with a zero mean value and a variance σ_Φ^2 [3.16]. This variance is directly related to the sum of the linewidths of the local oscillator laser and the transmitting laser according to the following relation [3.17]

$$\sigma_\Phi^2 = 2\pi(\Delta\nu_L + \Delta\nu_S)T = 2\pi\Delta\nu T \ . \tag{3.35}$$

Here $\Delta\nu_L$ and $\Delta\nu_S$ are the FWHM (Full-Width-Half-Maximum) laser linewidths of the local oscillator laser and the transmitting laser, respectively. $\Delta\nu$ represents the sum of both linewidths. T is the delay time introduced by the delay elements, which equals the bit time T_0. Rewriting the photocurrents in terms of the phase difference $\Delta\Phi$ leads to the following equations

$$I_{h,k}(t) = \frac{2}{3}R\sqrt{2P_L P_S\beta}.b(t).\cos(\omega_{IF}t + \Delta\Phi + \phi(t-T) + \rho + \frac{2}{3}\pi k) + n_k(t) \ ,$$

$$I_{v,k}(t) = \frac{2}{3}R\sqrt{2P_L P_S(1-\beta)}.b(t).\cos(\omega_{IF}t + \Delta\Phi + \phi(t-T) + \tau + \frac{2}{3}\pi k) + n_k'(t) \ ,$$

$$\text{with } k = 1, 2, 3 \ . \tag{3.36}$$

The noncentral parameters A_1 and A_2 can now easily be computed according to Equation (3.33). This results in

$$A_1^2 = \frac{8}{3}\cos^2(\frac{\Delta\Phi}{2}).\left[2P_L P_S\beta + 2P_L P_S(1-\beta)\right]R^2$$

$$= \frac{16}{3}R^2 P_L P_S \cos^2(\frac{\Delta\Phi}{2})$$

$$\Longrightarrow A_1 = \frac{4}{3}\sqrt{3}R\sqrt{P_L P_S}.\cos(\frac{\Delta\Phi}{2}) \ . \tag{3.37}$$

For A_2 can be calculated in the same way

$$==> A_2 = \frac{4}{3}\sqrt{3}R\sqrt{P_L P_S}.\sin(\frac{\Delta\Phi}{2}) \ . \tag{3.38}$$

Rewriting Equation (3.25) and taking into account the phase noise and shot noise leads to the following equation for the BER

$$BER = \frac{1}{\sqrt{2\pi}.\sigma_\Phi} \int_{-\infty}^{\infty} \exp\left[\frac{-\Delta\Phi^2}{2\sigma_\Phi^2} \right] . \int_{-\infty}^{\infty} f_1(r_1) . \int_{r_1}^{\infty} f_2(r_2)\ dr_1.dr_2.d(\Delta\Phi) \ , \tag{3.39}$$

where $f_1(r_1)$ and $f_2(r_2)$ are the error probability density functions in terms of A_1, r_1 and σ_1 {i = 1, 2} given by the following equations

$$f_1(r_1) = \frac{r_1^3}{A_1^2\sigma_1^2}.I_2\left[\frac{A_1 r_1}{\sigma_1^2} \right].\exp\left[- \frac{r_1^2 + A_1^2}{2\sigma_1^2} \right] \ , \tag{3.40}$$

and

$$f_2(r_2) = \frac{r_2^3}{A_2^2\sigma_2^2}.I_2\left[\frac{A_2 r_2}{\sigma_2^2} \right].\exp\left[- \frac{r_2^2 + A_2^2}{2\sigma_2^2} \right] \ . \tag{3.41}$$

The local oscillator photons are randomly distributed between both polarization states by the polarization beamsplitters. Therefore, the shot noises introduced by the local oscillator laser in the receiver for the horizontal and the vertical polarization state, are statistically independent. They have Gaussian probability density functions with zero mean and variance $\sigma_o^2 = eBRP_L \triangleq \langle N_n^2 \rangle = \langle N_n'^2 \rangle$ (n = 1, 2, 3). For mathematical convenience, we make a change of variable for the variances σ_1^2 and σ_2^2 of the vector components of the six dimensional vectors $\bar{u}$ and $\bar{s}$

$$\sigma_1^2 = \sigma_2^2 = \frac{2}{3}\sigma_0^2 \ . \tag{3.42}$$

The SNR of the {3x3} phase and polarization diversity DPSK receiver can be

defined as

$$\gamma = \frac{2\eta P_s T_0}{h\nu} . \tag{3.43}$$

This ratio γ can be interpreted as the average signal power received divided by the shot noise power in twice the Nyquist bandwidth. In this case of matched IF filtering with $B = 1/T_0$, γ can also be treated as the average number of signal photons received per bit time (T_0).
The following substitutions will be made in Equation (3.39) and (3.40)

$$s \triangleq \frac{\Delta\Phi}{\sqrt{2}.\sigma_\Phi} , \quad t \triangleq \frac{r_1}{\sqrt{2}.\sigma_1} , \tag{3.44}$$

$$\frac{A_1}{\sigma_1} = 2\sqrt{\gamma}.\cos\left[\frac{\sigma_\Phi s}{\sqrt{2}}\right] \triangleq \sqrt{2}.\alpha , \tag{3.45}$$

$$\frac{A_1^2}{2\sigma_1^2} = 2\gamma.\cos^2\left[\frac{\sigma_\Phi s}{\sqrt{2}}\right] = \alpha^2 . \tag{3.46}$$

In a similar way we make the following substitutions in Equation (3.41)

$$u \triangleq \frac{r_2}{\sqrt{2}.\sigma_2} , \tag{3.47}$$

$$\frac{A_2}{\sigma_2} = 2\sqrt{\gamma}.\sin\left[\frac{\sigma_\Phi s}{\sqrt{2}}\right] \triangleq \sqrt{2}.\beta , \tag{3.48}$$

$$\frac{A_2^2}{2\sigma_2^2} = 4\gamma.\sin^2\left[\frac{\sigma_\Phi s}{\sqrt{2}}\right] = \beta^2 . \tag{3.49}$$

Substitution of these variables in the Equations (3.47) to (3.49) results in the relation for the BER of the {3x3} phase and polarization diversity DPSK receiver analyzed. This as a function of the SNR (γ), which is a parameter for $\alpha(\gamma,s)$ and $\beta(\gamma,s)$.

$$BER = \frac{4}{\sqrt{\pi}} \int_{-\infty}^{\infty} e^{-s^2} \cdot \int_{0}^{\infty} \frac{t^3}{\alpha^2} I_2[2\alpha t]\, e^{-[t^2+\alpha^2]} \cdot \int_{t}^{\infty} \frac{u^3}{\beta^2} I_2[2\beta u]\, e^{-[u^2+\beta^2]}\, du.dt.ds \ . \tag{3.50}$$

3.4 Performance evaluation of the (3x3) phase and polarization diversity DPSK receiver

3.4.1 The performance for zero laser linewidths

For reasons of comparison with [3.2], the performance of the (3x3) phase and polarization diversity DPSK receiver has first been analyzed under zero laser linewidths conditions for both the local oscillator laser and the transmitting laser. Substitution of $\sigma_{\Phi} = 0$ in the Equations (3.45) and (3.48) gives $\alpha = \sqrt{2\gamma}$ and $\beta = 0$, respectively. Next, Equation (3.50) has been rewritten, making use of some mathematical identities [3.15]. If we use an approximation for a modified Bessel function with a very small argument, the argument of the third integral in Equation (3.50) can be rewritten. For small values of the argument z, we can substitute for $I_{\nu}(z)$ its asymptotic expansion

$$I_{\nu}(z) \cong \frac{(1/2.z)^{\nu}}{\Gamma(\nu + 1)} , \qquad \text{for } z << 1 , \tag{3.51}$$

$$\frac{I_2(z)}{z^2} \cong \frac{0.25}{\Gamma(3)} = \frac{1}{8} . \tag{3.52}$$

Therefore, in the limit for β approaching zero, the ratio $I_2[2\beta u]/\beta^2$ in the third integral of Equation (3.50) can be rewritten as

$$\lim_{\beta \Rightarrow 0} \frac{I_2[2\beta u]}{\beta^2} = \frac{u^2}{2} . \tag{3.53}$$

The first integral of Equation (3.50) equals $\sqrt{\pi}$, therefore, Equation (3.50)

can be recalculated which leads to the following integral

$$BER = 2 \int_0^\infty \frac{t^3}{\alpha^2} I_2[2\alpha t]\, e^{-[t^2+\alpha^2]} \int_t^\infty u^5 e^{-u^2}\, du.dt$$

$$= 2 \int_0^\infty \frac{t^3}{\alpha^2} \left(\frac{1}{2}t^4 + t^2 + 1\right).I_2[2\alpha t]\, e^{-[2t^2+\alpha^2]}\, dt \,, \qquad (3.54)$$

which can be calculated analytically to give

$$BER = \frac{e^{-N}}{64} (32 + 12N + N^2) \,, \qquad (3.55)$$

with N the number of signal photons/bit received. It is found that the SNR required to achieve a BER = 10^{-9} is 13.66 dB, which is equivalent to 23.2 photons/bit. This result is similar with Equation (57) of [3.2]* . In comparison with the ideal heterodyne DPSK receiver, which requires 20 photons/bit (SNR = 13.0 dB), this results in a sensitivity penalty of approximately 0.7 dB [3.2].

The BER according to Equation (3.55) has been calculated for values of the SNR varying from 10 to 15 dB, and the results are shown in Figure 3.3. In this figure, the performances are also depicted of the conventional heterodyne DPSK receiver and the (2x2) phase and polarization diversity DPSK receiver.

---

* *The coefficient of N^2 differs by a factor of 2. However, Equation (3.55) has been confirmed by the authors of [3.2,3.27].*

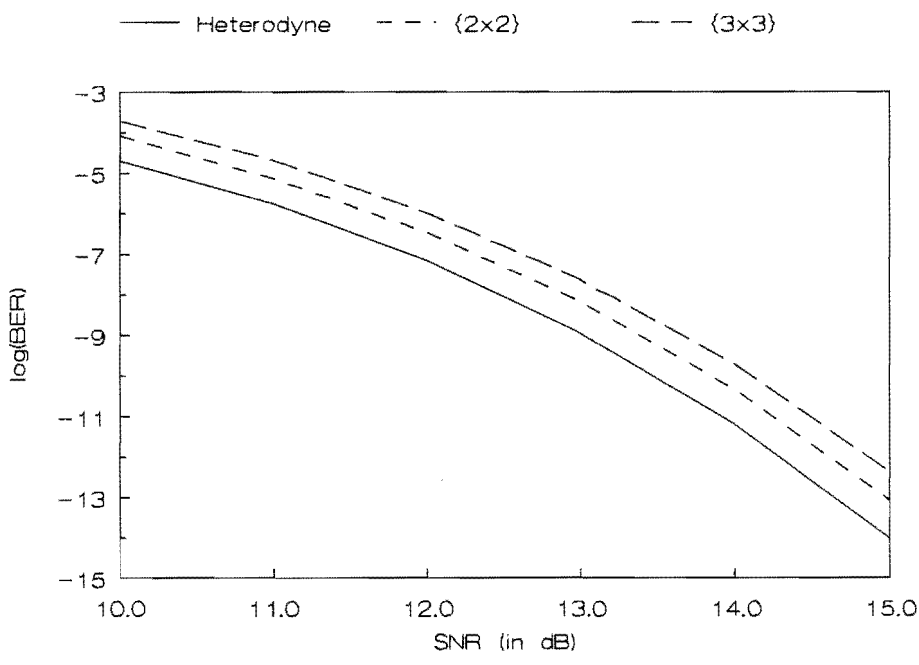

Figure 3.3 *The BER versus the SNR for the (3x3) phase and polarization diversity DPSK receiver for zero laser linewidths.*

The BER for the heterodyne DPSK receiver for nonzero laser linewidths is given by (see Appendix 3 for detailed derivation, [3.18])

$$BER = \frac{4}{\sqrt{\pi}} \int_{\infty}^{\infty} e^{-s^2} . \int_{0}^{\infty} tI_0[2\alpha t] \exp[-(t^2+\alpha^2)] \times$$

$$\int_{t}^{\infty} uI_0[2\beta t] \exp[-(u^2+\beta^2)] \, ds.dt.du \ , \qquad (3.56)$$

where

$$\alpha \triangleq \sqrt{2\gamma}.\cos(\frac{\Delta\Phi}{2}) \ , \qquad (3.57)$$

and

$$\beta \triangleq \sqrt{2\gamma}.\sin(\frac{\Delta\Phi}{2}) \ . \tag{3.58}$$

The parameter definitions are similar to those defined earlier for the {3x3} phase and polarization diversity DPSK receiver. For zero laser linewidths the integral of Equation (3.56) can be recalculated to give

$$BER = 2 \int_0^\infty tI_0[2\alpha t] \exp[-(2t^2 + \alpha^2)] \, dt \ , \tag{3.59}$$

which, after some mathematical manipulations can be calculated analytically. This results in the following relation for the BER

$$BER = \frac{1}{2}.e^{-N} \ . \tag{3.60}$$

It is found that the SNR required to achieve BER = 10^{-9} is 13.0 dB, which is equal to 20 photons/bit.
The BER for the {2x2} phase and polarization diversity DPSK receiver for zero laser linewidths reads [3.2,3.14,3.19]

$$BER = \left[\frac{1}{2} + \frac{1}{8}.N \right].e^{-N} \ . \tag{3.61}$$

For this receiver the SNR required to achieve BER = 10^{-9} is 13.4 dB (21.9 photons), which is 0.26 dB better than the performance of the {3x3} phase and polarization DPSK receiver. The SNR required for the {3x3} phase diversity DPSK receiver to achieve BER = 10^{-9} has been calculated by Nicholson [3.20] and appeared to be 13.2 dB. For matched IF filtering, this corresponds to 21 photons/bit. From Figure 3.3 it can be concluded that for BER = 10^{-9} the phase diversity DPSK receivers under investigation introduce a sensitivity penalty in comparison with the ideal heterodyne DPSK receiver of approximately 0.4 dB for the {2x2} phase and polarization diversity DPSK receiver [3.14], and approximately 0.7 dB for the {3x3} phase and polarization diversity DPSK receiver. For the {3x3} phase diversity DPSK receiver, the sensitivity penalty is approximately 0.2 dB.

3.4.2 The performance of the {3x3} phase and polarization diversity DPSK receiver including phase noise and shot noise

For nonzero laser linewidths, the integral of Equation (3.50) has been computed numerically for various laser linewidths. The results are depicted in Figure 3.4 as a function of the SNR (in dB) and the normalized laser linewidth $\Delta\nu.T_0$.

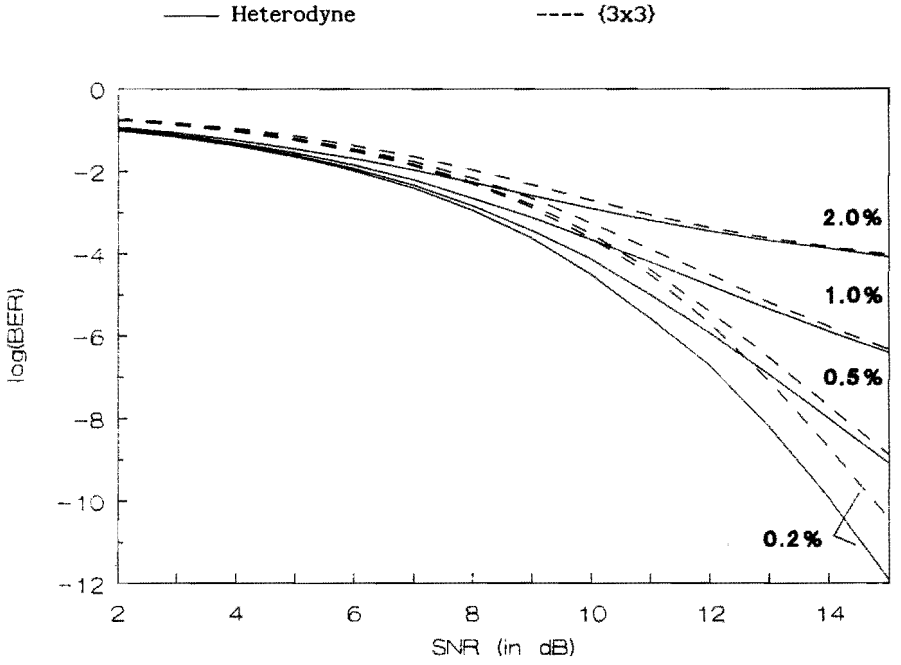

Figure 3.4 *The BER versus the SNR of the {3x3} phase and polarization diversity DPSK receiver for nonzero laser linewidths.*

In Figure 3.4, the BER curves of the ideal heterodyne DPSK receiver are also depicted [3.18]. For a normalized laser linewidth (= $\Delta\nu.T_0$) of 0.2% and a BER = 10^{-9}, the results are within 0.5 dB from the phase noise free case. For the heterodyne DPSK receiver, it results in an excess power penalty of 0.45 dB with respect to the shot noise limited case. For a normalized laser linewidth of 0.5%, the BER curves of the heterodyne DPSK receiver and the {3x3} phase and polarization diversity DPSK receiver merge for large SNR's,

comprising shot and phase noise only. For a normalized laser linewidth of 1.0%, the BER curves merge for SNR's > 13 dB. For even larger values of $\Delta\nu.T_0$, the performances of both receivers are almost identical for SNR's larger than approximately 11 dB. From the BER curves depicted in Figure 3.4 it can be concluded, that for both receivers the curves for $\Delta\nu.T_0$ = 1.0% and $\Delta\nu.T_0$ = 2.0% start to bottom out for large SNR's, implying the existence of a BER floor caused by phase noise. An increase of the signal power will not result in smaller BER's and for this reason these receivers are useless for large normalized laser linewidths in practical situations. These BER floors can be easily derived using the irreducible error probability expression as a function of the normalized laser linewidth $\Delta\nu$ [3.21]

$$BER_{floor} = \text{erfc}\left[\frac{\sqrt{\pi}}{4\sqrt{\Delta\nu T_0}}\right]. \qquad (3.62)$$

The BER floor, according to Equation (3.62), is plotted in Figure 3.5 for normalized laser linewidths varying from 0.2% to 2.0%.

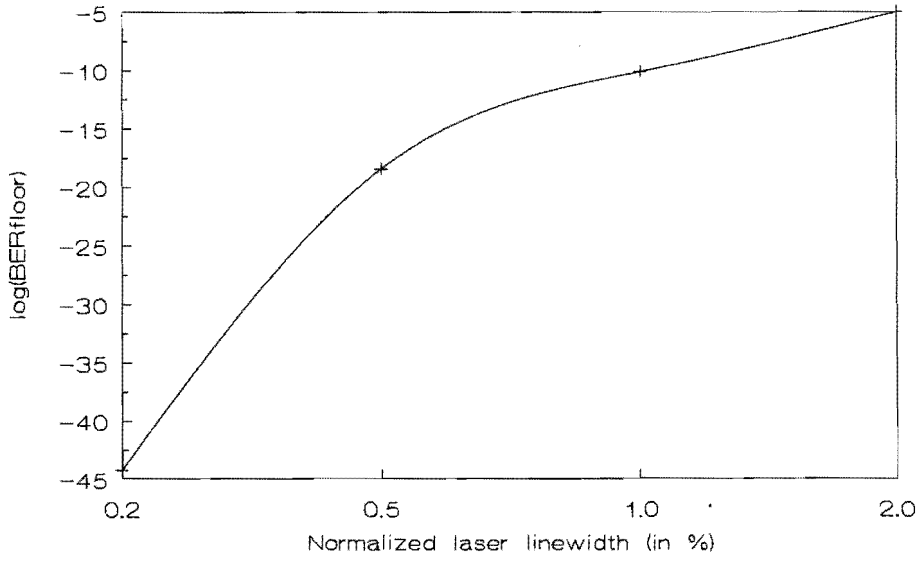

Figure 3.5 *The irreducible error probability as a function of the laser linewidths.*

We choose as criteria for the maximum allowable laser linewidth in the coherent receivers analyzed, that linewidth which increases the SNR required for the receivers to achieve a BER = 10^{-9} by maximal 1.0 dB. Computation of Equation (3.50) for a SNR of 14.66 dB and a BER of 10^{-9} results for the {3x3} phase and polarization diversity DPSK receiver in a maximum allowable normalized laser linewidth up to approximately 0.46%. For the conventional heterodyne DPSK receiver (Equation (36) of [3.18]), the maximum allowable normalized laser linewidth is approximately 0.36%. This for an optimal signal processing in all branches of the {3x3} phase diversity receiver depicted in Figure 3.1a, and comprising shot noise and phase noise only.

3.5 Discussion

The maximum allowable linewidths for both receivers have been derived for a IF filter matched to the signal, and it was assumed to have negligible influence on the laser phase noise. Some comparison with [3.21] reveals that neglecting the influence of IF filtering on the laser phase noise is not significant for DPSK receivers. It is shown that taking into account the IF filtering of laser phase noise leads to a slightly less severe condition for the maximum allowable laser linewidths. This has been calculated to increase by maximal a factor of 1.5. With this in mind, we expect an equal relaxation in the laser linewidth requirements for the {3x3} phase and polarization diversity DPSK receiver. It should be noticed that polarization diversity has no influence on the position of the BER floor. This can be concluded from the fact, that for significant laser phase noise and large SNR's the phase and polarization diversity DPSK receiver approaches the performance of the heterodyne DPSK receiver.

3.6 Sensitivity degradation of polarization diversity receivers due to non-ideal polarization beamsplitters

In non-ideal polarization beamsplitters (PBS's) a certain percentage of overcoupling of the power in both orthogonal polarization states takes

place. However, a conversion of polarization from one state into the other is not to be expected. In the (3x3) phase and polarization diversity DPSK receiver discussed in the preceding sections, two PBS's are used. One is applied to split up equally the power of the local oscillator laser (P_L) into two orthogonal polarization states. The second PBS is required to split up the power of the optical signal received (P_S) into two, usually not equally divided, orthogonal polarization states.

For two ideal PBS's (in Figure 3.2), the decomposition of the SOP of the local oscillator light and the optical signal received into orthogonal polarization states can be written as

$$B_{11} : 2P_S(1-k).\bar{e}_h \,, \qquad B_{12} : 2P_S k.\bar{e}_v \,,$$

$$B_{21} : P_L.\bar{e}_h \,, \qquad B_{22} : P_L.\bar{e}_v \,, \tag{3.63}$$

where $\bar{e}_h$ and $\bar{e}_v$ are the unit vectors of the horizontal and vertical polarization state, respectively. B_{1i} represents the i^{th} output branch of the PBS splitting the power P_S, and B_{2i} denotes the i^{th} output branch of the PBS splitting the power P_L (i = 1,2). The factors k and (1-k) are the relative amounts by which the signal power is split up into the vertical and horizontal polarization state.

For PBS's with polarization overcoupling, the splitting of the local oscillator power and the signal power received into two orthogonal polarization states can be written as

$$B_{11} : 2(1-k)P_S(1-\beta).\bar{e}_v + 2k\beta P_S.\bar{e}_h \,, \qquad B_{12} : 2(1-k)\beta P_S.\bar{e}_v + 2kP_S(1-\beta).\bar{e}_h \,,$$

$$B_{21} : P_L(1-\alpha).\bar{e}_v + \alpha P_L.\bar{e}_h \,, \qquad B_{22} : \alpha P_L.\bar{e}_v + (1-\alpha)P_L.\bar{e}_h \,, \tag{3.64}$$

where α and β are the percentages of power overcoupling between both orthogonal polarization states in the PBS's used. B_{1i} represents the i^{th} output of the PBS splitting the power P_S, and B_{2i} denotes the i^{th} output of the PBS splitting the power P_L (i = 1,2). The output powers of the branches

B_{11} and B_{21} mix at the IF stage of phase diversity receiver *I* (Figure 3.2). The output powers of the branches B_{12} and B_{22} mix at the IF stage of phase diversity receiver *II* (Figure 3.2). Remind, that the orthogonal polarization components do not mix constructively.

The average number of signal photons/bit received by the phase diversity receiver *I* which processes the vertically polarized signal components, can then be calculated to read

$$N_v = \frac{2P_S R[(1-\alpha)(1-\beta)(1-k) + k\alpha\beta]}{eB} . \tag{3.65}$$

The average number of signal photons/bit received for the phase diversity receiver *II* which processes the horizontally polarized signal components, is then given by

$$N_h = \frac{2P_S R[(1-\alpha)(1-\beta)k + (1-k)\alpha\beta]}{eB} . \tag{3.66}$$

Since N_h and N_v are the mean values of two independent processes and besides, the PBS's are assumed to be lossless, the total average number of signal photons/bit received is given by the sum of N_h and N_v. The total average number of signal photons/bit, N_{total}, then reads

$$N_{total} = \frac{2RP_S[(1-\alpha)(1-\beta) + \alpha\beta]}{eB} . \tag{3.67}$$

In this case of matched IF filtering, Equation (3.67) can be interpreted as the SNR of the (3x3) phase and polarization diversity DPSK receiver. According to reference [3.22], a typical percentage of polarization overcoupling is about 2%, and it is reasonable to assume that $\alpha = \beta$. The introduced sensitivity degradation for the (3x3) phase and polarization diversity DPSK receiver can then be calculated to be approximately 0.18 dB. In Figure 3.6 the degradation in receiver sensitivity (in terms of SNR) as a function of the percentage of polarization overcoupling between the orthogonal polarization states in the PBS's used, is depicted for $\alpha = \beta$ varying from 0

to 100%.

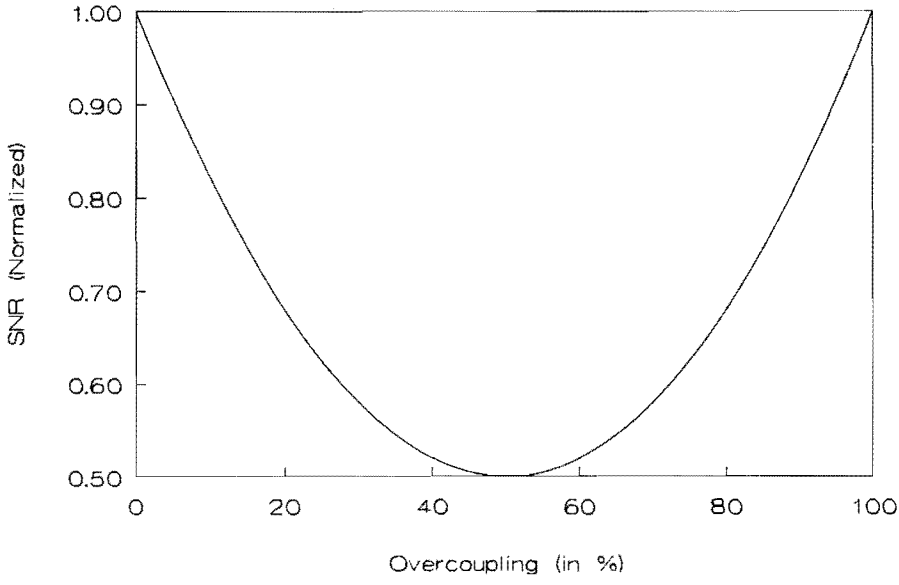

Figure 3.6 *Degradation in SNR of a {3x3} phase and polarization diversity receiver due to polarization overcoupling in the polarization beamsplitters.*

The impact of polarization overcoupling between the orthogonal polarization states has been analyzed for the {3x3} phase and polarization diversity DPSK receiver discussed in the previous sections. However, the results are valid for every polarization diversity receiver using two PBS's, and comprising shot and phase noise only.

3.7 Comparison of phase and polarization diversity ASK, DPSK, and CPFSK receivers with respect to the allowable laser phase noise

In this section, ASK, DPSK and CPFSK demodulation methods are compared in terms of maximum allowable laser phase noise for various receiver configurations,

- the {2x2} phase and polarization diversity ASK, DPSK and CPFSK, and
- the {3x3} phase and polarization diversity ASK, DPSK and CPFSK.

For nonzero laser linewidths, the phase and polarization diversity schemes are not included in the comparison, since they perform very similar as the phase diversity schemes, especially for greater laser linewidths [3.23]. For $\Delta\nu T_0 \cong 0$, the phase and polarization diversity schemes are less sensitive than the phase diversity scheme (penalty < 1 dB). For reasons of comparison, some results have been quoted from literature.

ASK modulation

For the shot noise limited case, the number of photons/bit (N) required to obtain the value of BER equal to 10^{-9} are given in Table 3.1 for various ASK demodulation schemes [3.2]. Notice that the values of N for the ASK schemes are average values, i.e. they also include the case in which a space is sent.

TABLE 3.1

Average number of photons/bit to obtain BER = 10^{-9} for various ASK receivers.

Ideal heterodyne ASK receiver	36
Phase diversity ASK receivers	
{2x2} receiver with squarers	38
{3x3} receiver with squarers	40
Phase and polarization diversity ASK receivers	
{2x2} receiver with squarers	41
{3x3} receiver with squarers	42.5

The impact of the laser phase noise and the influence of IF filtering on the performance of the ASK receivers can conveniently be visualized by studying

the IF power spectrum. We assume a Lorentzian laser lineshape (Chapter 2)

$$S_L(\nu) = \frac{\Delta\nu}{2\pi[(\Delta\nu/2)^2 + (\nu-\nu_0)^2]} , \tag{3.68}$$

where ν_0 is the resonant frequency, and $\Delta\nu$ is the sum of the linewidths of both lasers. If the intersymbol interference may be neglected, the power spectrum of the signal at the input of the IF filter is given by the following convolution

$$\Omega(\nu) = S_L(\nu) * S_M(f) , \tag{3.69}$$

where $S_M(f)$ is the modulation spectrum. In case of ASK modulation $S_M(f)$ is given by [3.24]

$$S_M(f) = \frac{A^2}{16}\left(\delta(f-f_c) + \delta(f+f_c) + \frac{\sin^2(\pi T_0(f-f_c))}{\pi^2 T_0(f-f_c)^2} + \frac{\sin^2(\pi T_0(f+f_c))}{\pi^2 T_0(f+f_c)^2}\right) , \tag{3.70}$$

where A is a constant, and f_c represents the carrier frequency. Equation (3.69) implies that when $\Delta\nu$ increases, the power spectrum $\Omega(f)$ of the signal at the input of the IF filter broadens. Consequently the bandwidth (B_{IF}) of the IF filter should be increased in order to accommodate the same amount of signal power as in case without laser phase noise. However, this also increases the (shot) noise bandwidth, and therefore, results in a sensitivity penalty. The loss in receiver sensitivity (SNR) due to the increase of the noise bandwidth, is depicted in Figure 3.7 versus the normalized laser linewidth $\Delta\nu T_0$. This for a in the frequency domain rectangular IF filter, which passes 95% of the incoming signal power.

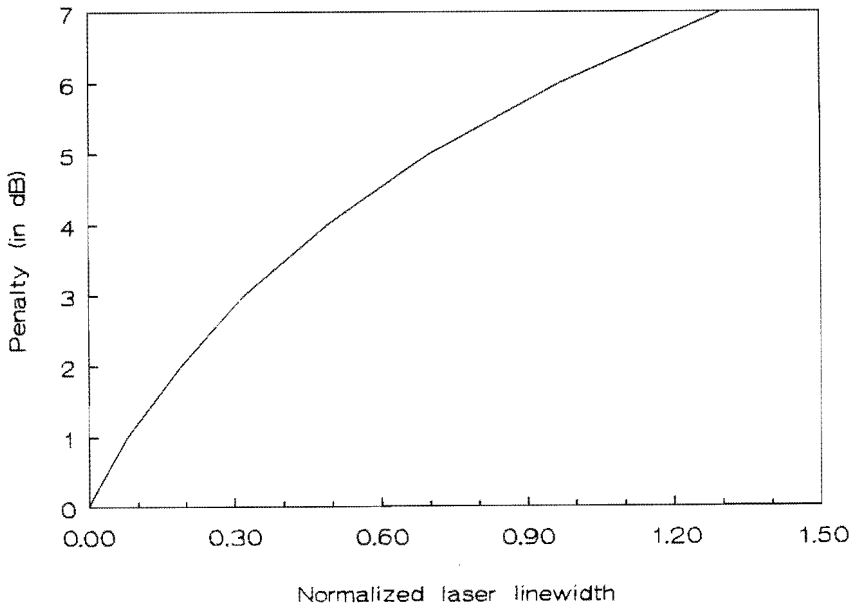

Figure 3.7 *Loss of SNR versus the normalized laser linewidth* $\Delta\nu T_0$.

When large IF filter bandwidths are used in ASK receivers to overcome the spectrum broadening due to laser phase noise, a post-detection filter, with a bandwidth much smaller than the IF filter bandwidth, is usually applied to improve the receiver sensitivity [3.4]. By matching of the IF filter and the post-detection filter, an optimal IF filter bandwidth can be found for which the sensitivity degradation is minimal. Further increasing of the bandwidth results in an excess sensitivity degradation, since too much (shot) noise is passed. On the other hand, if the IF filter bandwidth is too small, a BER floor seriously degrades the receiver performance, due to the conversion of laser phase noise into intensity noise and vice versa (Chapter 2). For ASK systems the BER floor depends on the relation between the normalized IF filter bandwidth ($B_{IF}T_0$) and the normalized laser linewidth ($\Delta\nu T_0$). The larger $B_{IF}T_0$, the lower the BER floor.

For optimized IF and post-detection filtering, phase diversity ASK receivers have the same phase noise performance as heterodyne ASK receivers, and they can tolerate the same amount of laser phase noise [3.25-3.27]. For ASK

receivers, the sensitivity penalty, due to laser phase noise versus the normalized laser linewidth, is given in Figure 3.8 for a BER = 10^{-9}, and optimized IF and post-detection filtering [3.26,3.27].

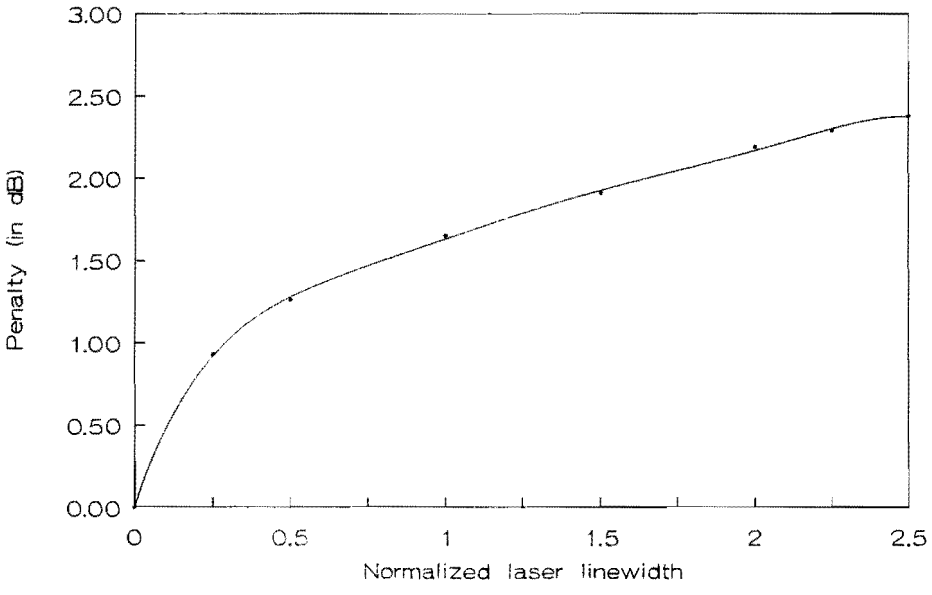

Figure 3.8 *Sensitivity penalty versus* $\Delta\nu T_0$ *for ASK receivers (BER =* 10^{-9}*).*

DPSK modulation

For zero linewidth conditions, the number of photons/bit required to obtain the value of BER equal to 10^{-9} for various (D)PSK demodulations schemes is given in Table 3.2.

TABLE 3.2

Average number of photons/bit to obtain BER = 10^{-9} for various DPSK receivers.

Ideal heterodyne PSK receiver	18
Phase diversity DPSK receivers	
{2x2} receiver	20
{3x3} receiver	21
Phase and polarization diversity DPSK receivers	
{2x2} receiver	22
{3x3} receiver	24

The shape of the modulation spectrum $S_M(f)$ of the DPSK signal and the ASK signal is similar. The only difference is that the DPSK modulation spectrum has no impulses at the carrier frequency. Therefore, as for ASK modulation, laser phase noise results in a broadening of the IF power spectrum (Equation (3.69)). For nonnegligible laser linewidths in ASK systems, significant improvement in receiver sensitivity can be obtained by optimal matching of the IF and post-detection filter. However, for DPSK systems the linewidth requirements are much more severe than for ASK systems, typically less than 0.5%. For this reason, the maximum allowable broadening of the spectrum at the input of the IF filter is insignificant. Therefore, increasing the IF bandwidth in order to accommodate broader laser linewidths as for ASK systems has no sense for error rates of interest and does not lower the BER floor [3.17]. By optimal matching of the IF filter and post-detection filter in DPSK systems, only little is gained in terms of tolerance to laser phase noise [3.17].

CPFSK modulation

For zero linewidth conditions, the number of photons/bit required to obtain the value of BER equal to 10^{-9} is given in Table 3.3 for various Continuous

Phase Frequency Shift Keying (CPFSK) demodulation schemes [3.28].

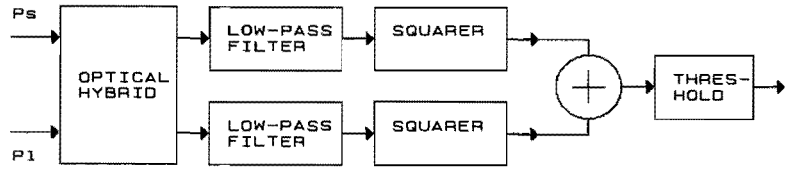

(a)

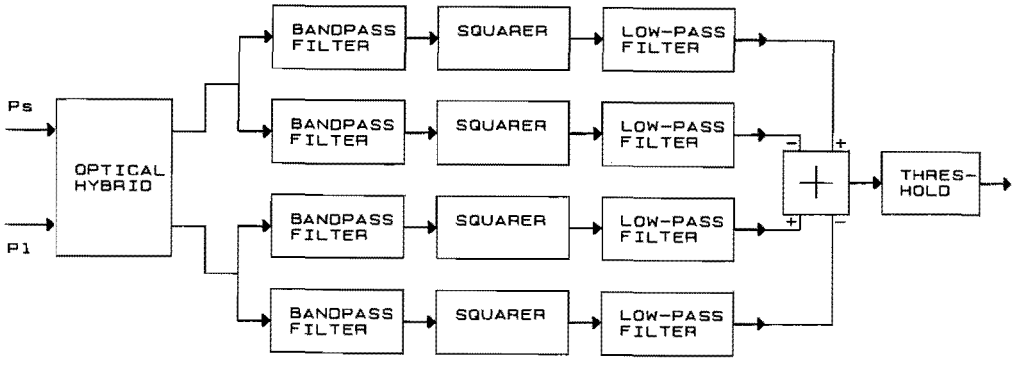

(b)

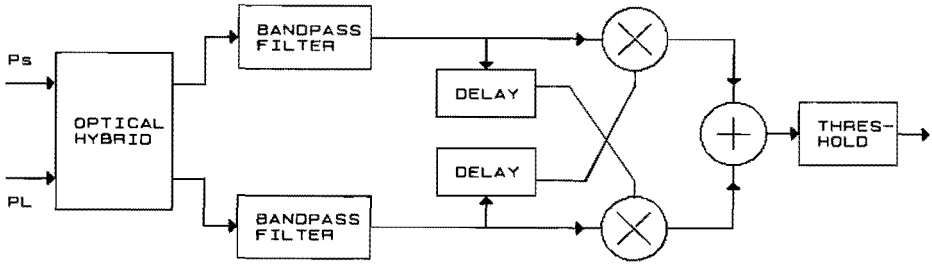

(c)

Figure 3.9 *Different methods of demodulation of CPFSK signals*

(a) single filter,

(b) dual filter, and

(c) delay-and-multiply.

TABLE 3.3

Average number of photons/bit to obtain BER = 10^{-9} for various CPFSK receivers.

	Single-filter	Dual-filter	Delay
Ideal heterodyne CPFSK receiver	72	36	18
Phase diversity CPFSK receivers			
{2x2} receiver	76	44	20
{3x3} receiver	80	46.5	18.5
Phase and polarization diversity CPFSK receivers			
{2x2} receiver	82	–	22
{3x3} receiver	85	–	19.5

The single-filter demodulation scheme (Figure 3.9a) is for the same peak power (mean power twice as large) conditions, fully equivalent to the ASK demodulation scheme [3.2,3.28]. During transmission of for example a mark, the frequencies of the local oscillator and the transmitting laser are set equal, and the spectrum is shifted to baseband. For transmitting a space the spectrum is swept out of baseband for a sufficient large modulation index.

The dual-filter demodulation scheme (Figure 3.9b) is more power efficient than the single-filter demodulation scheme, and the heterodyne CPFSK and ASK receiver have equal performance [3.29]. The modulation index is chosen large enough to avoid overlapping of the spectra corresponding to a mark and a space. There are two bandpass filters for each branch, each of them tuned to the frequency of the corresponding symbol. Notice that using the dual-filter scheme in combination with phase diversity reception has little sense, since one of the main advantages, namely the baseband signal processing, is lost.
In the delay-and-multiply demodulation scheme (Figure 3.9c), the frequency offset between the local oscillator and the transmitting laser can be taken

zero. The symbols space and mark occupy the same baseband spectrum. They may be distinguished only after the delay and multiply technique [3.28,3.30].

From the Tables 3.1 and 3.3 it can be concluded that for the shot noise limited case, the single-filter demodulation scheme is fully equivalent to the ASK demodulation scheme for a mean power twice as large. Besides, the {2x2} phase (and polarization) diversity CPFSK delay-and-multiply receiver has the same performance as a similar DPSK receiver. For nonnegligible laser linewidths, it is shown in reference [3.28], that a great advantage of CPFSK over DPSK is that by increasing the modulation index, which also implies greater bandwidth, it can handle substantially large laser linewidths. For DPSK receivers, little can be done to accommodate large laser linewidths. The delay-and-multiply demodulation scheme is superior over the dual-filter demodulation scheme for $\Delta\nu T_0 < 4\%$.

3.8 Conclusions

We choose as criterion for the maximum allowable laser linewidth in the coherent receivers analyzed, that linewidth which increases the signal power (P_s) required for the receiver to achieve a BER = 10^{-9} by maximal 1.0 dB. From Figure 3.4 it can then be concluded that the {3x3} phase and polarization diversity DPSK receiver can tolerate normalized laser linewidths of the same order as the conventional heterodyne DPSK receiver, namely approximately 0.46% and 0.36%, respectively. This implies that phase diversity reception of DPSK signals, in comparison with heterodyne reception, does not significantly increase the maximum allowable laser linewidth. However, the phase noise correlation at the IF stages of the DPSK receiver cancels to some extend the influence of nonzero laser linewidths, but does not shift the BER floor. For optical coherent DPSK receivers it is shown in [3.21], that optimal IF filtering of the laser phase noise results in a small relaxation of the laser linewidths requirements by maximal a factor 0.68.
Further, it is shown that it is possible to compensate for the influence of polarization fluctuations by using polarization diversity techniques. The {3x3} phase and polarization diversity reception of DPSK signals introduces a signal power penalty with respect to the ideal heterodyne DPSK receiver of

approximately 0.7 dB for a BER = 10^{-9}, in the shot noise limited case. For nonzero laser linewidths the performance of the {3x3} phase and polarization diversity DPSK receiver approaches the performance of the conventional heterodyne DPSK receiver for large SNR's.

It is shown, that for a typical value of polarization overcoupling of 2% in polarization beamsplitters, the degradation in receiver sensitivity (SNR) is about 0.18 dB. Therefore, polarization overcoupling can usually be neglected in practical polarization diversity receivers. This polarization overcoupling has only influence on the sensitivity of the receiver. The polarization insensitive operation of the receiver remains unaffected.

Appendix 3

Calculation of the BER of a heterodyne DPSK receiver for nonzero laser linewidths

We can model the photocurrent as a narrowband signal plus a noise signal, since i(t) is a narrowband process with a spectrum centered on ω_{IF}, the intermediate radial frequency. The photocurrent then reads

$$i(t) = S(t).\cos(\omega_{IF}t + \phi(t)) + x(t).\cos(\omega_{IF}t) - y(t).\sin(\omega_{IF}t) \ , \qquad \text{(A3.1)}$$

where x(t) and y(t) are, relative to the radial frequency ω_{IF}, slowly varying functions of time. They have zero mean Gaussian probability density functions since the shot noise is assumed to be Gaussian distributed [3.16]. For the amplitude S(t) we can calculate

$$S(t) = R\sqrt{P_L P_S}.b(t) \ . \qquad \text{(A3.2)}$$

The phase difference is given by

$$\Delta\Phi \triangleq \phi(t) - \phi(t-T) \ , \qquad \text{(A3.3)}$$

and it is assumed to have a Gaussian probability density function with zero mean and variance σ_Φ^2. We can rewrite Equation (A3.1) in terms of the phase difference by making use of some analytical identities. For the narrowband noise components in Equation (A3.1), we can calculate

$$\begin{aligned} &x(t).\cos(\omega t) - y(t).\sin(\omega t) \\ &= \{x(t).\cos\phi(t-T) + y(t).\sin\phi(t-T)\}.\cos(\omega t + \phi(t-T)) - \\ &\{-x(t).\sin\phi(t-T) + y(t).\cos\phi(t-T)\}.\sin(\omega t + \phi(t-T)) \\ &= x'(t).\cos(\omega t + \phi(t-T)) - y'(t).\sin(\omega t + \Phi(t-T)) \ , \end{aligned} \qquad \text{(A3.4)}$$

where

$$x'(t) \triangleq x(t).\cos\phi(t-T) + y(t).\sin\phi(t-T) ,$$

and (A3.5)

$$y'(t) \triangleq -x(t).\sin\phi(t-T) + y(t).\cos\phi(t-T) .$$

The signal component of Equation (A3.1) can be calculated to give

$$S(t).\cos(\omega t + \phi(t-T))$$
$$= S(t)\{\cos(\omega t + \phi(t-T)).\cos\Delta\Phi(t) - \sin(\omega t + \phi(t-T)).\sin\Delta\Phi(t)\} . \quad (A3.6)$$

Substitution of Equation (A3.4) and (A3.6) in Equation (A3.1) results in the following relation for the photocurrent

$$i(t) = \{S(t).\cos\Delta\Phi(t) + x'(t)\}.\cos(\omega t + \phi(t-T)) -$$
$$\{S(t).\sin\Delta\Phi(t) + y'(t)\}.\sin(\omega t + \phi(t-T)) . \quad (A3.7)$$

For the delayed version of the photocurrent can be calculated in the similar way

$$i(t-T) = \{S(t-T) + x'(t-T)\}.\cos(\omega t + \phi(t-T)) -$$
$$y'(t-T).\sin(\omega t + \phi(t-T)) . \quad (A3.8)$$

For the output voltage v(t) at the output of the low-pass filter is found

$$v(t)_{LPF} = \{c.i(t).i(t-T)\}_{LPF}$$

$$= 0.5\{S(t).S(t-T).\cos\Delta\Phi(t) + S(t).x'(t-T).\cos\Delta\Phi(t) +$$
$$x'(t).S(t-T) + x'(t).x'(t-T)\} +$$
$$0.5\{S(t).y'(t-T).\sin\Delta\Phi(t) + y'(t).y'(t-T)\}$$

$$= \frac{1}{8}c\{R_1^2 - R_2^2\} , \quad (A3.9)$$

where

$$R_1^2 = \{S(t).\cos\Delta\Phi(t) + S(t-T) + x'(t) + x'(t-T)\}^2 + \{S(t).\sin\Delta\Phi(t) + y'(t) + y'(t-T)\}^2 ,$$

$$R_2^2 = \{S(t).\cos\Delta\Phi(t) - S(t-T) + x'(t) - x'(t-T)\}^2 + \{S(t).\sin\Delta\Phi(t) + y'(t) - y'(t-T)\}^2 , \qquad \text{(A3.10)}$$

and c is a constant .

A decision error is made in two different situations, both assumed to have equal probability, namely when

1. $S(t) = S(t-T)$ and $v(t) < 0$, and
2. $S(t) = -S(t-T)$ and $v(t) > 0$.

Assume

1. $S(t) = S$,
2. the phase difference $\Delta\Phi(t) = \Delta\Phi$, implying that the phase change is negligible within one bit time T_0, and
3. no intersymbol interference.

Under those conditions we rewrite Equation (A3.10) to give

$$R_1^2 = \{S[\cos\Delta\Phi + 1] + x'(t) + x'(t-T)\}^2 + \{S.\sin\Delta\Phi + y'(t) + y'(t-T)\}^2 ,$$

and

$$R_2^2 = \{S[\cos\Delta\Phi - 1] + x'(t) - x'(t-T)\}^2 + \{S.\sin\Delta\Phi + y'(t) - y'(t-T)\}^2 . \qquad \text{(A3.11)}$$

From Equation (A3.11) it can be concluded that R_1 and R_2 are envelopes, whose probability density functions are Rician distributed under the conditions inflicted [3.16]. The envelopes can be written as

$$R_1 = \sqrt{[A_1 + x''(t)]^2 + y''(t)^2} \ , \qquad \text{(A3.12)}$$

and

$$R_2 = \sqrt{[A_2 + x^*(t)]^2 + y^*(t)^2} \ , \qquad \text{(A3.13)}$$

where

$$x''(t) \triangleq x'(t) + x'(t-T) \ ,$$
$$y''(t) \triangleq y'(t) + y'(t-T) \ ,$$

and

$$x^*(t) \triangleq x'(t) - x'(t-T) \ ,$$
$$y^*(t) \triangleq y'(t) - y'(t-T) \ .$$

The noncentral parameter $A_1^2 \triangleq \langle R_1^2 \rangle$ can be calculated to be

$$A_1 = \sqrt{S^2[\cos\Delta\Phi + 1]^2 + S^2\sin^2(\Delta\Phi)} = 2S.\left|\cos(\frac{\Delta\Phi}{2})\right| \ , \qquad \text{(A3.14)}$$

and the noncentral parameter $A_2^2 \triangleq \langle R_1^2 \rangle$ can be derived to be

$$A_2 = \sqrt{S^2[\cos\Delta\Phi - 1]^2 + S^2\sin^2(\Delta\Phi)} = 2S.\left|\sin(\frac{\Delta\Phi}{2})\right| \ . \qquad \text{(A3.15)}$$

The BER for shot noise limited conditions can now be given by the following equation

$$BER = P(R_1 < R_2) = \int_0^\infty P(R_1).\int_{R_1}^\infty P(R_2)\, dR_1.dR_2 \ , \qquad \text{(A3.16)}$$

where

$$P(R_i) = \frac{R_i}{\sigma_i^2}.I_0\left[\frac{A_i R_i}{\sigma_i^2}\right].\exp\left[-\frac{R_i^2 + A_i^2}{2\sigma_i^2}\right] \ . \qquad \text{for } i = 1,2 \qquad \text{(A3.17)}$$

For the BER, including phase noise we can calculate ($\sigma_1^2 = \sigma_2^2 = 2\sigma^2$)

$$BER = \frac{1}{\sqrt{2\pi}\sigma_\Phi} \int_{-\infty}^{\infty} \exp\left[-\frac{\Delta\Phi^2}{2\sigma_\Phi^2}\right] . \int_0^{\infty} \frac{R_1}{2\sigma^2} . I_0\left[\frac{A_1 R_1}{2\sigma^2}\right] \exp\left[-\frac{R_1^2 + A_1^2}{4\sigma^2}\right] \times$$

$$\int_{R_1}^{\infty} \frac{R_2}{2\sigma^2} . I_0\left[\frac{A_2 R_2}{2\sigma^2}\right] \exp\left[-\frac{R_2^2 + A_2^2}{4\sigma^2}\right] d\Delta\Phi . dR_1 . dR_2 \quad . \tag{A3.18}$$

After substitution of

$$\gamma = \frac{S}{2\sigma^2} , \qquad t = \frac{R_1}{2\sigma} ,$$

$$s = \frac{\Delta\Phi}{\sqrt{2}\sigma_\Phi} , \qquad u = \frac{R_2}{2\sigma} , \tag{A3.19}$$

we can recalculate Equation (A3.18) to give

$$BER = \frac{4}{\sqrt{\pi}} \int_{-\infty}^{\infty} e^{-s^2} . \int_0^{\infty} t I_0[2\alpha t] \exp[-(t^2 + \alpha^2)] \times$$

$$\int_t^{\infty} u I_0[2\beta t] \exp[-(u^2 + \beta^2)] \, ds . dt . du \quad , \tag{A3.20}$$

where

$$\alpha = \sqrt{2\gamma} . \cos\left(\frac{\Delta\Phi}{2}\right) , \tag{A3.21}$$

and

$$\beta = \sqrt{2\gamma} . \sin\left(\frac{\Delta\Phi}{2}\right) . \tag{A3.22}$$

For $\sigma_\Phi = 0$, we can calculate Equation (A3.20) to give

$$BER = 2 \int_0^{\infty} tI_0[2\alpha t] \exp-[2t^2 + \alpha^2] \, dt \; . \qquad \text{(A3.23)}$$

References

[3.1] A.W. Davis, M.J. Pettitt, J.P. King and S. Wright, "Phase diversity techniques for coherent optical receivers",
J. Lightwave Technol., vol. 5, no. 4, pp. 561-572, April 1987.

[3.2] J. Siuzdak and W. van Etten, "BER evaluation for phase and polarization diversity optical receivers using noncoherent ASK and DPSK demodulation",
J. Lightwave Technol., vol. 7, no. 4, pp. 584-599, April 1989.

[3.3] L.G. Kazovsky, "Phase- and polarization-diversity coherent optical techniques",
J. Lightwave Technol., vol. 7, no. 2, pp. 279-292, Febr. 1989.

[3.4] L.G. Kazovsky, P. Meissner and E. Patzak, "ASK multiport optical homodyne receivers",
J. Lightwave Technol., vol. 5, no. 6, pp. 720-780, June 1987.

[3.5] W.H.C. de Krom, "Impact of laser phase noise on the performance of a {3x3} phase and polarization diversity optical homodyne DPSK receiver",
J. Lightwave Technol., vol. 8, no. 11, pp. 1709-1716, Nov. 1990.

[3.6] I. Garrett and G. Jacobsen, "The effect of laser linewidth on coherent optical receivers with nonsynchronous demodulation",
J. Lightwave Technol., vol. 5, no. 4, pp. 551-560, April 1987.

[3.7] B. Glance, "Polarization independent coherent optical receiver",
J. Lightwave Technol., vol. 5, no. 2, pp. 274-276, Febr. 1987.

[3.8] M. Kavehrad and B. Glance, "Polarization-insensitive FSK optical heterodyne receiver using discriminator demodulation",
J. Lightwave Technol., vol. 6, no. 9, pp. 1386-1394, Sept. 1988.

[3.9] D. Kreit and R.C. Youngquist, "Polarization-insensitive optical heterodyne receiver for coherent FSK modulation",
Electron. Lett., vol. 23, pp. 168-169, 1987.

[3.10] E. Patzak and R. Langenhorst, "Sensitivity degradation of conventional and balanced 3x3 port phase diversity DPSK receivers due to thermal and local oscillator intensity noise",
Electron. Lett., vol. 25, pp. 545-547, 1989.

[3.11] T. Okoshi and Y.H. Cheng, "Four-port homodyne receiver for optical fiber communications comprising phase and polarization diversities", *Electron. Lett.*, vol. 23, pp. 377-378, 1987.

[3.12] H. Kuwahara et al., "New receiver design for practical coherent lightwave transmission systems", *Proc. 12th ECOC* (Barcelona, Spain), pp. 407-410, 1986.

[3.13] S. Stein and J.J. Jones, "Modern communication principles", *McGraw-Hill*, New York, 1965.

[3.14] Y. Cheng, T. Okoshi and O. Ishida, "Performance analysis and experiment of a homodyne receiver insensitive to both polarization and phase fluctuations", *J. Lightwave Technol.*, vol. 7, no. 2, pp. 368-374, Febr. 1989.

[3.15] M. Abramowitz and I. A. Stegun, "Handbook of mathematical functions", *Dover Publications*, New York, 1965.

[3.16] I. Garrett and G. Jacobsen, "Theoretical analysis of heterodyne optical receivers for transmission systems using (semiconductor) lasers with nonnegligible linewidth", *J. Lightwave Technol.*, vol. 4, no. 3, pp. 323-334, March 1986.

[3.17] G. Jacobsen and I. Garrett, "Theory for optical heterodyne DPSK receivers with post-detection filtering", *J. Lightwave Technol.*, vol. 5, no. 4, pp. 478-484, April 1987.

[3.18] K. Kikuchi, T. Okoshi, M. Nagamatsu and N. Henmi, "Degradation of the bit-error rate in coherent optical communications due to the spectral spread of the transmitter and the local oscillator", *J. Lightwave Technol.*, vol. 2, no. 6, pp. 1024-1033, Dec. 1984.

[3.19] T. Okoshi, "Simple formula for bit-error rate in optical heterodyne DPSK systems employing polarization diversity", *Electron. Lett.*, vol. 24, pp. 120-121, 1988.

[3.20] G. Nicholson, "Performance of coherent optical phase diversity receivers with DPSK modulation", *J. Lightwave Technol.*, vol. 7, no. 2, pp. 393-399, Febr. 1989.

[3.21] E. Patzak, P. Meissner, "Influence of IF-filtering on the bit error rate floor in coherent optical DPSK-systems", *IEE Proc.*, vol. 135, pp. 355-357, 1988.

[3.22] Melles Griot, *Optics Guide* 4, 1988.

[3.23] R. Noe, "Sensitivity comparison of coherent optical heterodyne, phase diversity, and polarization diversity receivers",
J. Optical Commun., no. 10, pp. 11-18, 1989.

[3.24] K.S. Shanmugam, "Digital and Analog Communication Systems",
John Wiley & Sons, New York, 1985.

[3.25] L.G. Kazovsky and O.K. Tonguz, "ASK and FSK coherent lightwave systems: a simplified approximate analysis",
J. Lightwave Technol., vol. 8, no. 3, pp. 338-352, March 1990.

[3.26] J. Siuzdak and W. van Etten, "Heterodyne ASK multiport optical receivers using postdetection filtering",
J. Lightwave Technol., vol. 8, no. 1, pp. 71-77, Jan. 1990.

[3.27] G.J. Foschini, L.J. Greenstein and G.V. Vannucci, "Noncoherent detection of coherent lightwave signals corrupted by phase noise",
IEEE Trans. on Commun., vol. 36, no. 3, pp. 306-314, March 1988.

[3.28] J. Siuzdak and W. van Etten, "BER performance for CPFSK phase and polarization diversity coherent optical receivers",
J. Lightwave Technol., vol. 9, no. 11, pp. 1583-1592, Nov. 1991.

[3.29] W. van Etten and J van der Plaats, "Fundamentals of Optical Fiber Communications",
Prentice Hall, New York, 1991.

[3.30] R. Noé et al., "New FSK phase diversity receiver in a 150 Mbit/s coherent optical transmission system",
Electron. Lett., vol. 24, no. 9, pp. 567-568, 1988.

CHAPTER 4.

IMPACT OF LOCAL OSCILLATOR INTENSITY NOISE ON THE PERFORMANCE OF A {2x2} AND {3x3} PHASE DIVERSITY ASK RECEIVER

4.1 Introduction

In the field of optical coherent communication systems, the phase diversity ASK receiver has proved to be tolerant to some of the effects of laser phase noise [4.1-4.3]. For ASK and FSK modulation, laser linewidths of the same order as the bit rate result in only a small degradation of the performance. However, the intensity noise, caused by random fluctuations of the optical power of both the transmitting and local oscillator lasers, has a nonnegligible influence on the performance of optical coherent phase diversity receivers (Chapter 2) [4.4,4.5]. In reference [4.4], the impact of the intensity noise on the performance of the {2x2} and {3x3} phase diversity ASK receivers has been investigated by means of computer simulations. The Probability Density Function (PDF) of the noise process at the input of the threshold comparator was assumed *a priori* to be Gaussian. In this chapter we shall investigate this PDF analytically and show that it differs substantially from Gaussian. The effects of shot noise, thermal noise and intensity noise on the performance of a {2x2} and {3x3} phase diversity ASK receiver have been investigated. Special attention is given to the non-Gaussian statistics of the noise process at the input of the threshold comparator and to the optimal threshold level in dependency of the local oscillator power and intensity noise level. The sensitivity penalty is computed with respect to the performance of an ideal heterodyne ASK receiver in the shot noise limited case for a BER = 10^{-9}. The bit rate is taken to be 150 Mbit/s and the influence of the phase noise is assumed to be negligible, implying zero laser linewidths. Since the local oscillator power is usually much larger than the optical power received from the transmitting laser, only the intensity noise and the shot noise introduced by the local oscillator laser are taken into account. The thermal noise introduced by each preamplifier, depicted in Figure 4.1, is assumed to show a white power spectrum for all

receiver branches. For the sake of clarity, some mathematical derivations are placed in the Appendices 4A and 4B.

4.2 Theory

The block-diagram of the {2x2} and {3x3} phase diversity ASK receiver analyzed is shown in Figure 4.1. It consists of a polarization controller, a {2x2} or {3x3} optical hybrid, photodiodes, low-pass filters, squarers, a summing circuit, and a threshold comparator.

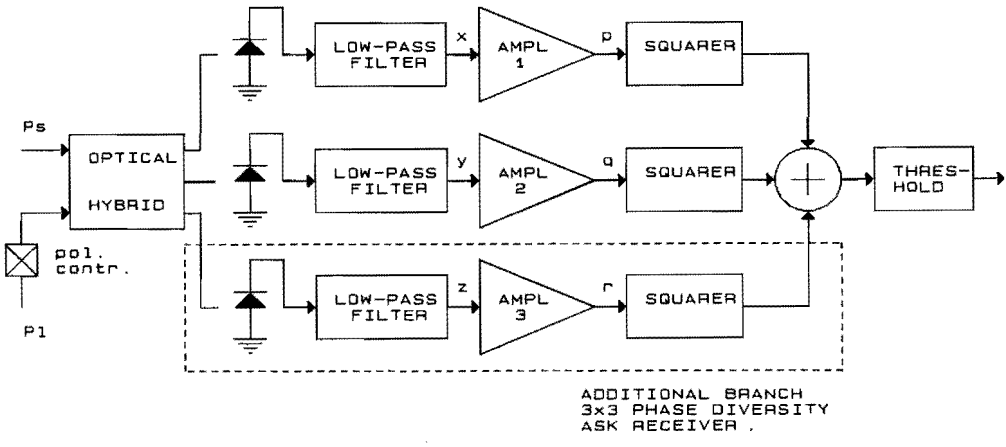

Figure 4.1 *Block-diagram of the optical coherent {2x2} and {3x3} phase diversity ASK receiver.*

The low-pass filtered photocurrent for each receiver branch is given by [4.4,4.6]

$$i_j(t) = \frac{2}{N}R\sqrt{P_L P_S}.b(t).\cos[f_j(t)] + i_{JS}(t) + i_{JT}(t) + i_{JR}(t), \qquad (4.1)$$

where

$j = 1,2,\ldots,N$ (N is the number of receiver branches),

$f_j(t) = \frac{\pi}{2}(j - 1) + \phi(t)$ for the {2x2} phase diversity ASK receiver,

$f_j(t) = \frac{2\pi}{3}(j - 1) + \phi(t)$ for the {3x3} phase diversity ASK receiver.

The local oscillator power is given by P_L, and P_S is the optical signal power received. The function b(t) represents the signaling waveform, which is modeled as the digital baseband signal $b(t) = \sum_k b_k.\mathrm{rect}(t-kT_0)$, where T_0 is the bit time. In case of ASK modulation, b_k takes the values 0 or 1. $\phi(t)$ is the phase offset between the local oscillator and the transmitting laser, and it also includes the frequency offset. R is the responsivity of the photodiodes used. The term $i_{jS}(t)$ represents the shot noise in the j^{th} branch, $i_{jT}(t)$ is the thermal noise in the j^{th} branch, and $i_{jR}(t)$ is the intensity noise in the j^{th} branch. The intensity noise in the receiver structures analyzed is assumed to have a Gaussian statistic, a flat power spectrum, and zero mean. The local oscillator intensity noise power (variance) at the IF stage, for each receiver branch, is given by

$$\sigma_R^2 = \frac{1}{2}\left[R \frac{P_L}{N} \right]^2 \gamma B \ , \tag{4.2}$$

where the local oscillator Relative Intensity Noise (RIN) is given by

$$\mathrm{RIN} = 10.\log \gamma \qquad \text{in dB/Hz} \ , \tag{4.3}$$

and B represents the double-sided receiver noise bandwidth. The RIN is actual amplitude noise and for this reason, in case of perfectly balanced receiver branches, each branch is corrupted by identical intensity noise components. This implies that the sample functions of the intensity noise process in each receiver branch are identical. The shot and thermal noise are assumed to be statistically independent and it is reasonable to assume that they have Gaussian statistics, a flat power spectrum, and zero means. The shot noise power plus the thermal noise power at the IF stage, for each receiver branch, is given by

$$\sigma^2 = \left[eR \frac{P_L}{N} + \frac{\langle i_{th}^2 \rangle}{2} \right] B \ . \tag{4.4}$$

Here $\langle i_{th}^2 \rangle$ represents the thermal noise spectral density of the preamplifier at the IF stage, which is taken to be equal to 9.10^{-24} A^2/Hz for each amplifier in both receiver structures ($\sqrt{\langle i_{th}^2 \rangle}$ = 3 pA/$\sqrt{Hz}$ is a practical

value [4.4]), and e is the electron charge.

For mathematical convenience, it will be easier if we normalize the total noise contribution $(\sigma^2 + \sigma_R^2)$ to unity noise variance in each receiver branch. This does not influence the BER characteristics, since it is equivalent to division by a constant. The values of the signals can be rewritten in terms of the SNR, and are given by

$$s_k(t) = \sqrt{2SNR}.b(t).\cos[\phi(t) + k\frac{\pi}{2}] , \qquad k = 0,1 \qquad (4.5)$$

for the {2x2} phase diversity ASK receiver. For mathematical convenience, the SNR is defined to be equal to

$$SNR \triangleq \frac{R^2 P_L P_S}{eRP_L B + \langle i_{th}^2 \rangle B + (RP_L/2)^2 \gamma B} , \qquad (4.6)$$

and B denotes the double-sided noise bandwidth of the low-pass filters, which are assumed to pass all the signal power. The intersymbol interference is assumed to be absent. Since the laser linewidths are assumed to be zero, the filter matched to the signal rect(t) may be applied (Chapter 3) [4.6]. Its impulse response is given by

$$h(t) = \begin{cases} 1/T_0 & \text{for } 0 < t < T_0 , \\ 0 & \text{elsewhere,} \end{cases} \qquad (4.7)$$

implying a double-sided noise bandwidth B of $1/T_0$.

For unity noise variance the values of the signals at the IF stage of the {3x3} phase diversity ASK receiver can be given by

$$s_k(t) = \frac{2}{\sqrt{3}}\sqrt{SNR}.b(t).\cos[\Phi(t) + \frac{2}{3}k\pi] , \qquad k = 0,1,2 \qquad (4.8)$$

where the SNR is defined as

$$SNR \triangleq \frac{\frac{2}{3}R^2 P_L P_s}{\frac{2}{3}eRP_L B + \langle i_{th}^2 \rangle B + (RP_L/3)^2 \gamma B} . \qquad (4.9)$$

If $P(b_k = 0) \triangleq p_0$ and $P(b_k = 1) \triangleq p_1 = 1 - p_0$, the BER is determined by the following relation

$$BER = p_0.P(V_{sample} > T | b_k = 0) + p_1.P(V_{sample} \leq T | b_k = 1) . \qquad (4.10)$$

Here V_{sample} is the realization of the process at the input of the threshold comparator at the sampling moment. T represents the threshold level, which for optimal sensitivity should be chosen as a function of the local oscillator power P_L and the RIN. $P_0 = P(V_{sample} > T | b_k = 0)$ is the probability that a mark is received, whereas a space is sent, and $P_1 = P(V_{sample} \leq T | b_k = 1)$ represents the probability that a space is received, whereas a mark is sent.

4.3 The (2x2) phase diversity ASK receiver

In case a space ($b_k = 0$) is sent, the Probability Density Function (PDF) of the process at the input of the threshold comparator is that of the sum of two squared Gaussian variables $i_1(t)$ and $i_2(t)$, respectively (Equation (4.1)), which have zero means. Each variable $i_1(t)$ and $i_2(t)$ consists of the sum of three Gaussian variables, indicating the shot noise current, the thermal noise current, and the local oscillator RIN current. They have zero means, unity total normalized noise power and are assumed to be statistically independent. The latter is in contrast to the contributions of the RIN in both receiver branches which are identical. Therefore, the shot noise and the thermal noise contributions in the different receiver branches are incoherent, whereas the RIN contributions are coherent.

Provided a space is sent, a detection error occurs if the value of V_{sample} at the sampling moments exceeds the threshold level (T). If the threshold level (T) is defined to be $2k^2SNR$ and k is the parameter to be optimized,

the conditional error probability P_0 is given by the following equation

$$P_0 = \int_T^{\infty} f_0(y)\, dy \ , \tag{4.11}$$

where $f_0(y)$ can be calculated to be (see Appendix 4A for details)

$$f_0(y) = \frac{(1+\delta)}{2\sqrt{(1+2\delta)}} . \exp\left[- \frac{y(1+\delta)^2}{2(1+2\delta)} \right] . I_0\left[\frac{\delta(1+\delta)y}{2(1+2\delta)} \right] \ . \tag{4.12}$$

Here the parameter δ is defined to be

$$\delta \triangleq \frac{\sigma_R^2}{\sigma^2} = \frac{\frac{1}{4}(RP_L)^2\gamma}{eRP_L + \langle i_{th}^2 \rangle} \ , \tag{4.13}$$

and $I_0[.]$ is the modified Bessel function of the first kind and zero order. When a mark ($b_k = 1$) is sent, a detection error occurs if V_{sample} at the sampling moments is less than the threshold level (T). V_{sample} is equal to the realization of $i_1^2 + i_2^2$ (Equation (4.1)), which has a nonzero mean. The expression for this conditional error probability has been calculated in Appendix 4A. It is shown, that the introduction of the RIN introduces a time varying character of the BER, depending on $\phi(t)$ (Equation (4.1)). In view of the long formulas, here and in the Appendices, we write $\phi(t)$ as ϕ. The average conditional bit error probability $\langle P_1 \rangle$ can then be calculated to give

$$\langle P_1 \rangle = \frac{1}{2\pi} \int_0^{2\pi} P_1(\phi)\, d\phi =$$

$$\frac{(1+\delta)}{4\pi^2\sqrt{(1+2\delta)}} \int_0^{2\pi} . \iint_V r . \exp\left[- \frac{(1+\delta)\{r^2 - 2r(s_0(\phi)\cos\vartheta + s_1(\phi)\sin\vartheta) + 2SNR\}}{2} \right] \times$$

$$\exp\left[\frac{\delta(1+\delta)[r(\cos\vartheta + \sin\vartheta) - \{s_0(\phi) + s_1(\phi)\}]^2}{2(1+2\delta)} \right] dr . d\vartheta . d\phi \ . \tag{4.14}$$

The final BER of the (2x2) phase diversity ASK receiver, can now be obtained by substitution of the Equations (4.11) and (4.14) in Equation (4.10).
Assuming $p_0 = 1/2$, the parameter k is chosen to minimize the BER as a function of P_L and the corresponding RIN. This is equal to the condition of jointly minimizing Equation (4.11) and (4.14). An optimum value for k results in equal values for the conditional error probabilities P_0 and P_1. The latter implies that the BER is independent of the bit sequence. The Equations (4.10), (4.11) and (4.14) have been analyzed numerically to determine the signal power (P_S) required to achieve a BER = 10^{-9} as a function of the local oscillator power, the local oscillator RIN, and the (optimal) threshold level (T). The sensitivity penalty is calculated with respect to the ideal heterodyne ASK receiver for three practical RIN levels, -150, -135, and -125 dB/Hz, respectively. The curves are depicted in Figure 4.2 and show an optimum value for P_L for which the sensitivity penalty is minimal.

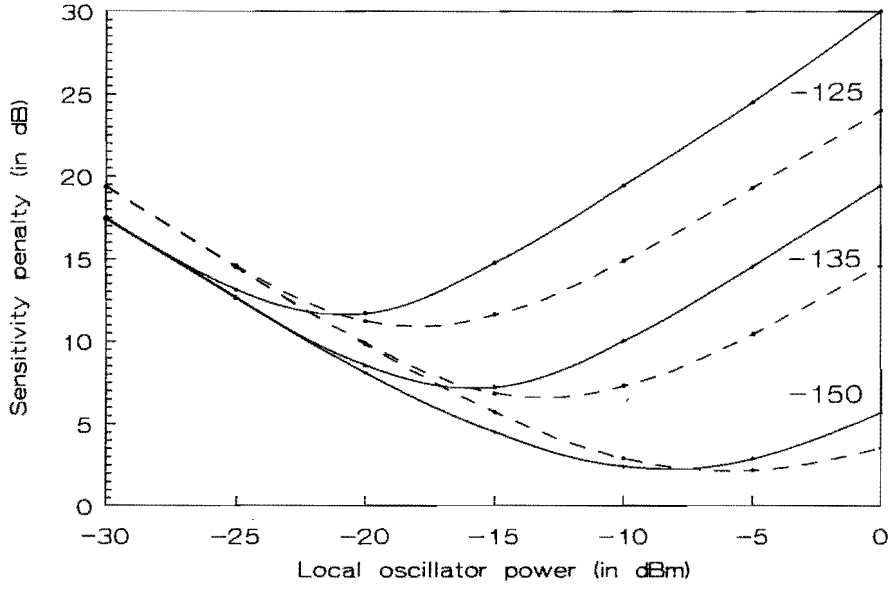

Figure 4.2 *Sensitivity penalty versus P_L for several RIN values and an optimal threshold level.*

A comparison of the exact results with those of the Gaussian approximation in [4.4] shows, that the sensitivity penalty is over-estimated by approximately 2 to 3 dB for small values of the local oscillator power. The opposite is true for large values of the local oscillator power, where the sensitivity penalty is worse than predicted by the Gaussian approximation. The optimum value of the k parameter versus P_L is shown in Figure 4.3 for the same RIN levels.

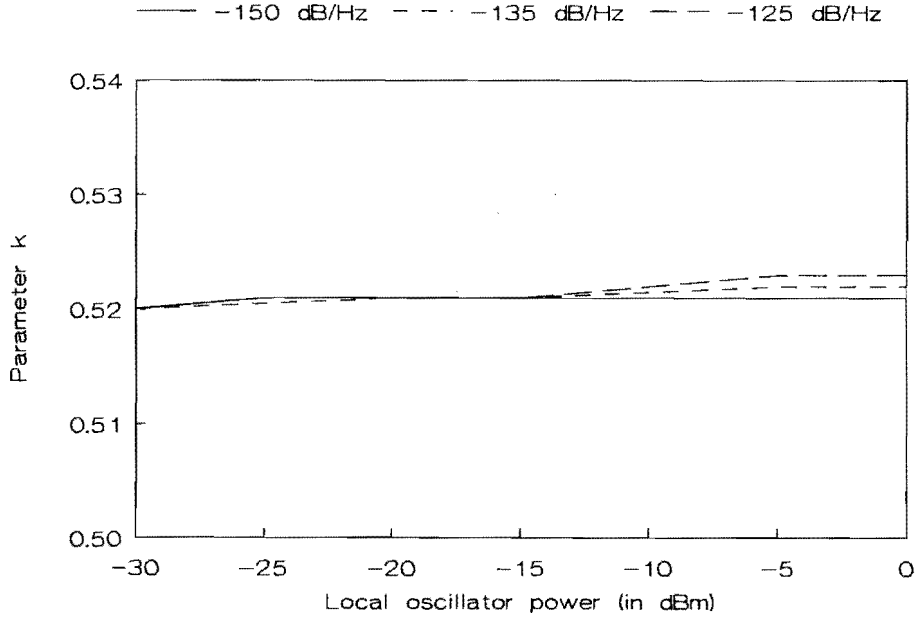

Figure 4.3 *The threshold parameter k versus the local oscillator power P_L for the {2x2} phase diversity ASK receiver.*

From this figure it can be concluded that for optimal performance the parameter k (threshold level) very slightly increases for larger values of the local oscillator power and the RIN level.

4.4 The {3x3} phase diversity ASK receiver

In case a space ($b_k = 0$) is sent, the PDF of the process at the input of the threshold comparator is that of the sum of three squared Gaussian variables $i_1(t)$, $i_2(t)$ and $i_3(t)$ (Equation (4.1)). Each variable consists of the sum of a shot noise term, a thermal noise term and a local oscillator RIN term. These noise terms are independent, have zero means and unity total noise power ($\sigma^2 + \sigma_R^2 \triangleq 1$). Remind that the contributions of the local oscillator RIN in all receiver branches are equal. The conditional probability of error P_0 is equal to the probability that the process at the input of the threshold comparator exceeds the threshold level at the moment of sampling. The conditional error probability, P_0, is (see Appendix 4B for the derivation)

$$P_0 = \int_T^\infty f_0(y)\, dy \,, \tag{4.15}$$

where

$$f_0(y) = \frac{\sqrt{y}(1+\delta)^{3/2}}{\sqrt{(2\pi(1+3\delta))}} . \exp\left[- \frac{y(1+\delta)}{2} \right] . \int_0^1 \exp\left[\frac{3y\delta(1+\delta)}{2(1+3\delta)} . x^2 \right] dx \tag{4.16}$$

and

$$\delta \triangleq \frac{\sigma_R^2}{\sigma^2} = \frac{\frac{1}{9}(RP_L)^2\gamma}{\frac{2}{3}eRP_L + \langle i_{th}^2 \rangle} \,. \tag{4.17}$$

When a mark is sent ($b_k = 1$), the process at the input of the threshold comparator is the sum of the three squared variables $i_1(t)$, $i_2(t)$, and $i_3(t)$ (Equation (4.1)). The only difference with the case in which $b_k = 0$ is, that they have nonzero means. The probability of error for the same threshold is equal to the probability that the realization of the process at the input of the threshold comparator is less than the threshold level. The conditional error probability P_1 has been calculated in Appendix 4B and is found to be equal to

$$P_I = \frac{\sqrt{(1+\delta)}}{\pi\lambda} \int_{-\infty}^{\infty} \left[\exp\left[-\frac{\lambda^2(1+\delta)}{2} \right] \int_0^{\sqrt{T}} \exp\left[-\frac{r^2(1+\delta)}{2} \right] . \sinh\left[\lambda(1+\delta) \right] \, dr \right] \times$$

$$\exp\left[-\frac{\rho^2}{2} \right] d\rho \, , \qquad (4.18)$$

where λ is defined in Appendix 4B. The BER of the {3x3} phase diversity ASK receiver can now be obtained by substitution of the Equations (4.15) and (4.18) in Equation (4.10). These equations have been analyzed numerically for the RIN levels mentioned earlier, in order to find the minimum required optical power received (P_S) to achieve a BER = 10^{-9}. The latter as a function of the threshold level (the parameter k), the local oscillator power (P_L), and the local oscillator RIN. The sensitivity penalty is calculated under the same conditions as mentioned in the previous section. The results are depicted in Figure 4.2. A comparison with the Gaussian approximation of [4.4] shows that the discrepancy in this case for large local oscillator power is of the same order as for the {2x2} phase diversity receiver. From Figure 4.2, it can be concluded that the optimum value for P_L (minimum sensitivity penalty) is larger than for the {2x2} phase diversity ASK receiver. The sensitivity penalty for small values of P_L is approximately 2.5 dB larger with respect to the {2x2} phase diversity receiver. However, for values of P_L larger than the optimum, the {3x3} phase diversity receiver outperforms the {2x2} phase diversity receiver by several dB's, depending on P_L and the RIN level.

In Figure 4.4, the parameter k is given as a function of the local oscillator power P_L for the three different RIN values. A comparison with Figure 4.3 reveals that for the {3x3} phase diversity ASK receiver, the parameter k increases significantly for large values of P_L and the RIN level. This in contrast to k parameter for the {2x2} phase diversity receiver which almost remains constant.

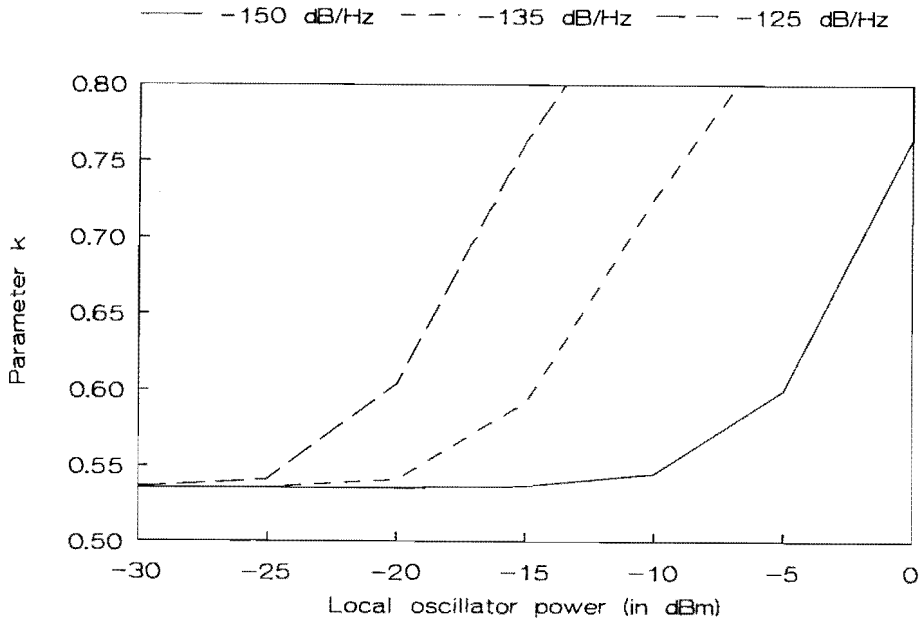

Figure 4.4 *The threshold parameter k versus the local oscillator power* P_L *for the {3x3} phase diversity ASK receiver.*

4.5 Discussion

The results are based on IF filters which are matched to the modulation signal. However, the use of pre- and postdetection filtering could probably offer some advantages as far as it the receiver sensitivity concerns [4.7]. Further, it should be noticed that we neglected the influence of laser phase noise on the performance of the receivers analyzed. However, according to reference [4.8], phase diversity ASK receivers can tolerate laser linewidths of the same order as the bit rate, resulting in an excess sensitivity penalty of less than 2 dB. For moderate and high bit rate ASK receivers, the latter can usually be neglected with respect to the degradation in receiver sensitivity due to the local oscillator intensity noise.

4.6 Comparison with a {3x3} phase diversity DPSK receiver

In this section the performances of the {3x3} phase diversity ASK and DPSK receiver are compared in terms of sensitivity degradation due to shot noise, thermal noise and RIN. The results for the DPSK receiver are quoted from reference [4.5]. In Figure 4.5, the sensitivity penalty versus the local oscillator power is given for the {3x3} phase diversity DPSK receiver, for different levels of local oscillator RIN. The penalty is calculated with respect to the ideal (shot noise limited) heterodyne PSK receiver.

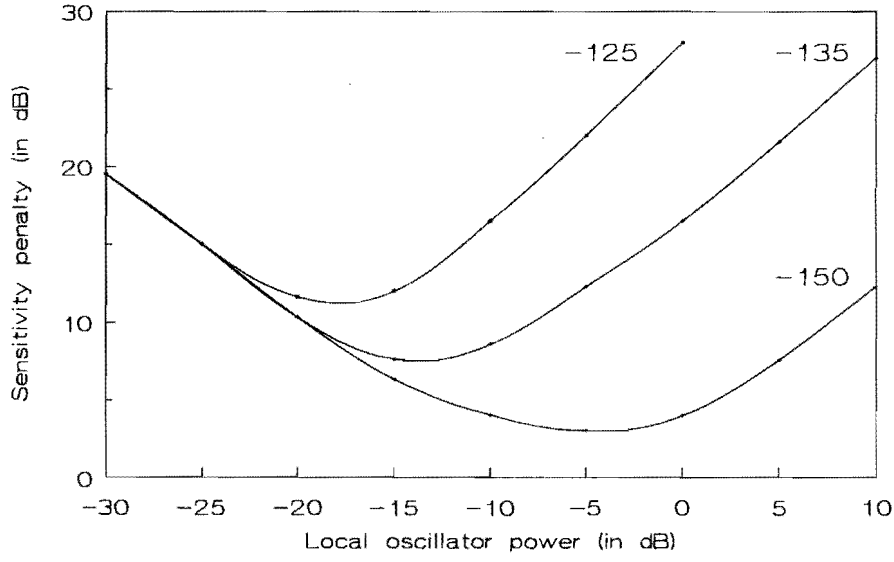

Figure 4.5 *Sensitivity penalty versus local oscillator power for a {3x3} phase diversity DPSK receiver.*

Since both receivers have equal system parameters (e.g., bit rate, IF noise bandwidth, thermal noise level, etc.), a comparison of the performances is possible. However, it should be noticed that for the ASK receiver the threshold level has been optimized as a function of the RIN level and the local oscillator power. For the DPSK receiver the threshold level is independent of these parameters. The fact that the threshold level of the DPSK receiver, even in case of RIN, does not have to be adjusted, implies a major practical

advantage over the ASK receiver.
In order to make a comparison more meaningful, the sensitivity penalties for both receiver structures should be calculated with respect to the ideal {3x3} phase diversity ASK and DPSK receiver, respectively. However, as already mentioned, the curves in the Figures 4.2 and 4.5 give the sensitivity penalty with respect to the ideal heterodyne ASK/PSK receiver. To accommodate for this, a correction of the curves is required.
From Table 3.1, it can be concluded that this can be accomplished by shifting the curves for the {3x3} phase diversity ASK receiver in Figure 4.2, 0.4 dB downwards. For the DPSK receiver (Table 3.2) the curves, given in Figure 4.5, should be shifted 0.7 dB downwards.
It can then be concluded that the sensitivity penalty, due to the RIN, for the {3x3} phase diversity DPSK receiver, is approximately 0.3 dB less then the sensitivity penalty for the {3x3} phase diversity ASK receiver, for the same RIN levels. The figure also reveals that for the given RIN levels, the values of P_L for which the sensitivity penalty is minimal, are almost identical for both diversity receivers.
In conclusion, the {3x3} phase diversity ASK and DPSK receiver perform very similar in case of RIN, except for an intrinsic difference in sensitivity of approximately 0.3 dB, due to the local oscillator RIN.

4.6.1 Intensity noise canceling receiver structures

As discussed in the preceding section, the local oscillator intensity noise (RIN) can substantially degrade the performance of optical coherent receivers. For this reason, intensity noise canceling receiver structures have been developed in order to relax the intensity noise requirement of the local oscillator laser.

A receiver structure, which possesses an intensity noise canceling capability, is the optical coherent heterodyne receiver given in Figure 4.6. It uses two photodiodes in a balanced mixer configuration [4.9].

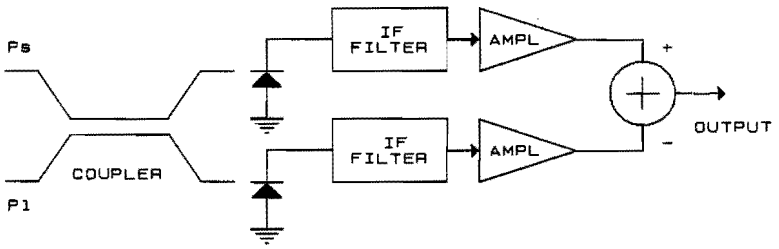

Figure 4.6 *A dual detector heterodyne receiver.*

The local oscillator intensity noise contributions in both photocurrents are identical, while the signal values are 180° out of phase. By subtracting the two photocurrents, the local oscillator intensity noise can be suppressed. A drawback of the dual detector receiver is that non-idealities such as, imbalance in the outputs of the coupler used, thermal noise, unmatched photodiodes and unequal electrical path lengths in the two branches of the receiver, may significantly degrade the performance.

The same principle of RIN suppression can also be applied to {3x3} and {4x4} phase diversity receivers. In reference [4.6], a modification of the {3x3} phase diversity ASK receiver has been proposed, which makes suppression of local oscillator intensity noise possible. The receiver is presented in Figure 4.7.

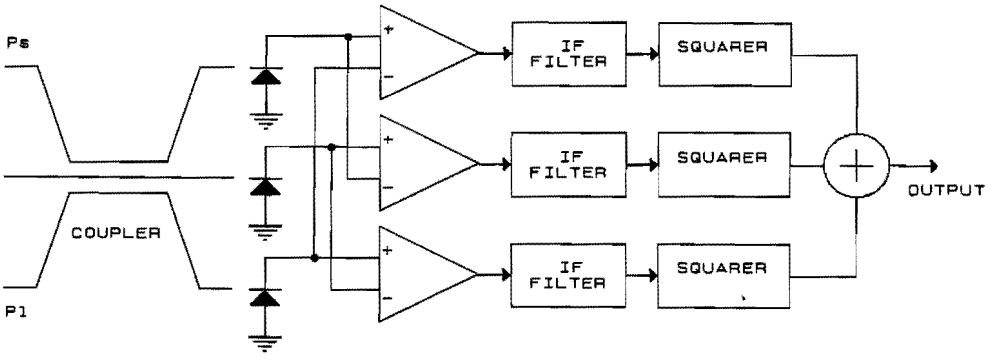

Figure 4.7 *The modified {3x3} phase diversity ASK receiver.*

The modified {3x3} phase diversity receiver uses subtractors which are placed between the squarers and the IF filter. The principle of operation is exactly the same as for the dual detector receiver. In reference [4.5] a more elegant way has been developed to obtain the same feature with less components. The three photodiodes are arranged in a closed triangle. In comparison with the preceding configuration, this balanced receiver does not require separate subtractors. The modified {3x3} and the balanced {3x3} phase diversity receiver suffer from the same drawbacks as mentioned for the dual detector receiver. The proposed balanced receiver configuration is shown in Figure 4.8.

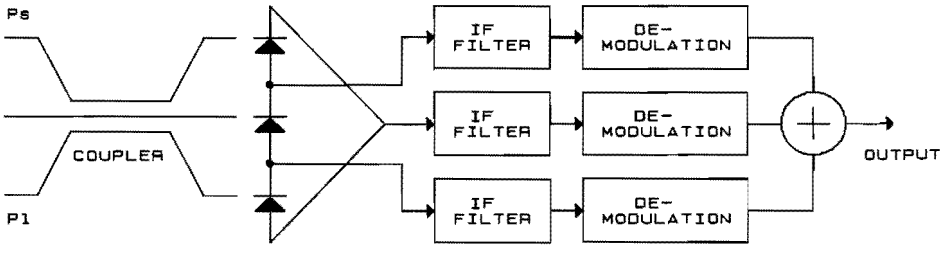

Figure 4.8 *The balanced {3x3} phase diversity receiver,*

For the {4x4} diversity receiver, suppression of the RIN can be obtained by subtracting the photocurrents, which are 180° out of phase. The resulting receiver configuration performs very similar as the ideal {2x2} phase diversity receiver. The proposed balanced receiver configuration is depicted in Figure 4.9.

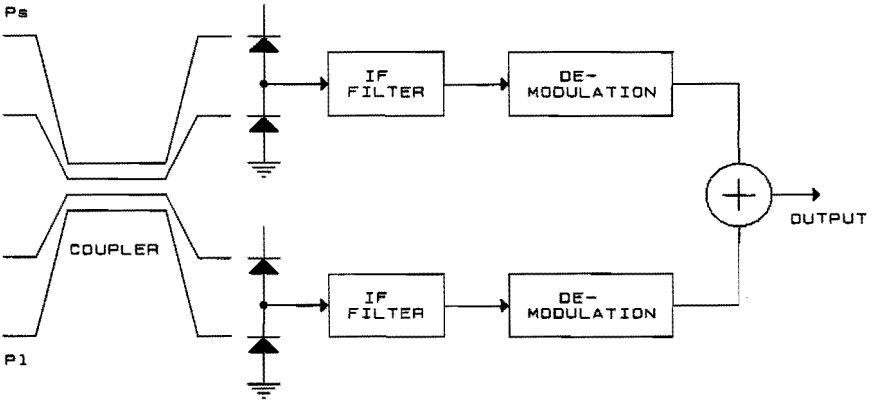

Figure 4.9 *The balanced {4x4} phase diversity receiver.*

4.7 Conclusions

For both the {2x2} and the {3x3} phase diversity ASK receiver an optimum value for the local oscillator power (P_L) is found, for which the sensitivity penalty with respect to the ideal heterodyne ASK receiver is minimal. This value depends on the position of the threshold level ($T = 2k^2SNR$) and the local oscillator laser RIN. For each combination of P_L and a RIN level, the value of k ought to be optimized in order to minimize the BER, implying a minimum sensitivity penalty. For an optimum value of k and a BER = 10^{-9}, the {3x3} receiver outperforms the {2x2} receiver for a local oscillator power larger than the optimum value of P_L. The reverse is true for values of P_L smaller than this optimum value.

A comparison with the results of [4.4], based on the Gaussian approximation of the PDF at the input of the threshold, shows that for both receiver structures the results differ substantially. Reference [4.4] over-estimates the sensitivity penalty for small values of the local oscillator by 2 to 3 dB. For large values of the local oscillator power the reverse is true.

The value of the parameter k varies little for the {2x2} phase diversity ASK receiver from approximately 0.520 for small values of P_L to approximately 0.522 for RIN = -125 dB/Hz and P_L = -10 dBm. For similar values of P_L and

the RIN as given just above, the parameter k varies from approximately 0.535 to 0.886 for the {3x3} phase diversity ASK receiver.

It is also shown that in presence of RIN, and for a perfect balancing of the receiver branches, the BER of the {3x3} phase diversity receiver is constant for a fixed value of the SNR. This in contrary to the BER of the {2x2} phase diversity receiver, which in this case shows a time varying character of the BER, with a frequency of twice the frequency and phase offset between the local oscillator and the transmitting laser.

Except for an intrinsic difference in sensitivity, the {3x3} phase diversity ASK receiver performs very similar to the equivalent DPSK receiver in case of shot noise, thermal noise and RIN. Even the optimum values of P_L are almost identical. However, for the {3x3} phase diversity DPSK receiver, the sensitivity penalty, due to the local oscillator RIN, is about 0.3 dB less.

Appendix 4A

Derivation of the PDF for the {2x2} phase diversity ASK receiver in case a space is sent

For the purpose of the derivation of Equation (4.11), the photocurrents are represented by

$$v = a + R \ ,$$
$$w = b + R \ . \qquad \text{(A4.1)}$$

The variables a and b (shot + thermal noise) have zero means and equal variances ($\triangleq \sigma^2$), are assumed to be statistically independent and have Gaussian PDF's $f_a(a)$ and $f_b(b)$, respectively. The variable R (the RIN) is assumed to have a Gaussian PDF ($f_R(R)$) with zero mean and a variance equal to σ_R^2. The joint probability density function of v and w can be calculated according to the following relation [4.10,4.13]

$$f_{v,w}(v,w) = \int_{-\infty}^{\infty} f_a(v-R).f_b(w-R).f_R(R)\ dR \qquad \text{(A4.2)}$$

$$= \frac{1}{(2\pi)^{3/2}\sigma^2\sigma_R} \int_{-\infty}^{\infty} \exp\left[-\frac{(v^2 - 2vR + w^2 - 2wR + 2R^2)}{2\sigma^2}\right].\exp\left[-\frac{R^2}{2\sigma_R^2}\right] dR \ . \qquad \text{(A4.3)}$$

Define

$$v \triangleq r.\cos\vartheta \ , \qquad 0 \le \vartheta \le 2\pi$$
$$w \triangleq r.\sin\vartheta \ , \qquad \text{(A4.4)}$$

$$\alpha \triangleq \frac{1}{(2\pi)^{3/2}\ \sigma^2\sigma_R} \ , \qquad \text{(A4.5)}$$

and

$$\delta \triangleq \frac{\sigma_R^2}{\sigma^2} = \frac{\frac{1}{4}(RP_L)^2\gamma}{eRP_L + \langle i_{th}^2 \rangle} . \qquad \text{(A4.6)}$$

Equation (A4.3) can be rewritten in terms of the Equations (A4.4) to (A4.6), which finally results in

$$f_{r,\vartheta}(r,\vartheta) = \alpha r.\exp\left[-\frac{r^2}{2\sigma^2}\right].\int_{-\infty}^{\infty} \exp\left[-\frac{R^2(1+2\delta)}{2\delta\sigma^2} + \frac{rR(\cos\vartheta + \sin\vartheta)}{\sigma^2}\right] dR. \qquad \text{(A4.7)}$$

Using the following identity [4.11]

$$\int_{-\infty}^{\infty} \exp[-p^2x^2 + qx]\, dx = \frac{\sqrt{\pi}}{p}.\exp[q^2/(4p^2)] , \qquad \text{(A4.8)}$$

and using the integral representation of the modified Bessel function of the first kind and zero order, $I_0[.]$, [4.12], Equation (A4.7) can, after normalization of the total noise power ($\sigma^2 + \sigma_R^2 \triangleq 1$) to unity and using Equation (A4.6), be rewritten in the following reduced form

$$f_0(r) = \frac{r(1+\delta)}{\sqrt{(1+2\delta)}}.\exp\left[-\frac{r^2(1+\delta)^2}{2(1+2\delta)}\right].I_0\left[\frac{\delta(1+\delta)r^2}{2(1+2\delta)}\right] . \qquad \text{(A4.9)}$$

Since the realization of the process at the input of the threshold comparator equals r^2 ($\triangleq y$) instead of r, the final PDF can be found to be [4.13]

$$f_0(y) = \frac{(1+\delta)}{2\sqrt{(1+2\delta)}}.\exp\left[-\frac{y(1+\delta)^2}{2(1+2\delta)}\right].I_0\left[\frac{\delta(1+\delta)y}{2(1+2\delta)}\right] . \qquad \text{(A4.10)}$$

Derivation of the PDF for the (2x2) phase diversity ASK receiver in case a mark is sent

In case a mark is sent, the realization of the process at the input of the threshold comparator differs from the one discussed in the preceding section only for the fact that the variables v and w have nonzero means.
For the purpose of the derivation of Equation (4.14), the photocurrents are represented by

$$\begin{aligned} v &= a + R + s_0 \,, \\ w &= b + R + s_1 \,, \end{aligned} \qquad \text{(A4.11)}$$

where the variables a and b are the (shot + thermal) noise terms, R is the RIN term, and s_i (i = 0,1) is the time dependent value of the signal given by Equation (4.5). Rewriting Equation (A4.2) for nonzero means results in the following equation for the joint probability density function of the variables v and w

$$f_{v,w}(v,w) = \int_{-\infty}^{\infty} f_a(v-s_0-R).f_b(w-s_1-R).f_R(R)\, dR$$

$$= \frac{1}{(2\pi)^{3/2}\,\sigma^2\sigma_R}.\exp\left[-\frac{v^2 + w^2 + s_0^2 + s_1^2 - 2(s_0 v + s_1 w)}{2\sigma^2}\right] \times$$

$$\int_{-\infty}^{\infty} \exp\left[\frac{-2R^2 - 2R(s_0 + s_1) + 2R(v + w)}{2\sigma^2}\right].\exp\left[-\frac{R^2}{2\delta\sigma^2}\right] dR \,. \qquad \text{(A4.12)}$$

By making use of the integration rule given by Equation (A4.8) and substituting $\sigma_R^2 \triangleq \delta\sigma^2$, the integral of Equation (A4.12) can be reduced to the following equation

$$f_{v,w}(v,w) = \frac{1}{2\pi\sigma^2\sqrt{(1+2\delta)}}.\exp\left[- \frac{v^2 + w^2 + s_0^2 + s_1^2 - 2(s_0 v + s_1 w)}{2\sigma^2} \right] \times$$

$$\exp\left[\frac{\delta(w + v - (s_0 + s_1))^2}{2\sigma^2(1+2\delta)} \right] . \qquad \text{(A4.13)}$$

After the introduction of polar coordinates for the variables v and w (Equation (A4.4)) and substituting $\sigma^2 = 1/(1+\delta)$, the conditional error probability P_1 can be calculated to read

$$P_1 = \frac{(1+\delta)}{2\pi\sqrt{(1+2\delta)}} \iint_V r.\exp\left[- \frac{(1+\delta)\{r^2 - 2r(s_0\cos\vartheta + s_1\sin\vartheta) + 2SNR\}}{2} \right] \times$$

$$\exp\left[\frac{\delta(1+\delta)\{r(\cos\vartheta + \sin\vartheta) - (s_0 + s_1)\}^2}{2(1+2\delta)} \right] dr.d\vartheta , \qquad \text{(A4.14)}$$

where the integration region $V = v^2 + w^2 = r^2 \leq T = 2k^2SNR$, and the relation $s_0^2 + s_1^2 = 2SNR$. From Equation (A4.14), it can be concluded, that due to the term $(s_0 + s_1)$, P_1 has a time varying character for $\delta \neq 0$ as function of $\phi(t)$ (the frequency and phase offset, see Equation (4.1)). Since near base-band operation is assumed, the period time of $\phi(t)$ is much larger than the bit time. Besides, s_0 and s_1 are trigonometric functions which implies that they show a periodical character for $\phi(t)$ between 0 and maximal 2π radians. Therefore, the average conditional bit error probability of P_1, $\langle P_1 \rangle$, can be computed by averaging P_1 of Equation (A4.14) over the interval $[0,2\pi]$. This results in the following equation for the average conditional error probability $\langle P_1 \rangle$ (with $\phi(t)$ written as ϕ)

$$\langle P_1 \rangle = \frac{1}{2\pi} \int_0^{2\pi} P_1(\phi)\, d\phi$$

$$= \frac{(1+\delta)}{4\pi^2\sqrt{(1+2\delta)}} \int_0^{2\pi} \cdot \iiint_V r.\exp\left[- \frac{(1+\delta)\{r^2 - 2r(s_0(\phi)\cos\vartheta + s_1(\phi)\sin\vartheta) + 2SNR\}}{2} \right] \times$$

$$\exp\left[\frac{\delta(1+\delta)[r(\cos\vartheta + \sin\vartheta) - \{s_0(\phi) + s_1(\phi)\}]^2}{2(1+2\delta)} \right] dr.d\vartheta.d\phi \ .$$

(A4.15)

Appendix 4B

Derivation of the PDF for the {3x3} phase diversity ASK receiver in case a space is sent

For the purpose of the derivation of Equation (4.16), the photocurrents are represented by

$$\begin{aligned} u &= a + R \ , \\ v &= b + R \ , \\ w &= c + R \ . \end{aligned} \tag{B4.1}$$

The variables a, b and c, indicating the contribution of the shot noise + the thermal noise, have zero means and equal variances ($\triangleq \sigma^2$). They are assumed to be statistically independent and Gaussian distributed. The variable R, indicating the RIN, is assumed to have a Gaussian PDF with zero mean and a variance equal to σ_R^2. The joint probability density function of the variables u, v and w can then be calculated according to the following relation [4.10,4.13]

$$f_{u,v,w}(u,v,w) = \int_{-\infty}^{\infty} f_a(u-R).f_b(v-R).f_c(w-R).f_R(R) \ . \ dR \tag{B4.2}$$

$$= \frac{1}{(2\pi)^2\sigma^3\sigma_R} \int_{-\infty}^{\infty} \exp\left[- \frac{(u^2 + v^2 + w^2 - 2R(u + v + w) + 3R^2)}{2\sigma^2} \right] \times$$

$$\exp\left[- \frac{R^2}{2\sigma_R^2} \right] dR \ . \tag{B4.3}$$

Let us introduce a new set of three variables $\bar{u}$, $\bar{v}$ and $\bar{w}$ which are implicitly defined by

$$
\begin{aligned}
u &\triangleq l_1\bar{u} + l_2\bar{v} + l_3\bar{w} \ , \\
v &\triangleq m_1\bar{u} + m_2\bar{v} + m_3\bar{w} \ , \\
w &\triangleq n_1\bar{u} + n_2\bar{v} + n_3\bar{w} \ ,
\end{aligned} \tag{B4.4}
$$

where

$$
\begin{aligned}
-n_1 &= -n_2 = l_3 = m_3 = n_3 = 1/\sqrt{3} \ , \\
l_1 &= m_2 = (1 + 1/\sqrt{3})/2 \ , \\
m_1 &= l_2 = -(1 - 1/\sqrt{3})/2 \ .
\end{aligned} \tag{B4.5}
$$

After the application of this transformation to Equation (B4.3), it can be rewritten in the following form

$$
f_{u,v,w}(\bar{u},\bar{v},\bar{w}) = \beta \int_{-\infty}^{\infty} \exp\left[- \frac{\bar{u}^2 + \bar{v}^2 + \bar{w}^2 - 2R\bar{w}\sqrt{3} + 3R^2}{2\sigma^2} \right] . \exp\left[- \frac{R^2}{2\sigma_R^2} \right] dR \ , \tag{B4.6}
$$

where β is given by

$$
\beta \triangleq \frac{1}{(2\pi)^2 \sigma^3 \sigma_R} \ . \tag{B4.7}
$$

A reduction of the number of variables can be obtained by using spherical coordinates

$$
\begin{aligned}
\bar{u} &= r.\sin\theta\sin\phi \ , \qquad 0 \le \theta \le \pi \\
\bar{v} &= r.\sin\theta\cos\phi \ , \qquad 0 \le \phi \le 2\pi \\
\bar{w} &= r.\cos\theta \ ,
\end{aligned} \tag{B4.8}
$$

leading to the following equation

$$
f_{r,\theta}(r,\theta) = (2\pi\beta r^2 \sin\theta) . \exp\left[- \frac{r^2}{2\sigma^2} \right] . \int_{-\infty}^{\infty} \exp\left[- \frac{R^2(1+3\delta)}{2\delta\sigma^2} + \frac{r\sqrt{3}R.\cos\theta}{\sigma^2} \right] dR \ , \tag{B4.9}
$$

where

$$\delta \triangleq \frac{\sigma_R^2}{\sigma^2} = \frac{\frac{1}{9}(RP_L)^2\gamma}{\frac{2}{3}eRP_L + \langle i_{th}^2 \rangle} . \qquad \text{(B4.10)}$$

The next step consists of the normalization of the total noise power to unity, integration of Equation (B4.9) over R by means of the identity given in (A4.8), and substitution of $\cos\theta \triangleq x$. After some mathematical manipulations, Equation (B4.8) can be calculated to give

$$f_0(r) = \frac{2r^2(1+\delta)^{3/2}}{\sqrt{(2\pi(1+3\delta))}} . \exp\left[- \frac{r^2(1+\delta)}{2} \right] . \int_0^1 \exp\left[\frac{3y^2\delta(1+\delta)}{2(1+3\delta)} . x^2 \right] dx . \qquad \text{(B4.11)}$$

However, the realization of the process at the input of the threshold comparator is equal to $r^2 \triangleq y$.

$$f_0(y) = \frac{\sqrt{y}(1+\delta)^{3/2}}{\sqrt{(2\pi(1+3\delta))}} . \exp\left[- \frac{y(1+\delta)}{2} \right] . \int_0^1 \exp\left[\frac{3y\delta(1+\delta)}{2(1+3\delta)} . x^2 \right] dx . \qquad \text{(B4.12)}$$

Derivation of the PDF for the (3x3) phase diversity ASK receiver in case a mark is sent

In case a mark is sent, the realization of the process at the input of the threshold comparator differs from the one discussed in the preceding section only for the fact that the variables u, v and w have nonzero time dependent means, s_0, s_1 and s_2.

For the purpose of the derivation of Equation (4.19), the photocurrents are

represented by

$$u = a + R + s_0 ,$$
$$v = b + R + s_1 , \qquad \text{(B4.13)}$$
$$w = c + R + s_2 .$$

Here s_i (i = 0,1,2) is the signal value given by Equation (4.8). The terms a, b and c are the contributions of the (shot + thermal) noise. The variable R stands for the RIN contribution, which is assumed to have a Gaussian PDF with zero mean and a variance equal to σ_R^2. The value of P_1 is given by the following fourfold integral

$$P_1 = \frac{1}{(2\pi)^2\sigma^3\sigma_R} \int_{-\infty}^{\infty} \cdot \iiint_V \exp\left[- \frac{(u-s_0-R)^2 + (v-s_1-R)^2 + (w-s_2-R)^2}{2\sigma^2} \right] \times$$

$$\exp\left[- \frac{R^2}{2\sigma_R^2} \right] du.dv.dw.dR , \qquad \text{(B4.15)}$$

where $V : u^2 + v^2 + w^2 < T = 2k^2SNR$. (B4.16)

Making use of the fact that the threefold integral over u, v and w is spherical-symmetrical, it can be rewritten as the following threefold integral by a rotation of the coordinates. This leads to the following equation

$$G(u,v,w,\lambda) \triangleq \iiint_V \exp\left[- \frac{u^2 + v^2 + w^2 - 2\lambda w + \lambda^2}{2\sigma^2} \right] du.dv.dw , \qquad \text{(B4.17)}$$

where

$$\lambda^2 \triangleq (s_0 + R)^2 + (s_1 + R)^2 + (s_2 + R)^2 = 2SNR + 3R^2 . \qquad \text{(B4.18)}$$

The sum of the signal values s_i (i = 1,2,3) is equal to zero. The latter also implies that the sum of the beat noise terms $R.(s_0 + s_1 + s_2)$ is zero.

The sum of the squares of the signal values is constant and equal to 2SNR. Using spherical coordinates (see Equation (B4.7)), the integral of Equation (B4.17) can be rewritten to give

$$G(r,\lambda) = \frac{4\pi\sigma^2}{\lambda}.\exp\left[-\frac{\lambda^2}{2\sigma^2}\right].\int_0^{\sqrt{T}} \exp\left[-\frac{r^2}{2\sigma^2}\right].\sinh\left[\frac{\lambda r}{\sigma^2}\right].r\ dr\ , \qquad \text{(B4.19)}$$

where sinh[.] is the hyperbolic sine function. The conditional error probability P_1 can now be written to be

$$P_1 = \frac{1}{(2\pi)^2\sigma^3\sigma_R}\int_{-\infty}^{\infty} G(r,\lambda).\exp\left[-\frac{R^2}{2\sigma_R^2}\right] dR\ . \qquad \text{(B4.20)}$$

The function $G(r,\lambda)$ is time independent, since λ is independent of $\phi(t)$ (the frequency and phase offset between the local oscillator and the transmitting laser). This in contrast to the {2x2} phase diversity ASK receiver, which has in the presence of RIN, a $\Phi(t)$ depending BER (the sum of the beat noise terms differs from zero). Substitution of $G(r,\lambda)$ and $R \triangleq \sigma_R\rho$ in Equation (B4.20) results in the following twofold integral for the conditional error probability P_1

$$P_1 = \frac{1}{\pi\sigma\lambda}\int_{-\infty}^{\infty}\left[\exp\left[-\frac{\lambda^2}{2\sigma^2}\right].\int_0^{\sqrt{T}}\exp\left[-\frac{r^2}{2\sigma^2}\right].\sinh\left[\frac{\lambda r}{\sigma^2}\right].r\ dr\right]\times$$

$$\exp\left[-\frac{\rho^2}{2}\right] d\rho\ . \qquad \text{(B4.21)}$$

Since the total noise power $(\sigma^2 + \sigma_R^2)$ is normalized to unit variance, and $\delta\sigma_R^2 = \sigma^2$, we can substitute in Equation (B4.21) $\sigma^2 = 1/(1+\delta)$, which results in the following equation for the conditional error probability P_1

$$P_1 = \frac{\sqrt{(1+\delta)}}{\pi\lambda} \int_{-\infty}^{\infty} \left[\exp\left[-\frac{\lambda^2(1+\delta)}{2} \right] . \int_0^{\sqrt{T}} \exp\left[-\frac{r^2(1+\delta)}{2} \right] . \sinh\left[\lambda(1+\delta) \right] . r \; dr \right] \times \exp\left[-\frac{\rho^2}{2} \right] d\rho \; .$$

(B4.22)

Computation of several values of P_1 in the interval $[0,2\pi]$ revealed that P_1 is periodic with π radians. This implies that the variation in the BER has a frequency of twice the frequency offset between the transmitting and local oscillator laser.

References

[4.1] A.W. Davis, M.J. Pettitt, J.P. King and S. Wright, "Phase diversity techniques for coherent optical receivers",
J. Lightwave Technol., vol. 5, no. 4, pp. 561-572, April 1987.

[4.2] L.G. Kazovsky, P. Meissner and E. Patzak, "ASK multiport optical homodyne receivers",
J. Lightwave Technol., vol. 5, no. 6, pp. 720-780, June 1987.

[4.3] W.H.C. de Krom, "Impact of laser phase noise on the performance of a {3x3} phase and polarization diversity optical homodyne DPSK receiver",
J. Lightwave Technol., vol. 8, pp. 1709-1716, Nov. 1990.

[4.4] A.F. Elrefaie, D.A. Atlas, L.G. Kazovsky, R.E. Wagner, "Intensity noise in ASK coherent lightwave receivers",
Electron. Lett., vol. 24, no. 3, pp. 158-159, 1988.

[4.5] E. Patzak, R. Langenhorst, "Sensitivity degradation of conventional and balanced 3x3 port phase diversity DPSK receivers due to thermal and local oscillator intensity noise",
Electron. Lett., vol. 25, no. 8, pp. 545-547, 1989.

[4.6] J. Siuzdak and W. van Etten, "BER evaluation for phase and polarization diversity optical receivers using noncoherent ASK and DPSK demodulation",
J. Lightwave Technol., vol. 7, no. 4, pp. 584-599, April 1989.

[4.7] J. Siuzdak and W. van Etten, "Heterodyne ASK multiport optical receivers using postdetection filtering",
J. Lightwave Technol., vol. 8, no. 1, pp. 71-77, Jan. 1990.

[4.8] L.G. Kazovsky, "Phase- and polarization-diversity coherent optical techniques",
J. Lightwave Technol., vol. 7, no. 2, pp. 279-292, Febr. 1990.

[4.9] G.L. Abbas, V.W.S. Chan, and T.K. Yee, "A dual-detector optical heterodyne receiver for local oscillator noise suppression",
J. Lightwave Technol., vol. 3, no. 5, pp. 1110-1122, Oct. 1985.

[4.10] C.W. Helstrom, "Probability and stochastic processes for engineers",
Macmillan Publishing Company, New York, 1984.

[4.11] I.S. Gradshteyn and I.M. Ryzhik, "Table of integrals, series, and products",
Academic Press, New York, 1965.

[4.12] M. Abramowitz and I.A. Stegun, "Handbook of mathematical functions"
Dover Publications, New York, 1965.

[4.13] A. Papoulis, "Probability, random variables, and stochastic processes",
McGraw-Hill, New York, 1965.

CHAPTER 5.

SENSITIVITY DEGRADATION OF A {2X2} AND {3X3} PHASE DIVERSITY ASK RECEIVER DUE TO GAIN IMBALANCE AND NON-IDEAL PHASE RELATIONS OF THE OPTICAL HYBRID

5.1 Introduction

The key component of all phase diversity receivers is an optical hybrid that provides the means of recovering the modulated optical signal [5.1,5.2]. All phase diversity receivers are sensitive to gain imbalance and an aberration in the phase relations between the different receiver branches. The aberration in the phase relations can originate from the optical hybrid, and the gain imbalance in the receiver branches can be caused, firstly, by an unequal amplification at the different IF stages, or secondly, by an unequal power distribution over the outputs of the optical hybrid. In this chapter the Bit Error Rates (BER's) will be calculated for a {2x2} and a {3x3} phase diversity ASK receiver, using non-Gaussian Probability Density Functions (PDF's) for the signals at the threshold comparator, and various values for the percentage of gain imbalance and the phase mismatch.

The phase diversity principle can be combined with the independent reception of the orthogonal polarization components of the optical signal received, the so called phase and polarization diversity receiver (Chapter 3) [5.2-5.6]. We found that the calculations of the sensitivity degradation for the phase and polarization diversity receiver are equivalent to that for the receivers employing phase diversity only. Therefore, the analyses are performed for the phase diversity receiver only, assuming that the state of polarization of both the local oscillator and the optical wave received are perfectly matched. The analyses are performed under the assumption that the shot noise originating from the local oscillator laser dominates all other receiver noise sources, for example the thermal noise and the noise due to the dark current of the photodiodes. The intersymbol interference is assumed to be absent, and the influence of laser phase noise and local oscillator intensity noise has been neglected. For the sake of clarity, some mathematical derivations are placed in the Appendices 5A and 5B.

5.2 Description of the receivers

The phase diversity receiver is depicted schematically in Figure 5.1. It consists of a {2x2} or {3x3} optical hybrid, photodiodes, low-pass filters, preamplifiers, and an ASK demodulation scheme. The latter scheme uses squarers for demodulation because they give a better performance than linear envelope detectors [5.2]. The {2x2} multiport is assumed to be a 90° optical hybrid [5.7,5.8], while the {3x3} multiport is assumed to be a threefold fused-fiber coupler [5.9] which in the lossless case, introduces a phase shift of 120° between the different output branches.

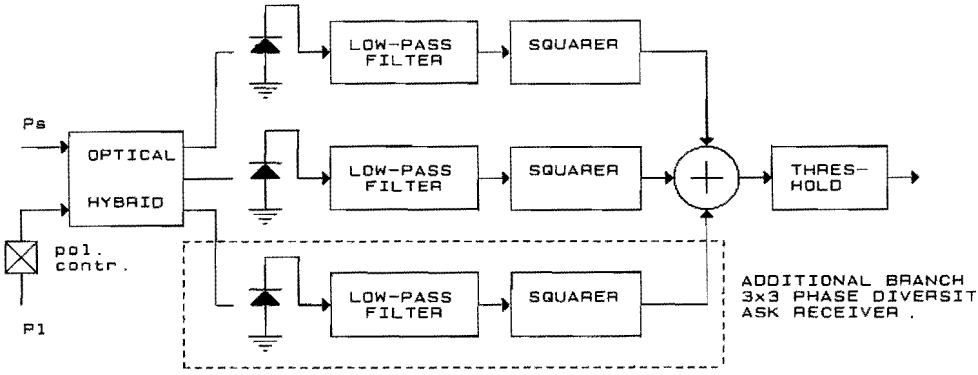

Figure 5.1 *Block-diagram of the analyzed {2x2} and {3x3} phase diversity ASK receiver.*

The gain imbalance is modeled by placing an additional amplifier in each receiver branch (Figure 5.1). One of the receiver branches is taken as a reference with an amplification factor equal to one. The amplification factor of the other branch in the {2x2} phase diversity receiver is given by $(1+\delta)$, introducing a gain imbalance of $100\times\delta\%$ $(-1 < \delta < 1)$. For the {3x3} phase diversity ASK receiver, the gain imbalance is introduced in the same way except for one difference. The percentage of gain imbalance is assumed to be symmetrical. The latter implies that the gain imbalance for two out of three receiver branches is assumed to be equal in magnitude and sign. The latter behaviour is characteristic for the output power distribution of

different commercially available (3x3) directional fused-fiber couplers. The optical power in the cross-coupled branches is less than the optical power in the transmitted branch. Besides, the optical powers in the cross-coupled branches are usually almost equal. The measured results of the commercially available "Sifam" (3x3) directional fused-fiber coupler [5.10] are shown in Figure 5.2.

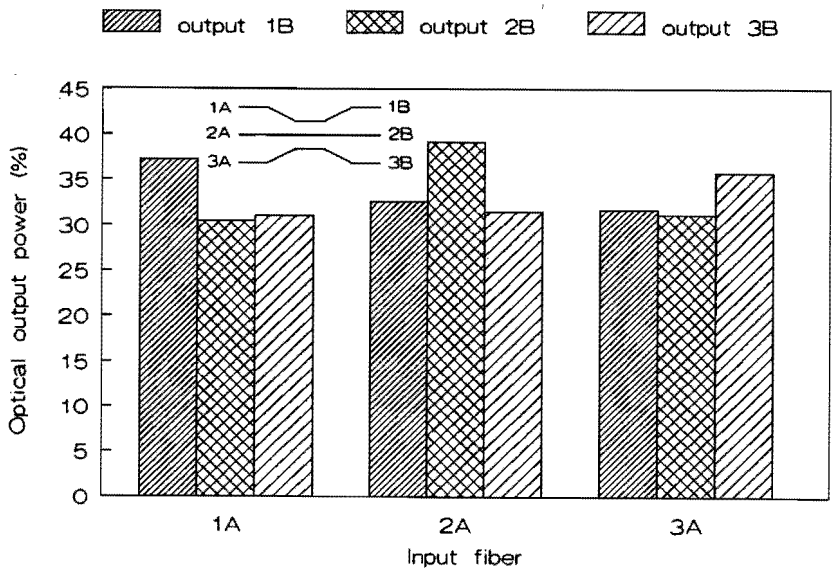

Figure 5.2 *Measured output power distribution of a "Sifam" (3x3) directional fused-fiber coupler.*

The phase mismatch for the (2x2) receiver is modeled by introducing an extra phase shift term ϕ in one of the two relations for the photocurrents at the IF stage, taking the phase of one receiver branch as a reference. This leads to a phase shift between the two outputs of the optical hybrid of $90^{\circ}+\phi$ or $90^{\circ}-\phi$. The values of the photocurrents are given by

$$i_0(t) = \sqrt{P_L P_S}\, R.b(t).\cos[\gamma(t)] + n_0(t) \,, \tag{5.1}$$

$$i_1(t) = (1+\delta).[\sqrt{P_L P_S}\, R.b(t).\cos[\gamma(t) - (\frac{\pi}{2} - \phi)] + n_1(t)] \,, \tag{5.2}$$

where the local oscillator power is given by P_L, and P_S is the signal power received. The function b(t) represents the signaling waveform. The radial frequency and phase offset between the local oscillator and the transmitting laser is given by $\gamma(t) = \omega_{IF}t + \varphi(t)$. R is the responsivity of the photodiodes used, and $n_0(t)$ and $n_1(t)$ are the shot noise currents. For the (3x3) receiver, the phase mismatch is modeled by introducing extra phase shift terms ϕ_1 and ϕ_2, respectively, in two out of the three relations for the photocurrents at the IF stage, taking one receiver branch as a reference. The values of the photocurrents are then given by

$$i_0(t) = \frac{2}{3}\sqrt{P_L P_S}\ R.b(t).\cos[\gamma(t)] + n_0(t)\ , \tag{5.3}$$

$$i_1(t) = (1+\delta).[\frac{2}{3}\sqrt{P_L P_S}\ R.b(t).\cos[\frac{2}{3}\pi + \gamma(t) + \phi_1] + n_1(t)]\ , \tag{5.4}$$

$$i_2(t) = (1+\delta).[\frac{2}{3}\sqrt{P_L P_S}\ R.b(t).\cos[\frac{4}{3}\pi + \gamma(t) + \phi_2] + n_2(t)]\ , \tag{5.5}$$

where $n_0(t)$, $n_1(t)$ and $n_2(t)$ are the shot noise currents. In the sequel we shall distinguish two situations :

1. $\phi_1 = \phi_2 = \phi$, which leads to a non-symmetrical vector diagram of the photocurrents $\{120^\circ - \phi,\ 120^\circ,\ 120^\circ + \phi\}$ (Figure 5.3a), and
2. $\phi_1 = -\phi_2 = \phi$, giving a symmetrical vector diagram, $\{120^\circ - \phi,\ 120^\circ + 2\phi,\ 120^\circ - \phi\}$ (Figure 5.3b).

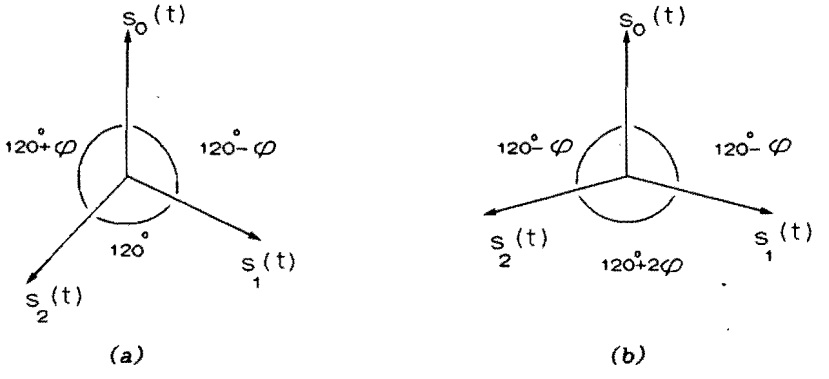

Figure 5.3 *(a) The non-symmetrical configuration of the photocurrents, (b) The symmetrical configuration of the photocurrents.*

The signaling waveform b(t) in the Equations (5.1) to (5.5) is modeled as a digital baseband signal and is given by

$$b(t) = \sum_k b_k.\mathrm{rect}(t - kT_0) \ , \tag{5.6}$$

where T_0 stands for the bit time, and the function rect(t) is equal to 1 for $t \in [0,T_0]$ and equal to 0 elsewhere. The term b_k is the symbol sequence, taking on the values 1 or 0.
It is reasonable to assume that the shot noise terms at the output of the photodiodes are independent and Gaussian distributed. The power spectrum is taken to be flat and the double-sided spectral density is equal to

$$N_1 = eRP_L/2 \ , \qquad (-\infty < f < \infty) \tag{5.7}$$

for the {2x2} receiver and

$$N_2 = eRP_L/3 \ , \qquad (-\infty < f < \infty) \tag{5.8}$$

for the {3x3} receiver, where e is the electron charge.

In this case of ASK demodulation, the low-pass filters, which follow the photodiodes, are assumed to pass all the signal power. For negligible laser linewidths (much smaller than the bit rate), a filter matched to rect(t) may be applied. Its impulse response is also rectangular and is given by

$$h(t) = \begin{cases} 1/T_0 & \text{for } 0 < t < T_0 \ , \\ 0 & \text{elsewhere.} \end{cases} \tag{5.9}$$

Under the above restrictions, the noise power at the output of each low-pass filter can be calculated to be

$$\langle n_1^2 \rangle = N_1.B = eRP_LB/2 \ , \qquad i = 0,1 \tag{5.10}$$

for the {2x2} receiver and

$$\langle n_i^2 \rangle = N_2.B = eRP_L B/3 \ , \qquad i = 0,1,2 \tag{5.11}$$

for the (3x3) receiver. Here B is the double-sided receiver bandwidth, which is defined by $1/T_0$. For mathematical convenience, the noise power is normalized to unit noise variance. The signal part of the Equations (5.1) and (5.2) can now be rewritten to give

$$s_0(t) = \sqrt{2SNR}.b(t).\cos[\gamma(t)] \ , \tag{5.11}$$

$$s_1(t) = \sqrt{2SNR}.b(t).\cos[\gamma(t) - (\frac{\pi}{2} - \phi)] \ , \tag{5.12}$$

where $SNR = \frac{RP_s}{eB}$ is the Signal-to-Noise Ratio of the (2x2) receiver which in this case of matched filtering, is equal to the number of signal photons received in a "1" bit. Performing the same procedure for the (3x3) receiver results in the following values for the signals

$$s_0(t) = 2\sqrt{SNR/3}.b(t).\cos[\gamma(t)] \ , \tag{5.13}$$

$$s_1(t) = 2\sqrt{SNR/3}.b(t).\cos[\tfrac{2}{3}\pi + \gamma(t) + \phi_1] \ , \tag{5.14}$$

$$s_2(t) = 2\sqrt{SNR/3}.b(t).\cos[\tfrac{4}{3}\pi + \gamma(t) + \phi_2] \ . \tag{5.15}$$

Here SNR is the signal-to-noise ratio of the (3x3) receiver. Provided a perfect gain balance (i.e. $\delta = 0$) and ideal phase relations (i.e. $\phi = 0$), it can be easily checked that for the shot noise limited case, the signal value at the input of the threshold comparator is constant for both receiver structures. This can be visualized by calculating the signal value at the input of the threshold comparator $V_{thres}(t)$, which is the sum of the squares of the signal values $s_i(t)$ $(i = 0,1,(2))$. For both receiver structures, this is given by the following relation

$$V_{thres}(t) = \sum_i s_i^2(t) = 2SNR \ . \qquad i = 0,1,(2) \tag{5.16}$$

After the introduction of the gain imbalance and the phase mismatch in the

way it has been discussed above, Equation (5.16) only holds if we take the sum of the MEAN squared values of the signal parts of Equation (5.1) and (5.2) for the {2x2} receiver. For the {3x3} receiver have to be taken the signal parts of the Equations (5.3) to (5.5). From the preceding it can be concluded, that $V_{thres}(t)$ averaged over the period time (T_{IF}) of $\gamma(t)$ equals 2SNR. Within this time interval T_{IF}, $V_{thres}(t)$ varies, which also includes a BER which changes in time. A more detailed study of the Equations (5.11) to (5.15) shows that in case of nonzero phase offset $\gamma(t)$, $V_{thres}(t)$ and the BER have a time varying character, which is determined by the radial offset frequency ω_{IF}. Since the BER of a particular receiver is measured over a large number of samples of the momentary BER, the problem of an IF dependent BER can be solved by averaging over one time interval T_{IF}, which is equal to $2\pi/\omega_{IF}$. For near baseband operation, the restriction that the bit period is much smaller than T_{IF}, is automatically fulfilled.

The Equations (5.11) to (5.15) are sufficient to calculate the BER of the diversity receivers. If the probability of sending a mark is equal to the probability of sending a space, the BER of the receivers is determined by the following relation

$$BER = \frac{1}{2}\left(P(V_{sample} > T \mid b_k = 0) + P(V_{sample} \leq T \mid b_k = 1)\right) , \qquad (5.17)$$

where T is the threshold level, and V_{sample} represents the realization of the stochastic process at the input of the threshold comparator. The term $P(V_{sample} > T \mid b_k = 0)$ is the probability of receiving a mark whereas a space is sent. $P(V_{sample} \leq T \mid b_k = 1)$ is the probability of receiving a space whereas a mark is sent.

5.3 The error probability of the {2x2} phase diversity ASK receiver

For the {2x2} diversity ASK receiver (Figure 5.1), the realization of the stochastic process at the input of the threshold comparator is given by $x^2(t) + y^2(t)$, where $x(t) = s_0(t) + n_0(t)$ and $y(t) = s_1(t) + n_1(t)$.

In case a space is sent ($b_k = 0$ and $s_0(t) = s_1(t) = 0$), the process at the input of the threshold comparator is the sum of two squared independent and

Gaussian distributed variables with zero-mean and unit variances. The resulting PDF can be written as a chi-square [5.2]. However, if gain imbalance is included, the resulting PDF changes due to the unequal variances. One with unit variance (related to the reference receiver branch) and one with a variance equal to $(1+\delta)^2$. From Figure 5.1 it can be concluded that $p \triangleq x$ and $q \triangleq (1+\delta)y$. Since in this case the signal values $s_0(t)$ and $s_1(t)$ are equal to zero, the phase mismatch (ϕ) has *no* influence on the PDF. Making use of some conventional mathematics, and the fact that the realization of the process at the input of the threshold comparator is equal to $p^2 + q^2$, the PDF can be calculated resulting in a twofold integral for the conditional error probability P_0. This integral consists of the joint probability density function of the Gaussian distributed variables p and βq.

$$P_0 = \frac{\beta}{2\pi} \iint_V \exp[-p^2/2].\exp[-(\beta q)^2/2]\ dp.dq\ , \qquad (5.18)$$

where $\beta = 1/(1+\delta)$ and δ stands for the gain imbalance. The integration region is given by $V = p^2 + q^2 > T$, where T is the threshold, which is set at $2k^2SNR$, and k is a parameter to be optimized. For an ideal {2x2} phase diversity ASK receiver and a BER = 10^{-9}, parameter k is set at 0.520 [5.2].
In case a mark is sent ($b_k = 1$), the conditional error probability P_1, for the same threshold T, is equal to the probability that the realization of the process at the input of the threshold comparator is less than T. The signal values $s_0(t)$ and $s_1(t)$ are functions of $\gamma(t)$, the radial frequency and phase offset, and $s_1(t)$ also of ϕ the phase mismatch (we write $s_0(\gamma)$ and $s_1(\gamma,\phi)$, see below Equation (5.2)). The expression for this probability is somewhat more difficult to compute, because of the time varying character. Following the same procedure as for the conditional error probability P_0, the conditional error probability P_1 as a function of $s_0(\gamma)$ and $s_1(\gamma,\phi)$, $P_1(\gamma,\phi)$, is given by

$$P_1(\gamma,\phi) = \frac{\beta}{2\pi}.\exp[-(s_0^2(\gamma) + s_1^2(\gamma,\phi))/2] \times$$

$$\iint_W \exp[-p(p-2s_0(\gamma))/2].\exp[-\beta q(\beta q-2s_1(\gamma,\phi))/2]\ dp.dq\ , \qquad (5.19)$$

where the integration region is $W = p^2 + q^2 \leq T$ and $\beta = 1/(1+\delta)$. Since $s_0(\gamma)$ and $s_1(\gamma,\phi)$ are periodical trigonometric functions with period time T_{IF}, $P_1(\gamma,\phi)$ will also show a periodical character. Therefore, it suffices to average $P_1(\gamma,\phi)$ just over one period time T_{IF} of $s_0(\gamma)$ or $s_1(\gamma,\phi)$. The time averaged value of $P_1(\gamma,\phi)$ is then given by

$$\langle P_1(\gamma,\phi)\rangle = \frac{1}{T_{IF}} \int_0^{T_{IF}} P_1(\gamma,\phi)\, d\gamma \ . \qquad (5.20)$$

Figure 5.4 has been obtained by numerical integration of Equation (5.20). In Figure 5.4a, $P_1(\gamma,\phi)$ is depicted for $\gamma(t)$ in the interval $[0,360^\circ]$, the threshold parameter k set to 0.520, a gain imbalance of +10% or -10% (in the sequel we write +/-..%), and a phase mismatch $\phi = 0^\circ$.

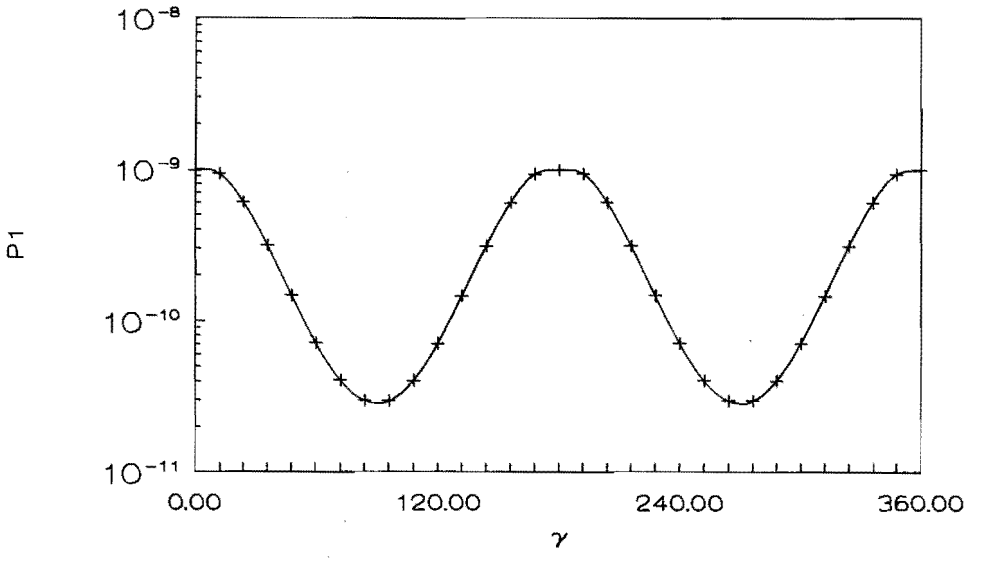

Figure 5.4 *(a) The conditional error probability P_1 versus γ for a gain imbalance of +10% and zero phase mismatch.*

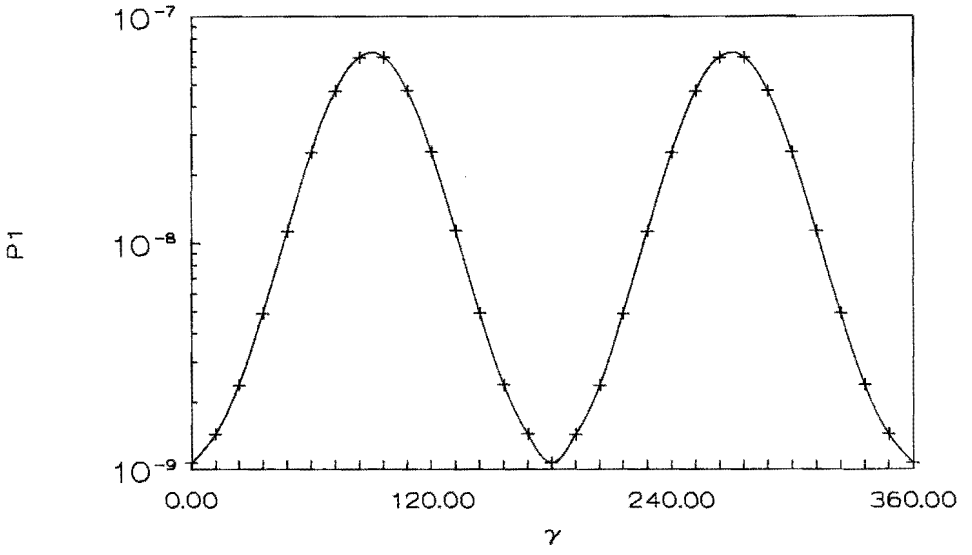

Figure 5.4 *(b) The conditional error probability P_1 versus γ for a gain imbalance of -10% and zero phase mismatch.*

From this figure it can be concluded, that due to the symmetrical and periodical structure of the curve, an averaging interval of 180° can be chosen. The value for the SNR is chosen so, that without gain imbalance the BER is equal to 10^{-9}. It can firstly be concluded that, in case of positive gain imbalance (Figure 5.4a), P_0 ($\cong 1.5\times10^{-9}$) determines the BER, because the maximum value of $P_1(\gamma,0)$ is less than 10^{-9}. Secondly, the conditional error probability $P_1(\gamma,0)$ has its maximum value for $\gamma(t) = \frac{\pi}{2} + k.\pi$, and k an integer (k = 0,1,2...). For negative gain imbalance the reverse is true, and the BER is determined by $P_1(\gamma,0)$ (Figure 5.4b). In Figure 5.5, $P_1(\gamma,\phi)$ is depicted for zero gain imbalance and a phase mismatch of 5°. It can be concluded that $P_1(\gamma,0)$ is periodic with 180°. The conditional error probability P_0 is constant and has been computed to be 1.19×10^{-9}.

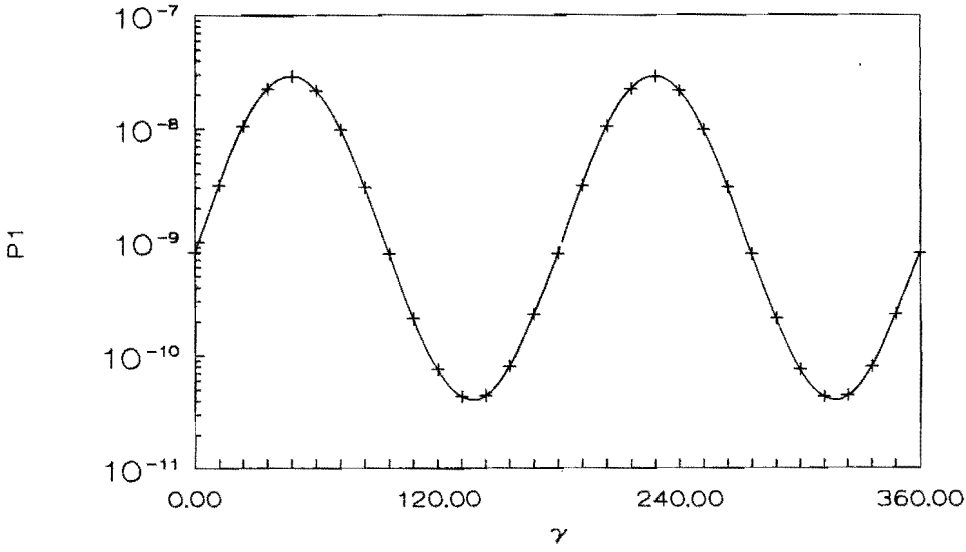

Figure 5.5 *The conditional error probability P_1 versus γ for zero gain imbalance and a phase mismatch of 5°.*

Inserting Equation (5.19) in Equation (5.20) leads to the following relation for the average conditional error probability $\langle P_1(\gamma,\phi)\rangle$

$$\langle P_1(\gamma,\phi)\rangle = \frac{\beta}{2\pi^2}\int_0^{\pi} \exp[-(s_0^2(\gamma) + s_1^2(\gamma,\phi))] \times$$

$$\iint_W \exp[-p(p-2s_0(\gamma))/2].\exp[-\beta q(\beta q-2s_1(\gamma,\phi))/2]\ dp.dq.d\gamma\ . \qquad (5.21)$$

The average BER can now be written as

$$BER = \frac{1}{2}\left(P_0 + \langle P_1(\gamma,\phi)\rangle\right)\ . \qquad (5.22)$$

Unfortunately, the equation for the BER is rather complicated and for this reason, numerical integration was necessary. For BER = 10^{-9}, the sensitivity penalty is computed with respect to the ideal phase diversity ASK receiver for an optimized threshold value (optimized in the presence of gain imbalan-

ce and a phase mismatch) and a non-optimized threshold value (assumed are a perfect gain balance and ideal phase relations). Optimization of the threshold value implies that the threshold level T is chosen such, that the conditional error probabilities P_0 and $\langle P_1(\gamma,\phi)\rangle$ are equal for a BER = 10^{-9}, which implies that the BER becomes independent of the bit pattern.

Gain imbalance

In Figure 5.6, the results are presented for positive and negative percentages of gain imbalance, zero phase mismatch and a BER = 10^{-9}. For a non-optimized threshold value, the degradation due to negative gain imbalance is much worse in comparison with positive gain imbalance. Optimization of the threshold value greatly reduces the sensitivity penalty to approximately 3 dB for a gain imbalance of -50% and approximately 1.5 dB for a gain imbalance of 50%.

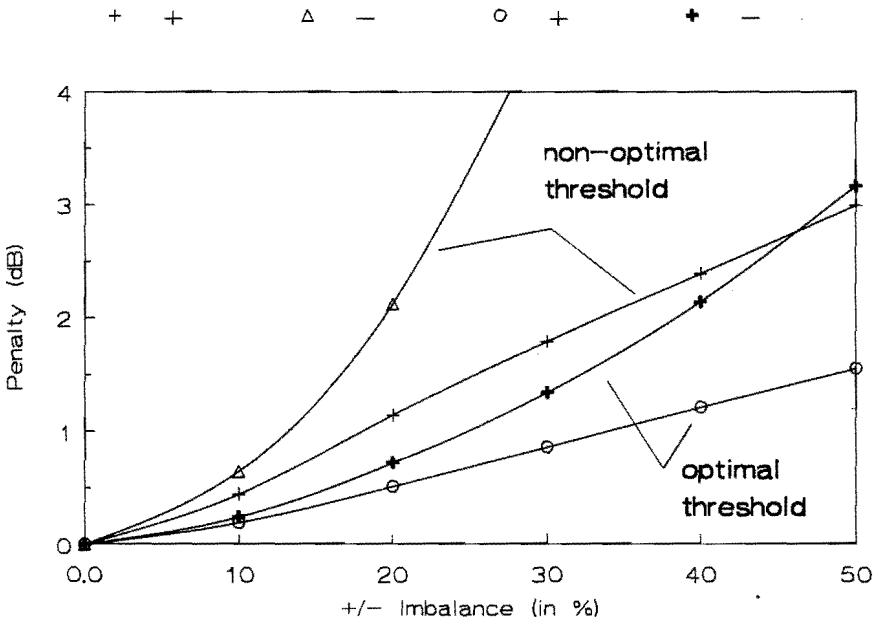

Figure 5.6 *Sensitivity penalty for a (2x2) receiver, for various (+) values of the gain imbalance, and zero phase mismatch.*

Phase mismatch

In Figure 5.7 the sensitivity degradation is depicted for a phase mismatch, varying from 0° to +/-10°, (non-)optimized threshold values, and an optimal gain balance. For a non-optimized threshold value, the degradation for a phase mismatch of +/-10° is approximately 1.2 dB, whereas for an optimized threshold value, this penalty can be reduced to approximately 0.6 dB.

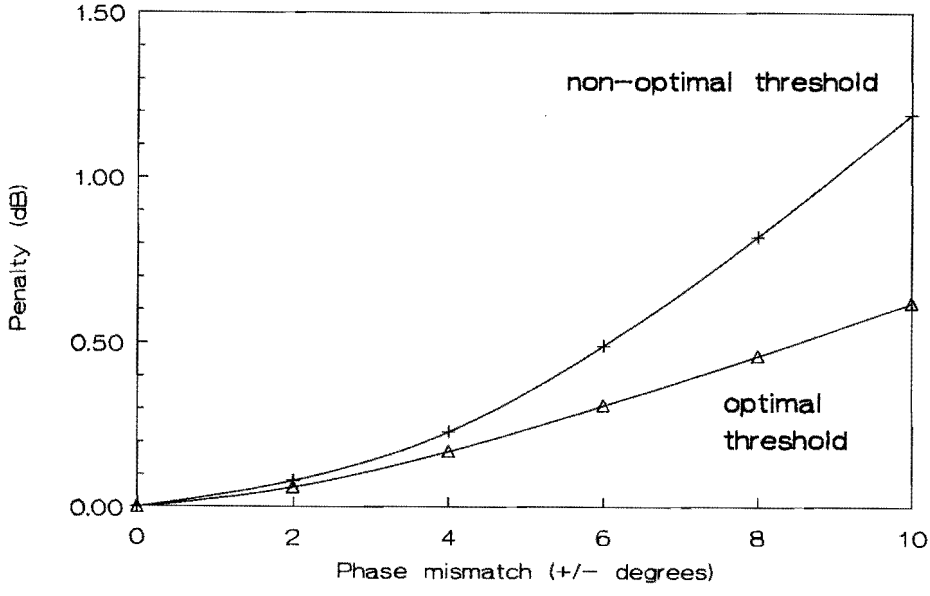

Figure 5.7 *Sensitivity penalty for a {2x2} receiver, for various (+) values of the phase mismatch, and zero gain imbalance.*

Gain imbalance and phase mismatch

So far the sensitivity degradation due to both imperfections has been dealt with separately. In practice both imperfections can occur simultaneously, however, their influence on $P_1(\gamma,\phi)$ is different and correlated as will be shown later. The results for non-optimized threshold values, a gain imbalance of +/-5% and +/-10%, and a phase mismatch varying from 0° to +/-10°, are presented in Figure 5.8.

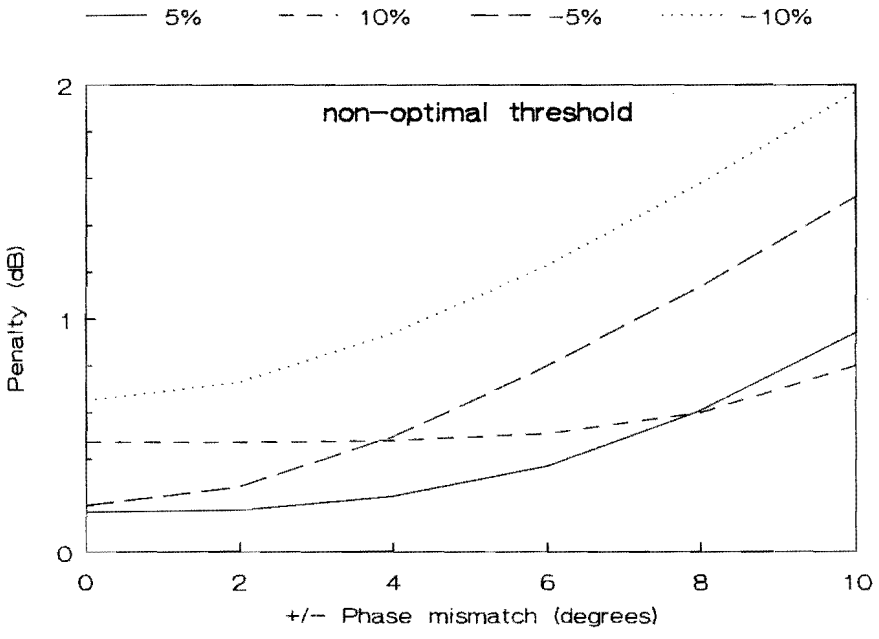

Figure 5.8 *Sensitivity penalty for a {2x2} receiver, for various combinations of phase mismatch and gain imbalance, and non-optimal threshold values.*

From this figure, it can be concluded that for positive gain imbalance the degradation is well below 1 dB for a phase mismatch less than 10°. For approximately 8°, the curves intersect and the penalty for a gain imbalance of 5% becomes worse than that for 10%. The latter is due to the threshold value, which should be optimized for optimal performance. The explanation is that for increasing phase mismatch, the optimal value for the threshold parameter k (see below Equation (5.18)) in case of 10% imbalance is closer to 0.520 than that for 5% imbalance. Besides, the gain imbalance and the phase mismatch are correlated. For an optimized threshold value, the latter will not occur as shown in the Figures 5.9 and 5.11. For negative imbalance, the sensitivity penalty is worse, but still less than 2 dB.

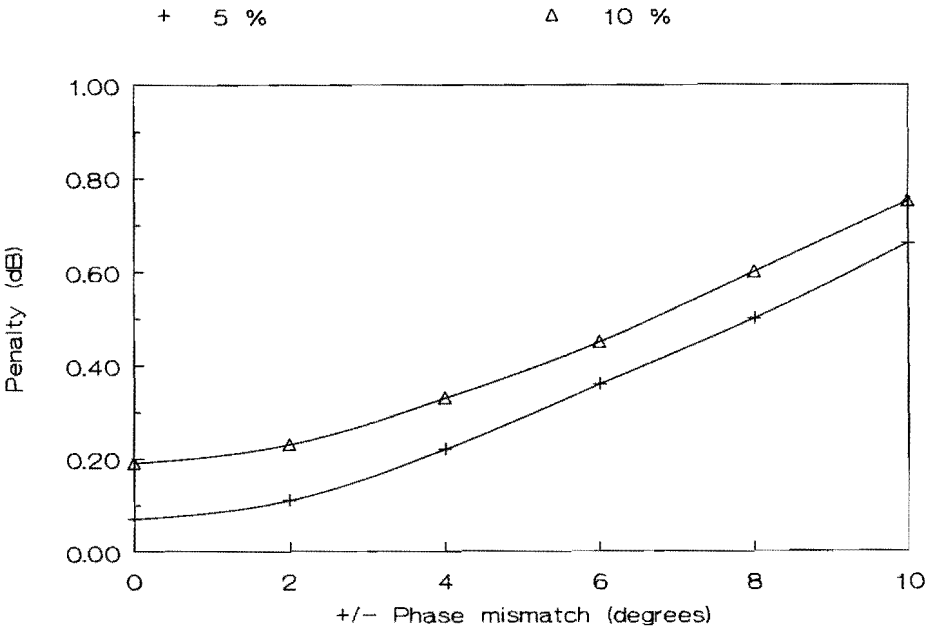

Figure 5.9 *Sensitivity penalty for a (2x2) receiver, a gain imbalance of 5% and 10%, and a phase mismatch varying from 0° to +/-10°, and optimal threshold values.*

A comparison of Figure 5.9 with the Figures 5.6 and 5.7 reveals that, for a BER = 10^{-9}, the sensitivity degradation due to (positive) gain imbalance and a phase mismatch is less than the sum of both imperfections separately. This has been visualized in the Figures 5.10a to 5.10d. In each of these figures two circles/ellipses are depicted. The outermost circle/ellipse represents the realization, $i_0^2(t) + i_1^2(t)$, of the process at the input of the threshold comparator, in case a mark is sent, and all the noise influences have been neglected. Under the same restriction, the origin represents the realization of the process at the input of the threshold comparator in case a space is sent. The innermost circle/ellipse equals the relation $i_0^2(t) + i_1^2(t) = T$ for a fixed threshold level (T). The conditional probability of error, P_0, is determined by the shortest distance, d_0, between the origin (point [0,0]) and the innermost curve. We can write $P_0 \propto \exp(-d_0^2/2)$. The conditional error

probability, $P_1(\gamma,\phi)$, is determined by the shortest distance, d_1, between the innermost and the outermost curve, and is given by $P_1(\gamma,\phi) \propto \exp(-d_1^2/2)$. It can then be concluded from Figure 5.10b, that in comparison with the ideal situation of Figure 5.10a, for a gain imbalance of 10% and zero phase mismatch, the minimum distance d_1 remains unchanged while d_0 decreases. This implies that P_0 increases while $P_1(\gamma,\phi)$ remains unchanged. In Figure 5.10c, the configuration is depicted for zero gain imbalance and a phase mismatch of 10°. It can be concluded, that the minimum distance, d_1, substantially decreases while d_0 almost remains constant. In this case, the conditional error probability, $P_1(\gamma,\phi)$, determines the total BER. For a combination of 10% gain imbalance and 10° phase mismatch, the configuration is given in Figure 5.10d. The distance d_0 equals the situation of 10% gain imbalance and zero phase mismatch, while d_1 has increased in comparison with Figure 5.10c. For this reason, the sensitivity degradation for the combination of both imperfections is less than the sum of the degradations of both imperfections separately (Figure 5.10b and 5.10c).

For a negative percentage gain imbalance of 10%, and a negative phase mismatch of 10°, the configurations are given in the Figures 5.10e to 5.10g. It can be concluded, that in this case the sensitivity penalty due to both imperfections is more pronounced than to each of these imperfections separately. The minimum distance, d_0, remains constant in these figures. However, in comparison with the Figures 5.10e and 5.10f, the minimum distance, d_1, in Figure 5.10g is significantly smaller. The latter agrees with our computations. From Figure 5.6 we have a penalty of approximately 0.6 dB for a gain imbalance of -10%. From Figure 5.7, it can be concluded, that a phase mismatch of -10° results in a penalty of approximately 1.2 dB. The combination of both imperfections results in a penalty of approximately 2 dB, as can be concluded from Figure 5.8, and is approximately 0.2 dB worse than the sum of both imperfections separately.

For the {2x2} phase diversity receiver analyzed, it can be concluded from the Figures 5.9 and 5.11, that for a gain imbalance of less than +/-10% and a phase mismatch of less than $+/-10^\circ$, the sensitivity degradation is approximately 0.80 dB for a BER = 10^{-9}, and an optimized threshold value.

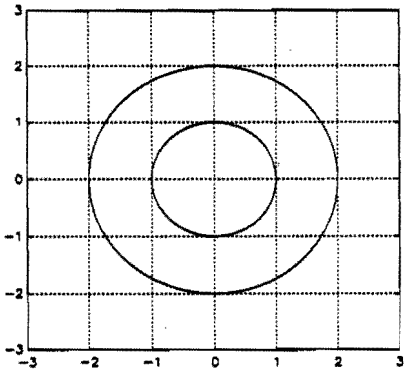

(a) (0%, 0°)

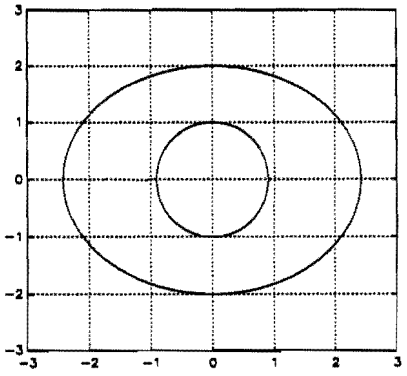

(b) (10%, 0°)

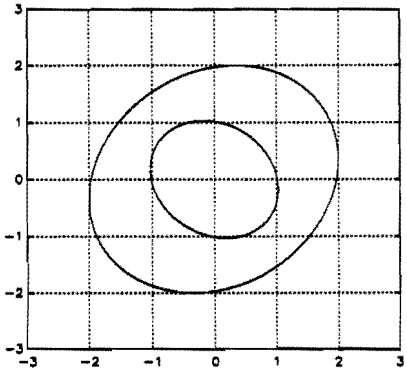

(c) (0%, 10°)

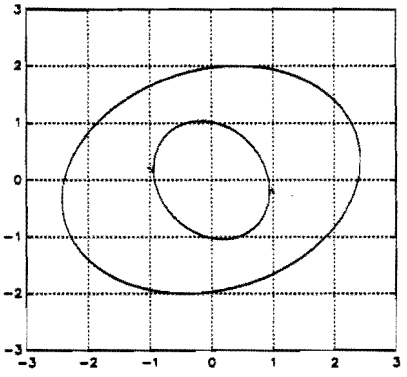

(d) (10%, 10°)

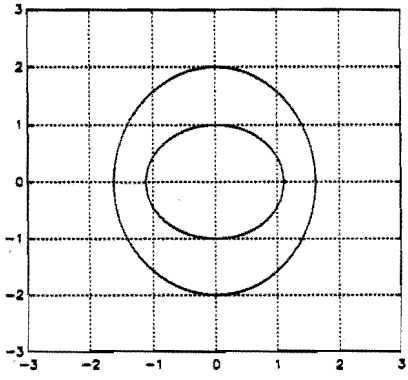

(e) (-10%, 0°)

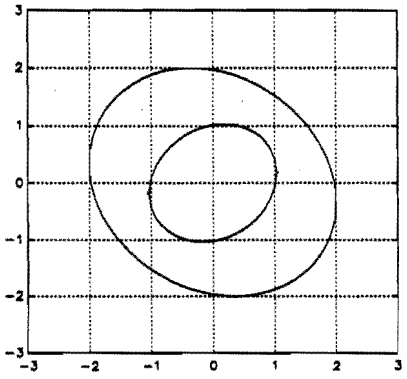

(f) (0%, -10°).

Figure 5.10 *Geometrical visualization of the conditional error probabilities* P_0 *and* $P_1(\gamma,\phi)$ *for the {2x2} phase diversity ASK receiver.*

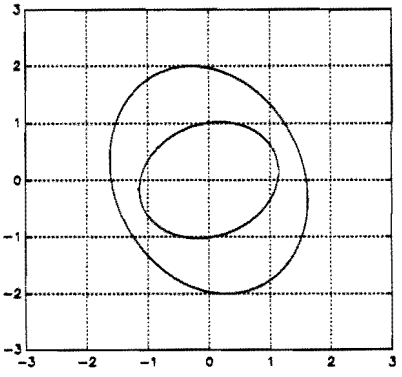

(g) (-10%, -10°)

Figure 5.10g *Geometrical visualization of the conditional error probabilities P_0 and $P_1(\gamma,\phi)$ for the {2x2} phase diversity ASK receiver.*

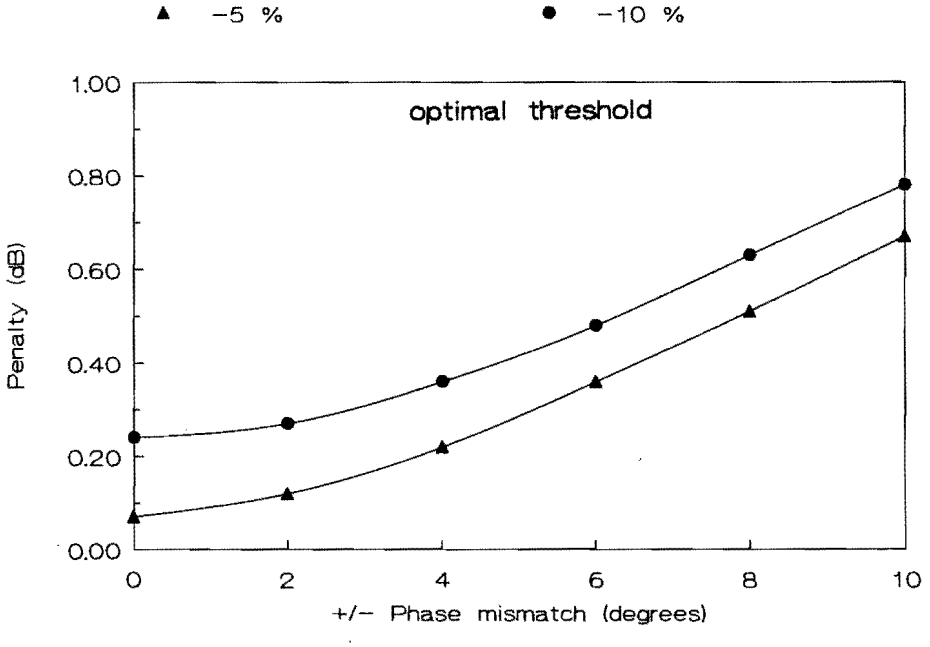

Figure 5.11 *Sensitivity penalty for a {2x2} receiver, a gain imbalance of -5% and -10%, a phase mismatch varying from 0° to +/-10°, and optimal threshold values.*

5.4 The error probability of the {3x3} phase diversity ASK receiver

Following the same procedure as for the {2x2} receiver, the realization of the stochastic process at the input of the threshold comparator can be written as $x^2(t) + y^2(t) + z^2(t)$ for zero gain imbalance and phase mismatch, where $x(t) = s_0(t) + n_0(t)$, $y(t) = s_1(t) + n_1(t)$ and $z(t) = s_2(t) + n_2(t)$. From Figure 5.1 it can be concluded, that after the introduction of the gain imbalance, $p \triangleq x$, $q \triangleq (1+\delta)y$ and $r \triangleq (1+\delta)z$.

In case a space is sent, $s_0(t) = s_1(t) = s_2(t) = 0$ and the phase mismatch (ϕ) has *no* influence on the PDF. The realization of the process at the input of the threshold comparator is that of the sum of three squared Gaussian distributed and independent variables with zero means, and variances equal to 1, $(1+\delta)^2$ and $(1+\delta)^2$, respectively. The conditional error probability P_0 is the probability that the realization of the process at the input of the threshold comparator is larger than the threshold T. The resulting equation for P_0 is a threefold integral of the product of three Gaussian functions given by

$$P_0 = \frac{\beta^2}{(2\pi)^{3/2}} \iiint_V \exp[-\{p^2 + (\beta q)^2 + (\beta r)^2\}/2]\, dp.dq.dr \ , \qquad (5.23)$$

where $\beta = 1/(1+\delta)$, and δ is the gain imbalance. $V = p^2 + q^2 + r^2 > T$ stands for the integration region and T is the threshold level ($T = 2k^2SNR$). Rewriting Equation (5.23), and using some conventional mathematics, results in the following integral for the conditional error probability P_0 (see Appendix 5A for detailed derivation)

$$P_0 = 1 - \frac{1}{(2\pi)^{1/2}} \int_{-\sqrt{T}}^{\sqrt{T}} \exp[-p^2/2].\left[1 - \exp[-\beta^2(T - p^2)/2]\right] dp \ . \qquad (5.24)$$

In case a mark is sent, the probability of error as a function of $\gamma(t)$, the radial frequency and phase offset, and ϕ the phase mismatch, $P_1(\gamma,\phi)$, is the conditional error probability that the realization of the process at the

input of the threshold comparator is less than T. The process is the sum of three squared Gaussian distributed variables, which are independent, with nonzero means and unequal variances due to the gain imbalance (see above Equation (5.23)). The resulting equation for the conditional error probability $P_1(\gamma,\phi)$ is given by

$$P_1(\gamma,\phi) = \frac{\beta^2}{(2\pi)^{3/2}} \int_{-\sqrt{T}}^{\sqrt{T}} \exp[-(p-s_0(\gamma))^2/2] \times$$

$$\iint_W \exp[-(\beta^2(q^2+r^2)-2\beta[qs_1(\gamma,\phi)+rs_2(\gamma,\phi)]+s_1^2(\gamma,\phi)+s_2^2(\gamma,\phi))/2]\ dp.dq.dr, \tag{5.25}$$

where $W : q^2 + r^2 \le T - p^2$ the integration region and $\beta = 1/(1+\delta)$. Changing coordinates, and using the integral representation of the modified Bessel function, results in the following twofold integral for $P_1(\gamma,\phi)$ (see Appendix 5B for detailed derivation)

$$P_1(\gamma,\phi) = \frac{\beta^{3/2}}{2\pi\sqrt{\xi}} \int_{-\sqrt{T}}^{\sqrt{T}} \exp[-(p-s_0(\gamma))^2/2].\int_0^{(T-p^2)^{1/2}} \sqrt{s}.\exp[-(\beta s-\xi(\gamma,\phi))^2/2]\ dp.ds\ , \tag{5.26}$$

where $\xi(\gamma,\phi) = [s_1^2(\gamma,\phi) + s_2^2(\gamma,\phi)]^{1/2}$, and $\beta = 1/(1+\delta)$. Applying the same procedure as for the (2x2) receiver, the time averaged value of the conditional error probability $P_1(\gamma,\phi)$, $\langle P_1(\gamma,\phi)\rangle$, is then given by

$$\langle P_1(\gamma,\phi)\rangle = \frac{\beta^{3/2}}{2\pi^2\sqrt{\xi}} \int_0^{\pi}. \int_{-\sqrt{T}}^{\sqrt{T}} \exp[-(p - s_0(\gamma))^2/2] \times$$

$$\int_0^{(T-p^2)^{1/2}} \sqrt{s}.\exp[-(\beta s - \xi(\gamma,\phi))^2/2]\ dp.ds.d\gamma\ . \tag{5.27}$$

The BER can then be calculated according to Equation (5.22). The results for zero phase mismatch and a gain imbalance varying from 0 to +/-50%, are

depicted in Figure 5.12. Since in this case the phase mismatch is zero, these results are valid for the *symmetrical* configuration as well as for the *non-symmetrical* configuration of the photocurrents (see below Equation (5.5)).

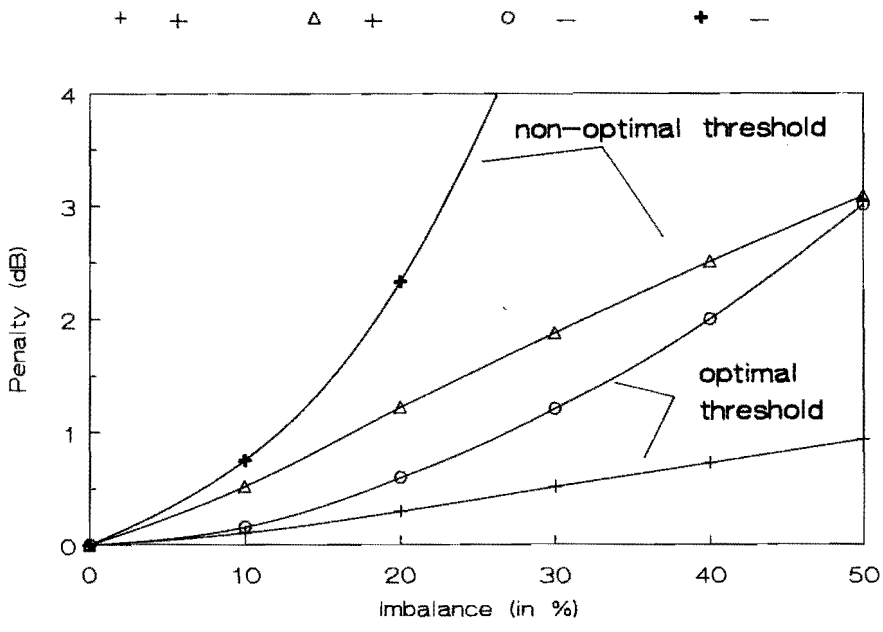

Figure 5.12 *Sensitivity penalty for the {3x3} receiver with zero phase mismatch and a gain imbalance varying from 0 to +/-50%.*

For positive and negative percentages of gain imbalance, the sensitivity degradation has been calculated for an optimized and a non-optimized threshold value (k = 0.535, [5.2]). From Figure 5.12, it can be concluded that the degradation due to negative gain imbalance is much worse than the degradation due to positive values of gain imbalance. The impact can be greatly reduced by an optimization of the threshold value. For +/-10% gain imbalance, the penalty can be reduced to approximately 0.1 dB for positive values of gain imbalance, and approximately 0.5 dB for negative values of gain imbalance. In case of nonzero phase mismatch, one has to distinguish the two configurations of the photocurrents as mentioned below Equation (5.5).

5.4.1 The non-symmetrical configuration of the photocurrents

In Figure 5.13 the sensitivity degradation is given for nonzero phase mismatch and zero gain imbalance.

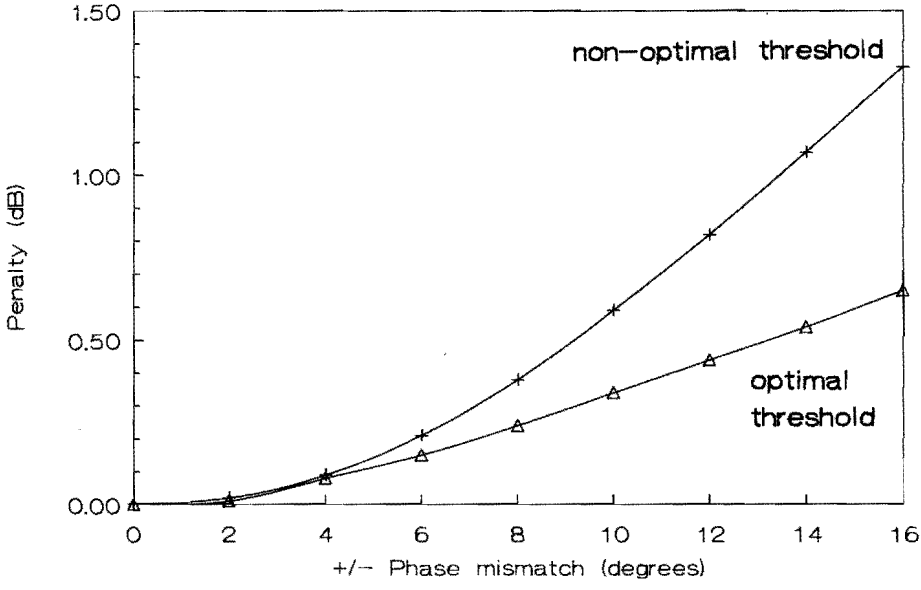

Figure 5.13 *Sensitivity penalty for the {3x3} receiver for zero gain imbalance and a phase mismatch varying from 0° to +/-16°.*

For a phase mismatch of +/-16°, and a non-optimized threshold value, the penalty is less than 1.4 dB. By optimization of the threshold level, the degradation can be reduced to approximately 0.7 dB. The sensitivity penalty due to both imperfections has been computed for a gain imbalance of +/-5%, +/-10%, and a phase mismatch varying from 0 to +/-16°. The results are shown in the Figures 5.14 and 5.15 for optimized and non-optimized values of the threshold level and a BER = 10^{-9}.

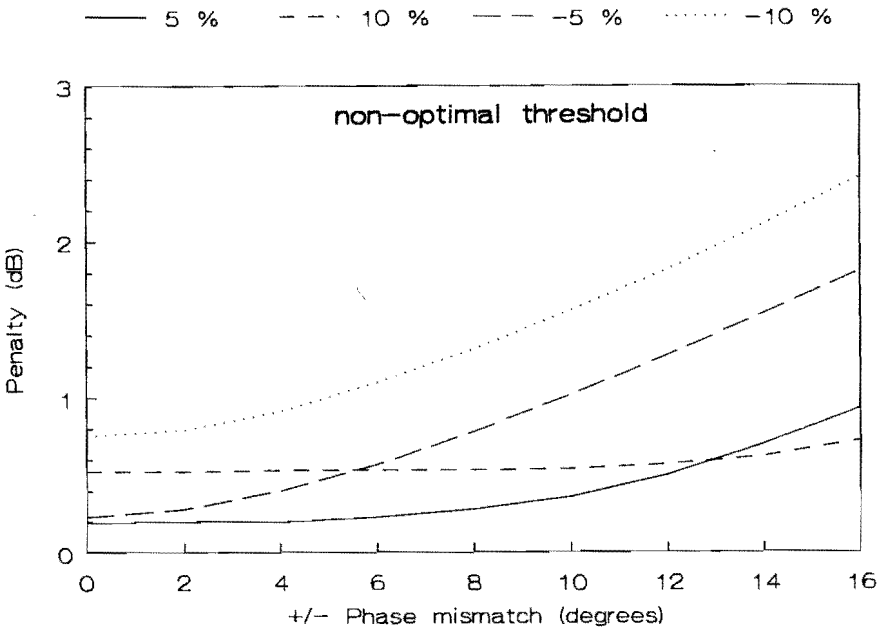

Figure 5.14 *Sensitivity penalty for the {3x3} receiver for various combinations of gain imbalance and phase mismatch, and non-optimal threshold levels.*

The sensitivity degradation is computed with respect to the ideal {3x3} phase diversity ASK receiver. For positive gain imbalance (Figure 5.14), the curves are flat over a wide range of the phase mismatch. For a phase mismatch of approximately 13°, both curves intersect and the penalty for a gain imbalance of 10% becomes smaller than that for a gain imbalance of 5%. This is due to the non-optimized threshold value, which has already been discussed for the {2x2} receiver. For a gain imbalance of 5% and 10%, respectively, the penalty is less than 1 dB for a phase mismatch smaller than 16°. For a gain imbalance of -5% and -10%, respectively, the penalty, under the same conditions, is less than approximately 2.5 dB.

In Figure 5.15 the results are depicted for optimized threshold values and the same values for the phase mismatch and the gain imbalance as in the previous figure. The sensitivity degradation remains well below 0.9 dB.

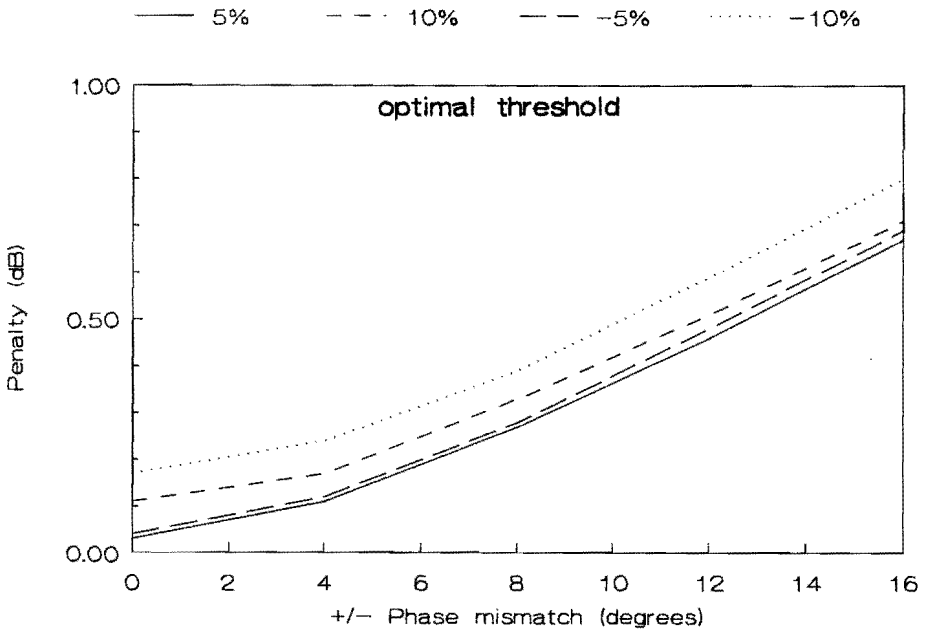

Figure 5.15 *Sensitivity penalty for the {3x3} receiver for various combinations of gain imbalance and phase mismatch, and optimal threshold levels.*

5.4.2 The symmetrical configuration of the photocurrents

In the case of a symmetrical configuration of the photocurrents, one should distinguish positive and negative values of the phase mismatch. The sensitivity degradation has been computed for a phase mismatch varying from 0° to $+/-16^{\circ}$, and a BER = 10^{-9}. The results are given in Figure 5.16 for both situations where the threshold value both has and has not been optimized.

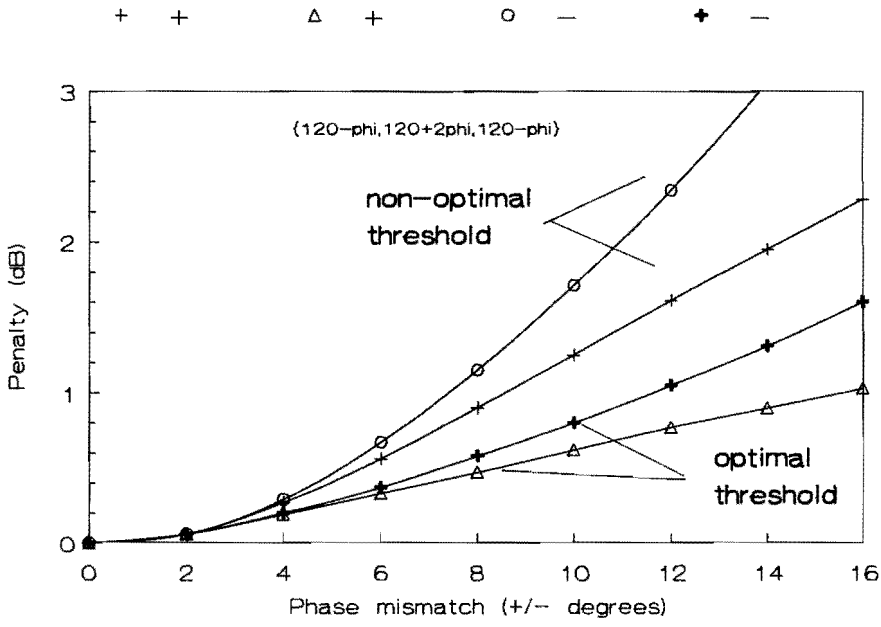

Figure 5.16 *Sensitivity penalty for the {3x3} receiver for zero gain mismatch and a phase mismatch varying from 0° to +/-16°.*

The curves show the same behaviour as for the non-symmetrical configuration, except for the fact that in this case, the penalties are somewhat larger. For an optimized threshold value, the penalty is approximately 1 dB for a phase mismatch of 16°, and 1.6 dB for a phase mismatch of -16°. For both a phase mismatch and a gain imbalance, the results are presented in Figure 5.17 for a non-optimized threshold value.

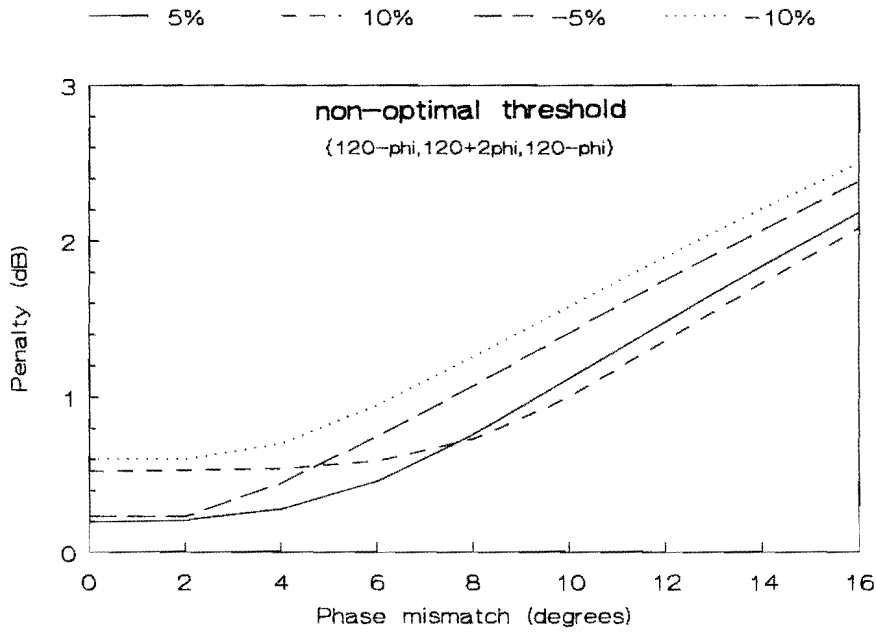

Figure 5.17 *Sensitivity penalty for the {3x3} receiver for various combinations of gain imbalance and (+) phase mismatch, and non-optimal threshold levels.*

In comparison with Figure 5.14, the degradation for large values of phase mismatch becomes more pronounced, and the curves for the different values of gain imbalance merge. The same curves have also been computed for optimized threshold values and are depicted in Figure 5.18.

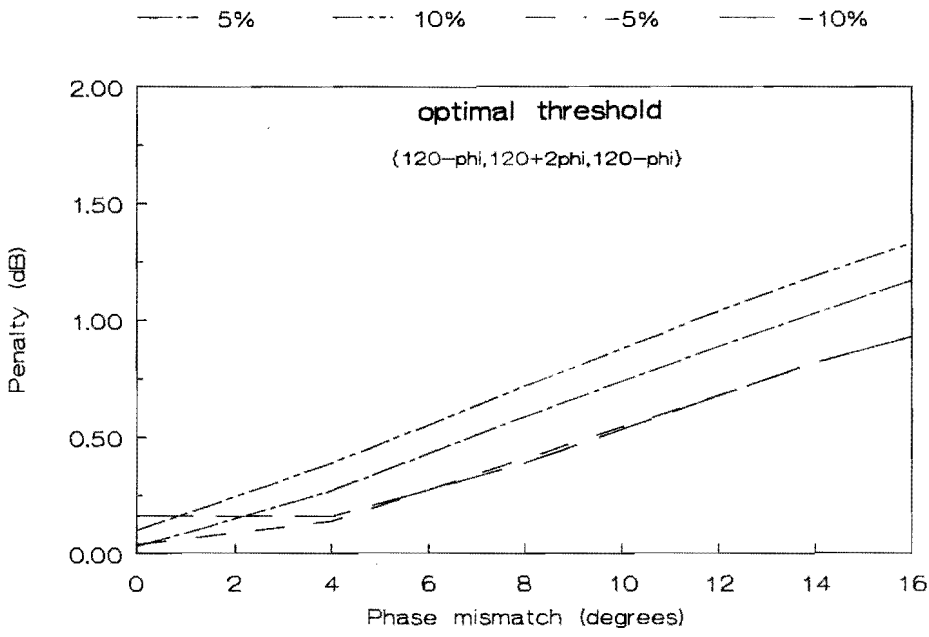

Figure 5.18 *Sensitivity penalty for the (3x3) receiver for various combinations of gain imbalance and (+) phase mismatch, and optimal threshold levels.*

The main difference with Figure 5.17 is that in this case, the degradation due to negative values of gain imbalance is less than for positive values of gain imbalance, this in contrary with Figure 5.17. Similar curves as shown in the Figures 5.17 and 5.18 have been computed for negative values of phase mismatch and show a larger sensitivity penalty than in case of positive values of the phase mismatch (Figures 5.19 and 5.20).

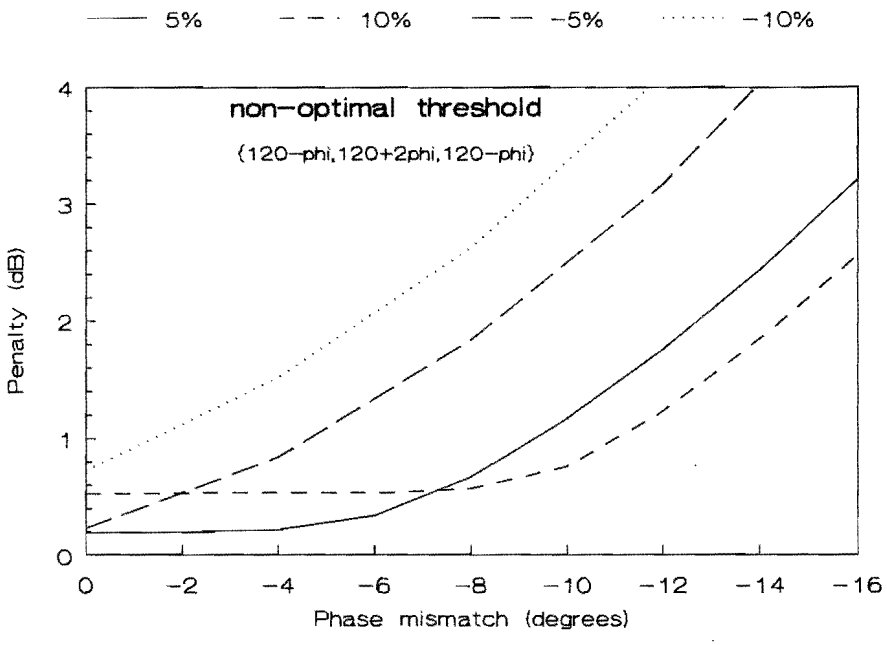

Figure 5.19 *Sensitivity penalty for the {3x3} receiver for various combinations of gain imbalance and (-) phase mismatch, and non-optimal threshold levels.*

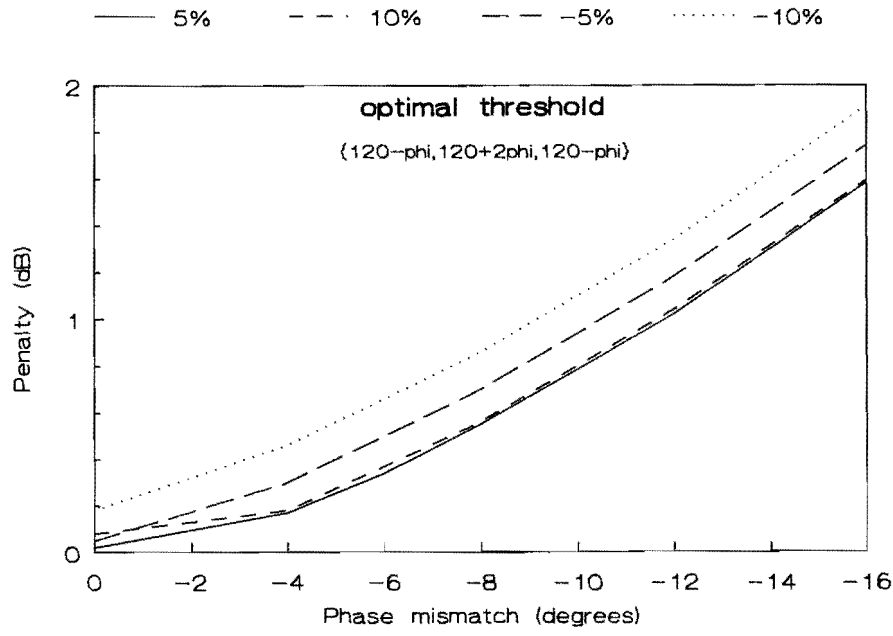

Figure 5.20 *Sensitivity penalty for the (3x3) receiver for various combinations of gain imbalance and (-) phase mismatch, and optimal threshold levels.*

5.5 Discussion

Based on the results presented in the previous sections, upper-bounds for the gain imbalance and the phase mismatch in both receiver structures can be found. We choose as criteria for the maximum allowable combination of phase mismatch and gain imbalance in the phase diversity ASK receivers analyzed, that combination which increases the signal power P_s required to achieve a BER = 10^{-9} by maximal 0.5 dB. In the Tables 5.1 and 5.2, maximum values for the phase mismatch are presented, for a gain imbalance of +/-5% and +/-10%, respectively.

TABLE 5.1

Maximum allowable phase mismatch for a {2x2} and a {3x3} phase diversity ASK receiver as a function of the gain imbalance. BER = 10^{-9}, non-optimal threshold, penalty margin = 0.5 dB

Gain imbalance	0%	5%	10%	-5%	-10%
{2x2} ASK receiver	±6.0°	±7.0°	±5.5°	±4.0°	-----
{3x3} ASK receiver non-symmetrical configuration	±9.0°	±11.8°	----	±4.5°	-----
{3x3} ASK receiver symmetrical configuration	5.5°	6.2°	----	4.0°	-----
	-5.0°	-7.0°	----	-1.5°	-----

---- = not possible within a penalty margin of 0.5 dB

± = for positive and negative values of the phase mismatch

TABLE 5.2

Maximum allowable phase mismatch for a {2x2} and a {3x3} phase diversity ASK receiver as a function of the gain imbalance. BER = 10^{-9}, optimal threshold, penalty margin = 0.5 dB

Gain imbalance	0%	5%	10%	-5%	-10%
{2x2} ASK receiver	±8.5°	±8.0°	±6.5°	±8.0°	±6.2°
{3x3} ASK receiver non-symmetrical configuration	±13.0°	±13.0°	±12.0°	±12.0°	±10.0°
{3x3} ASK receiver symmetrical configuration	8.0°	7.0°	5.5°	9.1°	9.0°
	-7.8°	-7.8°	-7.8°	-5.8°	-4.0°

± = for positive and negative values of the phase mismatch

The analyses do not cover the situation in which the imbalance, for example, is introduced in the squarers. Besides, it has been assumed that the influence of laser phase noise is negligible. However, the degradation due to

laser phase noise for ASK receivers can conveniently be taken into account by increasing the necessary IF bandwidth [5.11]. The IF spectrum is broadened by the laser phase noise. Therefore, the IF bandwidth has to be increased to avoid loss of signal power. By an increase of the IF bandwidth the (shot) noise power increases, which results in a degradation of the receiver sensitivity. Since the broadening of the IF spectrum is independent of the gain imbalance and the phase mismatch, the penalty introduced by the laser phase noise can be added to the penalty due to the gain imbalance and the phase mismatch. However, the intensity noise introduced by the local oscillator laser in combination with gain imbalance is much more difficult to implement in these receiver models (Chapter 4) [5.12]. It is expected to have considerable influence on the performance in case of gain imbalance.

5.6 Conclusions

All phase diversity receivers are sensitive to IF gain imbalance and an aberration of the phase relations at the output branches of the optical hybrid used. The phase mismatch is introduced as an extra phase shift in the photocurrents, and the gain imbalance is introduced by placing additional amplifiers at the IF stages of the {2x2} and {3x3} phase diversity ASK receivers. In comparison with the ideal situation, without any of these imperfections, the signal value at the input of the threshold comparator becomes a function of the radial offset frequency ω_{IF}. This results in a time varying character of the BER, which leads to a sensitivity degradation. The sensitivity degradation has been calculated with respect to the ideal {2x2} or {3x3} phase diversity ASK receiver for a BER = 10^{-9}. Since ASK demodulation highly depends on the threshold value, the BER's have been calculated for a threshold value optimized for the case without any imperfections, and for a threshold value optimized for a certain combination of gain imbalance and phase mismatch. By optimizing the threshold level, the sensitivity penalty can be significantly reduced (see Table 5.1 and 5.2).

Appendix 5A

Due to the structure of the receiver, the realization of the stochastic process at the threshold comparator is the sum of three independent, Gaussian distributed variables with variances equal to 1, $(1+\delta)^2$ and $(1+\delta)^2$, respectively. The conditional error probability P_0 is then given by the threefold integral of the product of three Gaussian functions. This equals the integral of the joint probability density function of the three independent Gaussian variables p, βq, and βr, respectively.

$$P_0 = 1 - \frac{\beta^2}{(2\pi)^{3/2}} \iiint_V \exp[-(p^2 + (\beta q)^2 + (\beta r)^2)/2]\, dp.dq.dr \ , \qquad (A5.1)$$

where the integration region is given by $V = p^2 + q^2 + r^2 \leq T$, and the term $\beta = 1/(1+\delta)$. Rewriting Equation (A5.1), and changing coordinates to polar ones,

$$\begin{aligned} q &= s.\cos\varphi \ , & s &\geq 0 \\ r &= s.\sin\varphi \ , & 0 &\leq \varphi \leq 2\pi \end{aligned} \qquad (A5.2)$$

results in the following twofold integral

$$P_0 = 1 - \frac{\beta^2}{(2\pi)^{1/2}} \int_{-\sqrt{T}}^{\sqrt{T}} \exp[-p^2/2].\int_0^{(T - p^2)^{1/2}} s.\exp[-(\beta s)^2/2]\, ds.dp \ , \qquad (A5.3)$$

which can be calculated to give

$$\boxed{P_0 = 1 - \frac{1}{(2\pi)^{1/2}} \int_{-\sqrt{T}}^{\sqrt{T}} \exp[-p^2/2\ ] \left\{1 - \exp[-\beta^2(T - p^2)/2]\right\} dp \ .} \qquad (A5.4)$$

Here, $T = 2k^2SNR$ is the threshold value and $\beta = 1/(1+\delta)$. The term δ denotes the parameter which represents the gain imbalance.

Appendix 5B

Following the same procedure as in Appendix 5A for the calculation of P_0, and taking into account the signal values, which are a function of the radial frequency offset $\gamma(t)$, and the phase mismatch ϕ, $s_0(\gamma)$, $s_1(\gamma,\phi)$, and $s_2(\gamma,\phi)$, results in the following threefold integral for the conditional error probability $P_1(\gamma)$, as a function of the phase offset $\gamma(t)$ (we write $\gamma(t) = \gamma$)

$$P_1(\gamma,\phi) = \frac{\beta^2}{(2\pi)^{3/2}} \int_{-\sqrt{T}}^{\sqrt{T}} \exp[-(p-s_0(\gamma))^2/2] \times$$

$$\iint_{q^2+r^2 \le T-p^2} \exp[-(\beta^2(q^2+r^2) - 2\beta(qs_1(\gamma,\phi)+rs_2(\gamma,\phi))+s_1^2(\gamma,\phi)+s_2^2(\gamma,\phi))/2]\, dp.dq.dr \,, \tag{B5.1}$$

Equation (B5.1) can be rewritten using the coordinate transformation for the variables q and r given by the following relations,

$$q = ax + by \,,$$
$$r = cx - dy \,. \tag{B5.2}$$

The coefficients are given by $a = (1 + s_2^2/s_1^2)^{-1/2}$, $b = (1 + s_1^2/s_2^2)^{-1/2}$, $c = \sqrt{(1 - a^2)}$, and $d = \sqrt{(1 - b^2)}$, respectively. The error probability can now be written as follows

$$P_1(\gamma,\phi) = \frac{\beta^2}{(2\pi)^{3/2}} \int_{-\sqrt{T}}^{\sqrt{T}} \exp[-(p-s_0(\gamma))^2/2] \times$$

$$\iint_{x^2+y^2 \le T-p^2} \exp[-(\beta^2(x^2+y^2) - 2\beta x.\sqrt{s_1^2(\gamma,\phi)+s_2^2(\gamma,\phi)}+s_1^2(\gamma,\phi)+s_2^2(\gamma,\phi))/2]\, dp.dx.dy \,, \tag{B5.3}$$

where $\beta = 1/(1+\delta)$, and δ represents the gain imbalance. Using Equation

(B5.3), the integral representation of the modified Bessel function of the first kind and zero order, and changing coordinates to polar ones (Appendix 5A) for the variables x and y, results in the following twofold integral as a function of γ

$$P_1(\gamma,\phi) = \frac{\beta^2}{(2\pi)^{1/2}} \int_{-\sqrt{T}}^{\sqrt{T}} \exp[-(p-s_0(\gamma))^2/2] \times$$

$$\int_0^{(T - p^2)^{1/2}} s.\exp[-(\beta^2 s^2 + s_1^2(\gamma,\phi) + s_2^2(\gamma,\phi))/2].I_0[\beta.\sqrt{s_1^2(\gamma,\phi) + s_2^2(\gamma,\phi)}.s]\ dp.ds\ .$$

(B5.4)

Let us substitute for the modified Bessel function in Equation (B5.4) its asymptotic expansion [5.13] $I_0[x] = \exp[x]/\sqrt{2\pi x}$. The conditional error probability, $P_1(\gamma,\phi)$, can then be written to be

$$\boxed{P_1(\gamma,\phi) = \frac{\beta^{3/2}}{2\pi.\sqrt{\xi}} \int_{-\sqrt{T}}^{\sqrt{T}} \exp[-(p-s_0(\gamma))^2/2].\int_0^{(T - p^2)^{1/2}} \sqrt{s}.\exp[-(\beta s - \xi(\gamma,\phi))^2/2]\ dp.ds\ ,}$$

(B5.5)

where $\xi(\gamma,\phi) = \sqrt{s_1^2(\gamma,\phi) + s_2^2(\gamma,\phi)}$, $T = 2k^2SNR$, and $\beta = 1/(1+\delta)$.

References

[5.1] A.W. Davis, M.J. Pettitt, J.P. King, and S. Wright, "Phase diversity techniques for coherent optical receivers",
J. Lightwave Technol., vol. 5, pp. 561-572, April 1987.

[5.2] J. Siuzdak and W. van Etten, "BER evaluation for phase and polarization diversity optical receivers using noncoherent ASK and DPSK demodulation",
J. Lightwave Technol., vol. 7, no. 4, pp. 584-599, April 1989.

[5.3] W.H.C. de Krom, "Impact of laser phase noise on the performance of a (3x3) phase and polarization diversity optical homodyne DPSK receiver",
J. Lightwave Technol., vol. 8, no. 11, pp. 1709-1716, Nov. 1990.

[5.4] T. Okoshi et al., "Polarization-diversity receiver for heterodyne/coherent optical fiber communications",
Proc. IOOC '83, pap. 30C3-2, pp. 386-387, June 1983.

[5.5] B. Glance, "Polarization independent coherent optical receiver",
J. Lightwave Technol., vol. 5, pp. 274-276, Febr. 1987.

[5.6] L.G. Kazovsky, "Phase- and polarization-diversity coherent optical techniques",
J. Lightwave Technol., vol. 7, no. 2, pp. 279-292, Febr. 1990.

[5.7] W.R. Leeb, "Realization of a 90° and 180° hybrids for optical frequencies",
Arch. Elek. Ubertragung, vol. 37, pp. 203-206, 1983.

[5.8] L.G. Kazovsky et al., "All-fiber 90° optical hybrid for coherent communications",
Appl. Opt., vol. 26, pp. 437-439, 1987.

[5.9] J. Siuzdak, "Optical couplers for coherent optical phase diversity systems",
EUT Report 88-E-190, March 1988, ISBN 90-6144-190-0.

[5.10] *Sifam LTD - Fiber Optics Division*, England

[5.11] L.G. Kazovsky, "Impact of laser phase noise on optical heterodyne communication systems",
J. of Optical Communications, vol. 7, pp. 66-87, Febr. 1986.

[5.12] A.F. Elrefaie, D.A. Atlas, L.G. Kazovsky, R.E. Wagner, "Intensity noise in ASK coherent lightwave receivers", *Electron. Lett.*, vol. 24, pp. 158-159, 1988.

[5.13] M. Abramowitz and I.A. Stegun, "Handbook of mathematical functions" *Dover Publications*, New York, 1965.

CHAPTER 6.

IMPACT OF NONZERO EXTINCTION RATIO OF AN EXTERNAL AMPLITUDE MODULATOR ON THE PERFORMANCE OF A {2x2} AND {3x3} PHASE DIVERSITY ASK RECEIVER

6.1 Introduction

A problem encountered in most optical coherent ASK communication systems, is the impact of non-ideal amplitude modulators on the performance of phase diversity ASK receivers. The ASK modulation of the optical signal wave transmitted is usually obtained by means of an external amplitude modulator (Chapter 2), [6.1]. The modulator switches the amplitude of the optical wave transmitted between two levels, corresponding to the information signal. In case of ideal operation, the amplitude of the wave transmitted should be switched between zero and a certain maximum level. However, for practical available amplitude modulators, the lowest level of zero (no power transmission) is difficult to obtain at high bit rates. The ratio of the amplitude of the signal part of the IF photocurrent in case a space is sent and in case a mark is sent is an important parameter. This ratio is defined as the Extinction Ratio (ER) of the external amplitude modulator. In this chapter, the sensitivity degradation, due to the use of an amplitude modulator with nonzero ER, has been investigated for a {2x2} and {3x3} phase diversity ASK receiver, comprising shot noise only. The analyses are an extension of the calculations performed in reference [6.2]. The sensitivity degradation has been computed with respect to the ideal {2x2} and {3x3} phase diversity ASK receiver, respectively. The BER of both receivers has been expressed analytically. However, the results are evaluated numerically for various ER's, as a function of the SNR. Special attention is given to the optimal threshold level in dependency of the ER, and the impact of nonzero ER's on the shape of the IF modulation spectrum. The receivers have been investigated under the assumption that the shot noise related to the local oscillator dominates all other receiver noise sources. It is also assumed that intersymbol interference is absent, and that the local oscillator relative intensity noise (RIN in Chapter 4) and the laser phase noise due to both lasers (Chapter 3)

are negligible. Furthermore, the amplitude modulator introduces no chirping of the transmitting laser. For proper comparison, the system parameters of both receivers are taken to be equal (e.g., bit rate, IF bandwidth, etc.).

6.2 Theory

The block-diagram of the analyzed {2x2} and {3x3} phase diversity ASK system is presented in Figure 6.1.

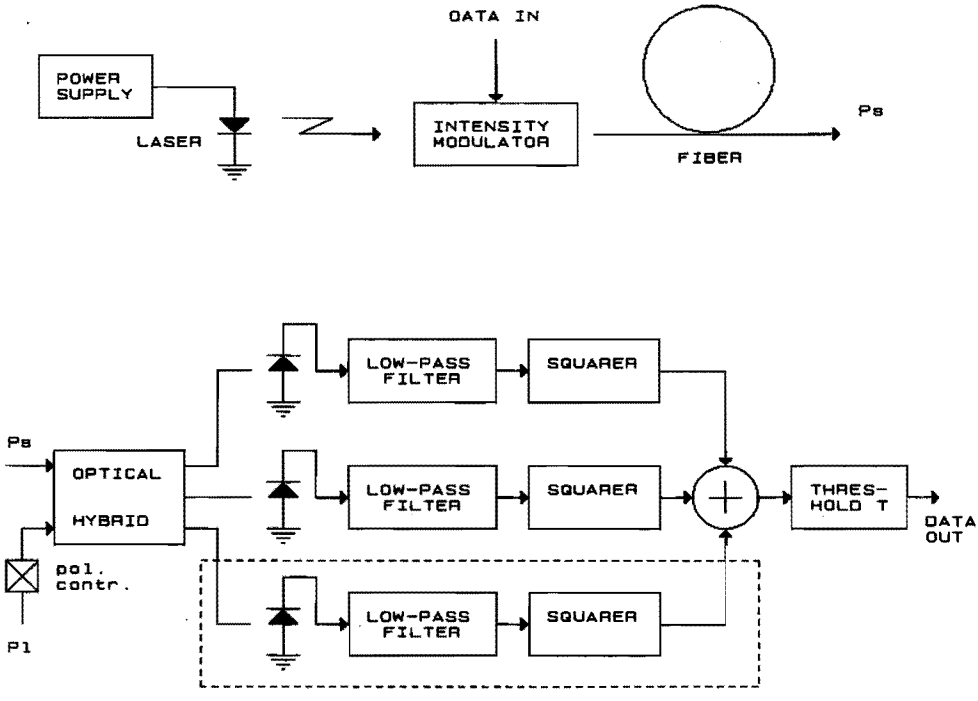

Figure 6.1 *Block-diagram of an optical coherent {2x2}/{3x3} phase diversity system.*

The low-pass filtered photocurrent for each receiver branch is given by the following relation (Chapter 4), [6.2,6,3]

$$i_j(t) = \frac{2}{N}R\sqrt{P_L P_S}.b(t).\cos[f_j(t)] + i_{JS}(t) , \qquad j = 0,1,2 \qquad (6.1)$$

where

$N = 2,3$ (the number of receiver branches),

$f_j(t) = \frac{\pi}{2}j + \phi(t)$ for the {2x2} phase diversity ASK receiver,

$f_j(t) = \frac{2}{3}\pi j + \phi(t)$ for the {3x3} phase diversity ASK receiver.

The local oscillator power is given by P_L, and P_S denotes the signal power received. The function b(t) represents the signaling waveform, which is given by $b(t) = \sum_k b_k.\mathrm{rect}(t-kT_0)$, where T_0 is the bit time. In case of ASK modulation, b_k takes the values 0 or 1. For a nonzero value of the ER, b_k switches between η (= b_k("0")) and 1 (= b_k("1")), where η can be interpreted as the ER, and is defined according to the following relation

$$0 \le \eta = b_k("0")/b_k("1") \le 1 . \qquad (6.2)$$

The term $\phi(t)$ represents the frequency and phase offset between the local oscillator and the transmitting laser. R is the responsivity of the photodiodes used. The term $i_{JS}(t)$ is the shot noise current in the j^{th} receiver branch. It is reasonable to assume for the shot noise to have Gaussian statistics with zero mean, and a flat power spectrum. The shot noise power for each photodiode at the IF stage is then given by

$$\sigma^2 = eRBP_L/N , \qquad N = 2,3 \qquad (6.3)$$

where B is the double-sided receiver bandwidth and e is the electron charge. After normalization the shot noise has unity variance in each receiver branch, and the values of the signals can then be written in terms of the SNR according to the following relation

$$s_k(t) = \sqrt{2SNR}.b(t).\cos[\phi(t) + k\frac{\pi}{2}] , \qquad k = 0,1 \qquad (6.4)$$

for the {2x2} phase diversity ASK receiver, and

$$s_k(t) = \frac{2}{\sqrt{3}}\sqrt{SNR}.b(t).\cos[\phi(t) + \frac{2}{3}k\pi] \ , \qquad k = 0,1,2 \qquad (6.5)$$

for the (3x3) phase diversity ASK receiver. The SNR for both ASK receiver structures is defined to be equal to

$$SNR \triangleq \frac{RP_s}{eB} \ . \qquad (6.6)$$

According to similar considerations as in the Chapters 4 and 5, an IF filter matched to the signal rect(t) may be applied with an impulse response

$$h(t) = \begin{cases} 1/T_0 & \text{for } 0 < t < T_0 \ , \\ 0 & \text{elsewhere,} \end{cases} \qquad (6.7)$$

implying a double-sided bandwidth B of $1/T_0$ (T_0 = bit time).

If the probability of sending a space is $P(b_k = \eta) \triangleq p_0$, and the probability of sending a mark is $P(b_k = 1) \triangleq p_1 = 1 - p_0$, the BER is determined by the following relation

$$BER = p_0.P(V_{sample} > T|b_k = \eta) + p_1.P(V_{sample} \leq T|b_k = 1) \ . \qquad (6.8)$$

Here, V_{sample} is the realization of the process at the input of the threshold comparator at the sampling moment. T represents the threshold level, which for optimum sensitivity should be chosen as a function of the ER.
$P_0 = P(V_{sample} > T|b_k = 0)$ is the conditional error probability that a mark is received whereas a space is sent. $P_1 = P(V_{sample} < T|b_k = 1)$ denotes the conditional error probability that a space is received whereas a mark is sent. If the probability of sending a mark is equal to the probability of sending a space, the BER of both receivers is determined by the following equation

$$BER = \frac{1}{2}\left(P(V_{sample} > T|b_k = 0) + P(V_{sample} \leq T|b_k = 1)\right) \ . \qquad (6.9)$$

6.3 The error probability of the (2x2) phase diversity ASK receiver

In case $b_k = 0$ (space is sent), implying an ER = 0 ($\eta = 0$) for the amplitude modulator used, the PDF of the process at the input of the threshold comparator is that of the sum of two squared Gaussian variables with zero means. Since both variables are statistically independent, the resulting PDF is a chi-square with two degrees of freedom [6.2,6.4]. However, for a nonzero values of the ER, the PDF changes and can be rewritten into a noncentral chi-square distribution with two degrees of freedom (see Appendix 6A for a detailed derivation). Hence, the conditional error probability P_0 reads

$$P_0 = 2.\exp[-\eta^2 SNR] \int_{\sqrt{T/2}}^{\infty} r.\exp[-r^2].I_0[2\eta\sqrt{SNR}.r]\, dr \ , \qquad (6.10)$$

where the threshold level T is set at $2k^2SNR$, and k is the parameter to be optimized. For an ideal (2x2) phase diversity receiver, this is set at 0.520 for a BER = 10^{-9} [6.2]. $I_0[.]$ represents the modified Bessel function of the first kind and zero order, and $0 \leq \eta \leq 1$.

When $b_k = 1$ (mark is sent), implying that $\eta = 1$, the conditional probability of error, P_1, for the same threshold is equal to the probability that the realization of the process at the input of the threshold comparator is less than T. Following the same procedure as for the conditional error probability P_0, the probability P_1 can be calculated to give (see Appendix 6B for a detailed derivation)

$$P_1 = \frac{1}{\sqrt{\pi}(SNR)^{-1/4}} \int_0^{\sqrt{T/2}} \sqrt{s}.\exp[-(s - \sqrt{SNR})^2]\, ds \ . \qquad (6.11)$$

The final BER of the (2x2) phase diversity ASK receiver equals the following

relation (see Equation (6.9))

$$BER = \frac{1}{2}.(P_0 + P_1) \ . \qquad (6.12)$$

The form of the BER (Equation (6.12)) is rather complicated, and for this reason numerical integration was necessary. For BER = 10^{-9}, the sensitivity degradation has been computed with respect to the ideal (2x2) phase diversity ASK receiver, for both an optimized threshold value (optimized for $\eta \neq 0$) and a non-optimized threshold value. In the optimization, the condition is imposed that the BER = 10^{-9}, and besides that it is independent of the bit pattern. This implies that the conditional error probabilities P_0 and P_1 are equal. In Figure 6.2, the results are presented for a (non-)optimized threshold value, and η varying from 0.0 to 0.25.

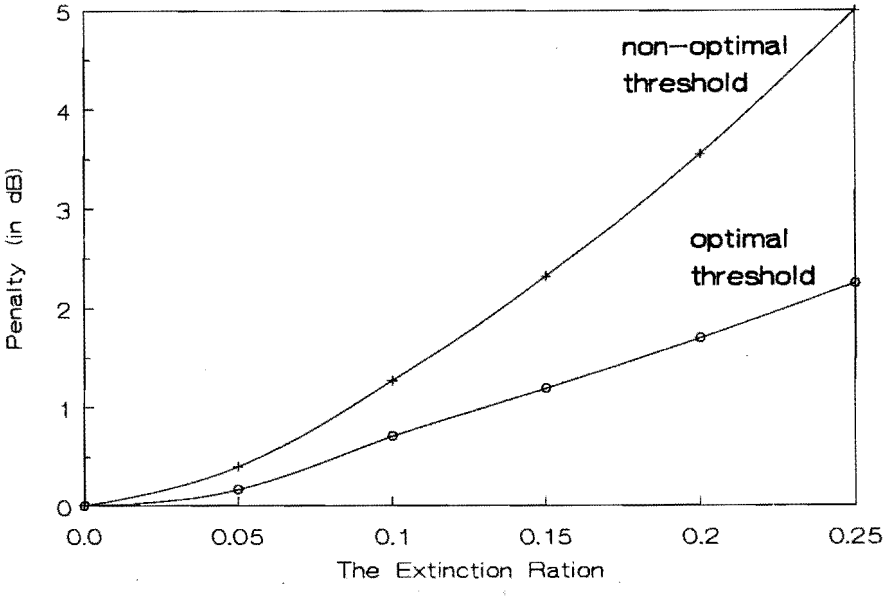

Figure 6.2 *Sensitivity penalty versus extinction ratio for a (2x2) phase diversity ASK receiver, and a BER = 10^{-9}.*

From Figure 6.2, it can be concluded that the degradation due to nonzero values of the ER, can be significantly reduced by optimization of the thres-

hold level parameter k. For an optimal threshold level and an ER = 0.25, the sensitivity penalty can be reduced from approximately 5.0 dB to approximately 2.25 dB. The optimized value of the threshold parameter k as a function of the ER, is depicted in Figure 6.3 for $0 \leq \eta \leq 0.25$ and BER = 10^{-9}.

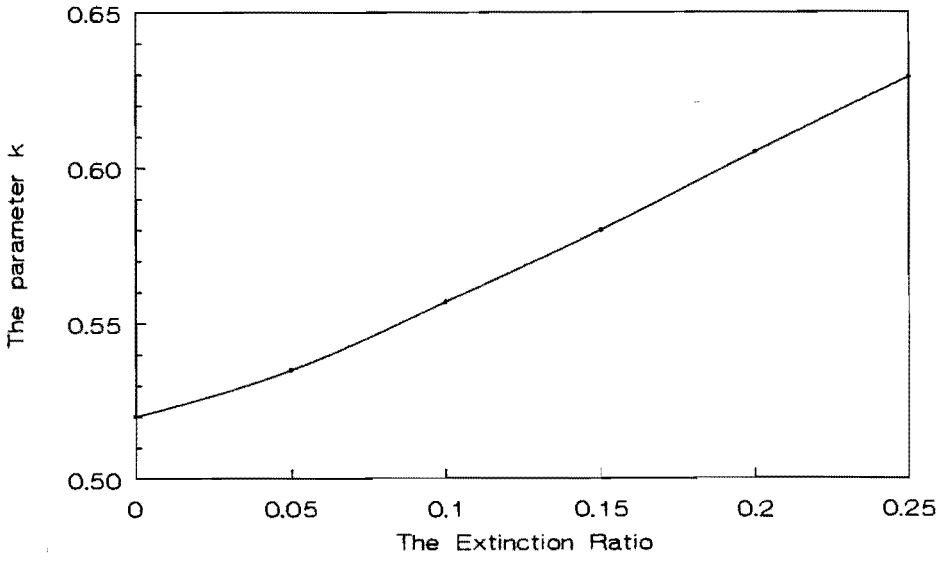

Figure 6.3 *The threshold parameter k versus the extinction ratio.*

Since the optimal threshold value for ASK demodulation is usually approximately midway between the mark and the space level, it is obvious that for nonzero ER's the value of the threshold parameter k increases.

6.4 The error probability of the {3x3} phase diversity ASK receiver

The procedure for the calculation of P_0 for the {3x3} receiver is similar to that of the {2x2} receiver, except for the extension from two to three independent Gaussian distributed variables. In case the ER ≠ 0, and for this reason $0 < b_k \leq 1$ (space is sent), the PDF of the process at the input of the threshold comparator is the sum of three independent squared Gaussian variables with nonzero means. After some mathematical manipulations, the

resulting PDF can be written as (see Appendix 6C for a detailed derivation)

$$P_0 = \frac{2}{\sqrt{\pi}}.\exp[-\eta^2 SNR] \int_{\sqrt{T/2}}^{\infty} s^2.\exp[-s^2].\int_0^{\pi} \exp[2\eta\sqrt{SNR}.s.\cos\theta].\sin\theta \; d\theta.ds \; , \tag{6.13}$$

where $T = 2k^2SNR$ is the threshold level with k the parameter to be optimized, and $0 \leq \eta \leq 1$.

In case a mark is sent, $b_k = 1$ and $\eta = 1$. The conditional probability of error P_1 for the same threshold can be calculated according to the same procedure as for the (2x2) receiver. Changing the integration region in Equation (6.13), and substitution of $\eta = 1$ results in the conditional error probability P_1

$$P_1 = \frac{2}{\sqrt{\pi}}.\exp[-SNR] \int_0^{\sqrt{T/2}} s^2.\exp[-s^2].\int_0^{\pi} \exp[2\sqrt{SNR}.s.\cos\theta].\sin\theta \; d\theta.ds \; . \tag{6.14}$$

The final BER of the (3x3) phase diversity ASK receiver can be calculated according to Equation (6.9).

For a BER = 10^{-9}, the sensitivity degradation has been computed with respect to the ideal (3x3) phase diversity ASK receiver, for a (non-)optimized threshold value. In Figure 6.4, the results are depicted for (non-)optimized threshold values, and η varying from 0.0 to 0.25.

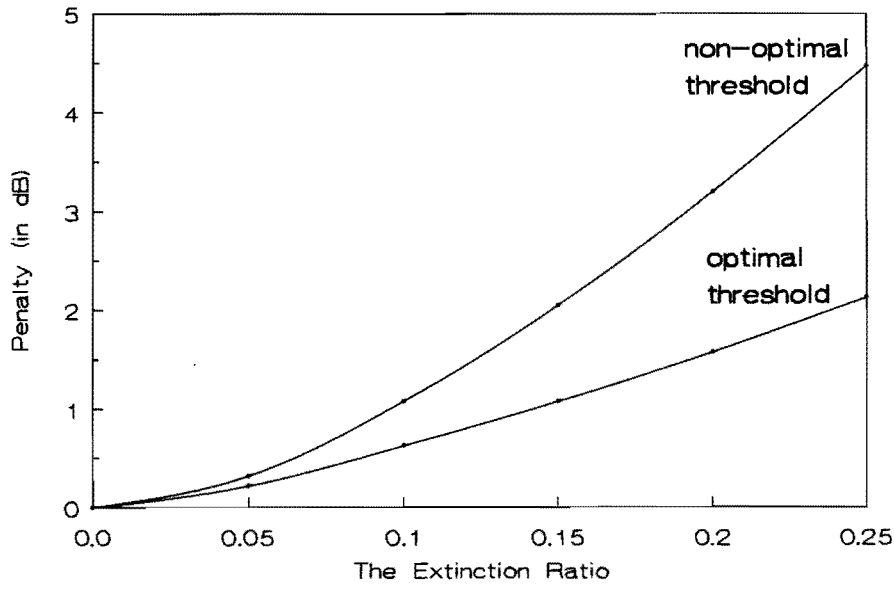

Figure 6.4 *Sensitivity penalty versus extinction ratio for a {3x3} phase diversity ASK receiver, and a BER = 10^{-9}.*

From Figure 6.4, it can be concluded that similar as for the {2x2} receiver, the degradation due to a nonzero ER can be reduced by optimization of the threshold level. For an optimal threshold level (T) and an ER = 0.25, a reduction of the sensitivity penalty by 2.45 dB can be obtained. A comparison of the Figures 6.1 and 6.4 reveals that the {3x3} phase diversity ASK receiver is slightly less sensitive for nonzero ER's than the {2x2} phase diversity ASK receiver. In Figure 6.5, the optimized value of the parameter k is depicted as a function of the ER, for $0 \leq \eta \leq 0.25$ and BER = 10^{-9}.

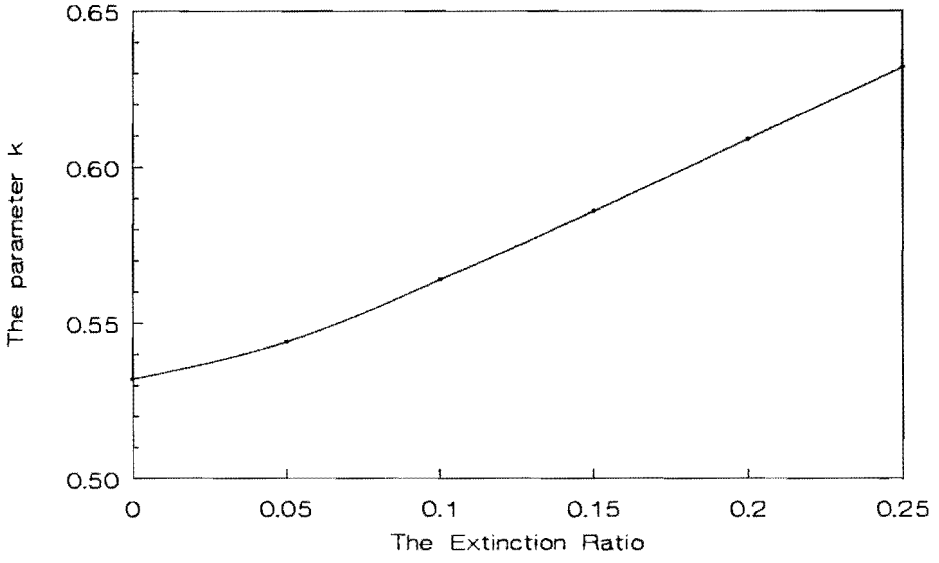

Figure 6.5 *The threshold parameter k versus the extinction ratio.*

A comparison of Figure 6.5 with Figure 6.3 shows that for increasing values of the ER the curves for both receivers merge.

6.5 The shape of the ASK IF spectrum for nonzero extinction ratios

6.5.1 Measuring the IF spectrum

For an optimal IF filter design, it is of utmost importance to have knowledge about the shape of the IF power spectrum. In this section, the IF power spectrum for ASK modulation has been calculated for (non)zero ER's. The results are compared with the measured power spectrum of an ASK modulated laser. The FWHM laser linewidth is obtained by means of the self-homodyning principle [6.5]. In Figure 6.6, an example of a power spectrum is depicted for a local oscillator (or transmitting) laser after self-homodyning. From this figure, it can be seen that the FWHM laser linewidth is approximately 30 MHz. This is the single-sided 3 dB bandwidth in case of self-homodyning.

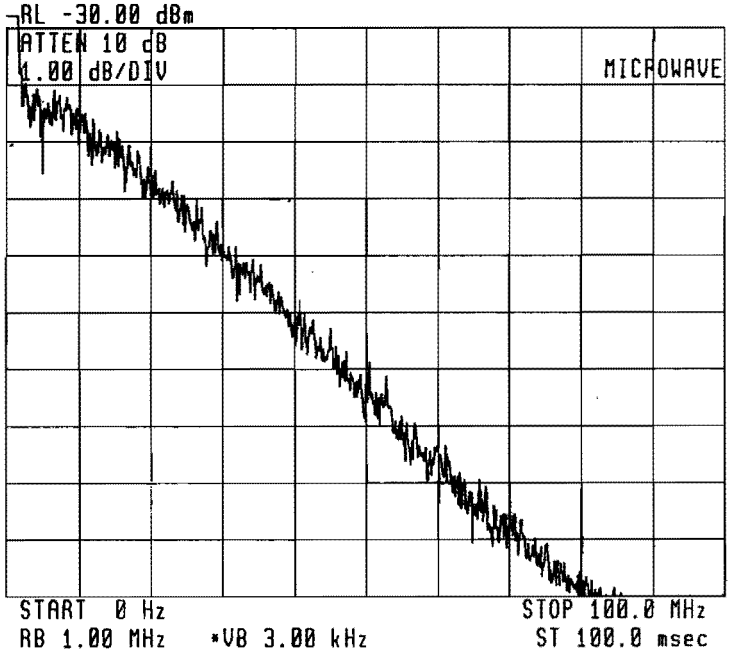

Figure 6.6 *The laser power spectrum obtained after self-homodyning.*

The system-setup for measuring the modulated laser power spectrum is shown in Figure 6.7. It consists of two DFB (Distributed FeedBack) lasers, an external amplitude modulator with an ER of 1/8, a directional coupler, a photodiode, and an electrical spectrum analyzer.

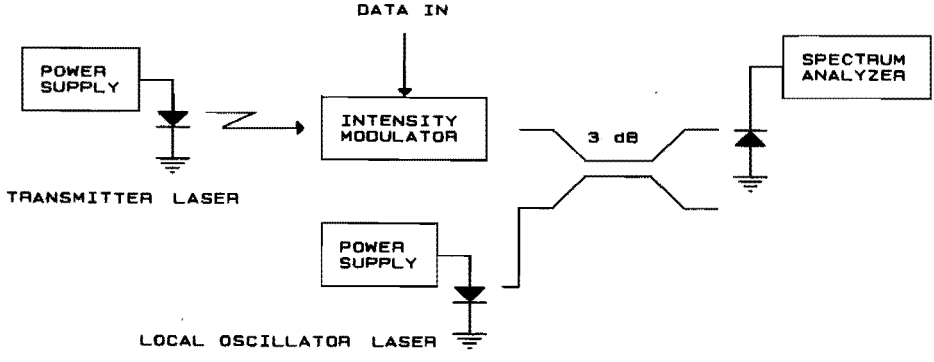

Figure 6.7 *The system-setup for measuring the ASK modulated IF spectrum.*

The ASK modulated optical wave is superimposed on the local oscillator wave by means of the directional coupler. The subsequent mixing of the composite wave is performed by the photodiode. By carefully tuning and controlling the temperature and bias current of the local oscillator laser, the mean beat frequency is stabilized at about 0 MHz. In Figure 6.8, the measured ASK modulated power spectrum is depicted for a 140 Mbit/s Pseudo Random Bit Sequence (PRBS) and an ER of 1/8. The FWHM laser linewidth of each laser is approximately 30 MHz.

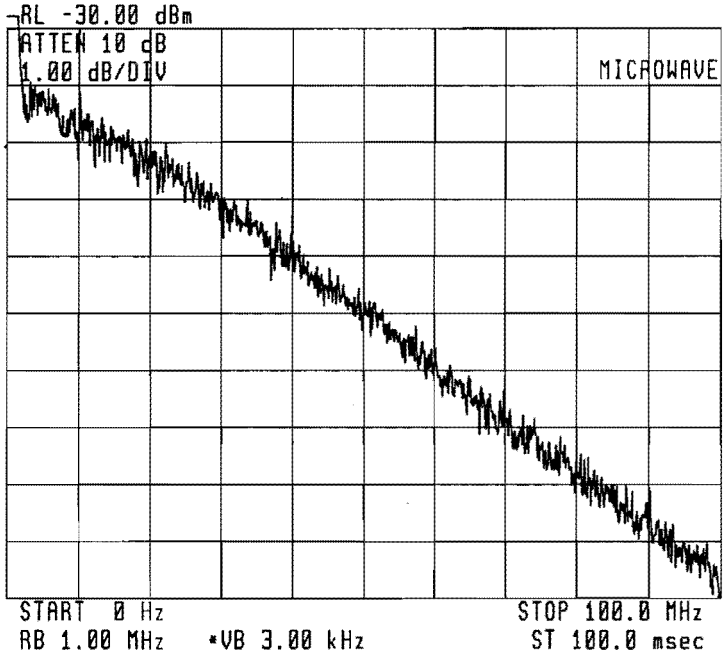

Figure 6.8 *The measured ASK modulation spectrum for a PRBS with a bit rate of 140 Mbit/s, an extinction ratio of 1/8, and FWHM laser linewidths of 30 MHz.*

From this figure, it can be concluded that the FWHM bandwidth is approximately 80 MHz. This is two times the single-sided 3 dB bandwidth (= 40 MHz) of the power spectrum measured.

6.5.2 Derivation of the IF spectrum for nonzero extinction ratios

After detection of the composite wave (see Figure 6.7 and Equation (6.1)), and appropriate IF low-pass filtering, the signal values in both receiver structures are given by

$$s_j(t) = \frac{2}{N} R\sqrt{P_L P_S}.b(t).\cos[f_j(t)] \ , \tag{6.15}$$

where $f_j(t)$, N and b(t) are explained below Equation (6.1). It is a known feature of two lasers with a Lorentzian power spectrum and laser linewidths of $\Delta\lambda_1$ and $\Delta\lambda_2$, respectively, that after combining and mixing, the resulting power spectrum is also Lorentzian. It has a FWHM linewidth which equals the sum of both laser linewidths separately [6.6]. This implies that for the computation of the ASK modulated laser spectrum, it is sufficient to perform the following convolution

$$S_m(f) = S_{laser}(f) * M(f) \ , \tag{6.16}$$

where $S_{laser}(f)$ is the equivalent baseband laser power spectrum, which has a Lorentzian line shape (Section 2.3.1). Moreover, since the transmitting and local oscillator laser have equal characteristics, the FWHM bandwidth is twice the laser linewidth of a single laser. M(f) represents the modulation spectrum of b(t), the signaling waveform. In Figure 6.9, the (normalized) modulated waveform is depicted for an ER of α. For a nonzero ER of the amplitude modulator and a random binary ASK signal, the modulation spectrum, M(f), can be derived according to the following procedure. If the probability of sending a mark is equal to the probability of sending a space, the autocorrelation function of b(t) can be calculated to be given by (see Figure 6.9b)

$$R_{bb}(\tau) = \frac{(T_0 - \tau)(1 + \alpha^2)/2 + \tau(1 + 2\alpha + \alpha^2)/4}{T_0}$$

$$= \frac{1 + \alpha^2}{2} - \left(\frac{1}{4}(1 + \alpha^2) - \alpha/2 \right) \frac{|\tau|}{T_0} . \quad \text{for } |\tau| \le T_0$$

$$R_{bb}(\tau) = \left(\frac{1}{4}(1 + \alpha^2) + \alpha/2 \right) \quad \text{for } |\tau| > T_0 \qquad (6.17)$$

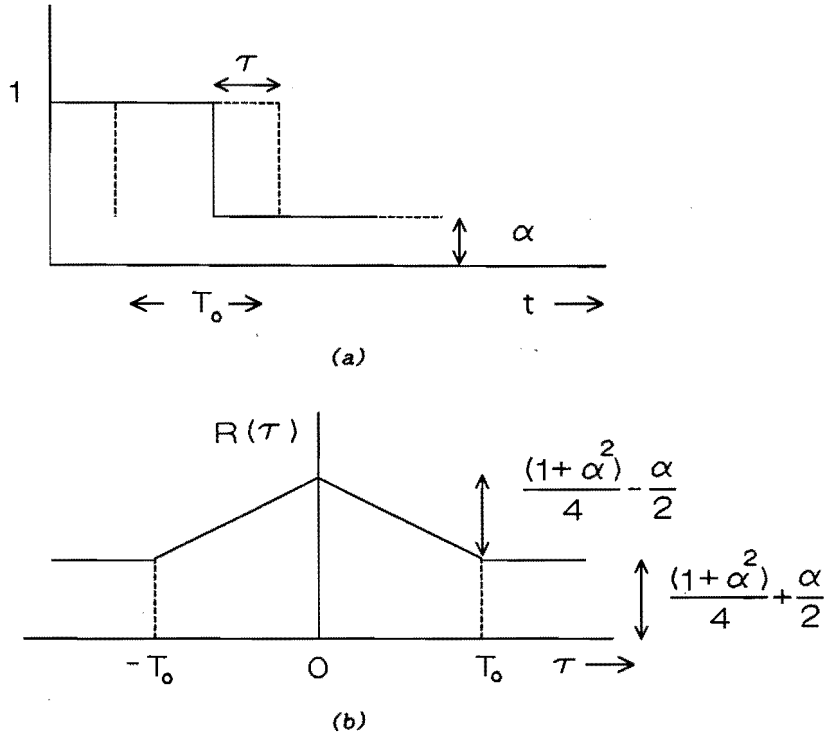

Figure 6.9 *(a) Modulated waveform for and extinction ratio of α and a bit time T_0,*
(b) The autocorrelation function.

The modulation spectrum M(f) of the signaling waveform b(t), can be obtained by Fourier transformation of the autocorrelation function $R_{bb}(\tau)$. After normalization to unity, the modulation spectrum M(f) is depicted in

Figure 6.10, for a PRBS of 140 Mbit/s. For the sake of clarity, the delta function at the center of the spectrum has been omitted in this figure.

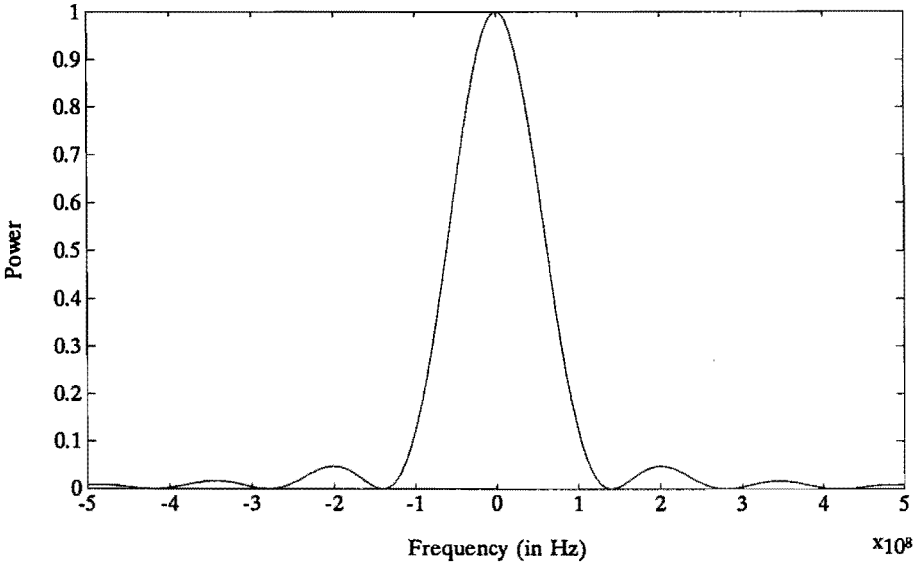

Figure 6.10 *The normalized power spectrum of the signaling waveform b(t), for a PRBS of 140 Mbit/s.*

Substitution of M(f) in Equation (6.16) finally results in the (equivalent baseband) ASK modulated power spectrum $S_m(f)$ for an ER of α.

$$S_m(f) = \left(\frac{1}{4}(1+\alpha^2) - \alpha/2 \right) . \frac{\sin^2(\pi f T_0)}{\pi^2 f^2 T_0} * S_{laser}(f) + \left(\frac{1}{4}(1+\alpha^2) + \alpha/2 \right) * S_{laser}(f) . \qquad (6.18)$$

Unfortunately, the form of the power spectrum $S_m(f)$ is rather complicated, and for this reason numerical convolution was necessary. For an ER of 1/8, a FWHM laser linewidth of 30 MHz for each laser, and a 140 Mbit/s ASK modulated PRBS, the (equivalent baseband) power spectrum $S_m(f)$ is depicted in Figure 6.11 for two different frequency scales.

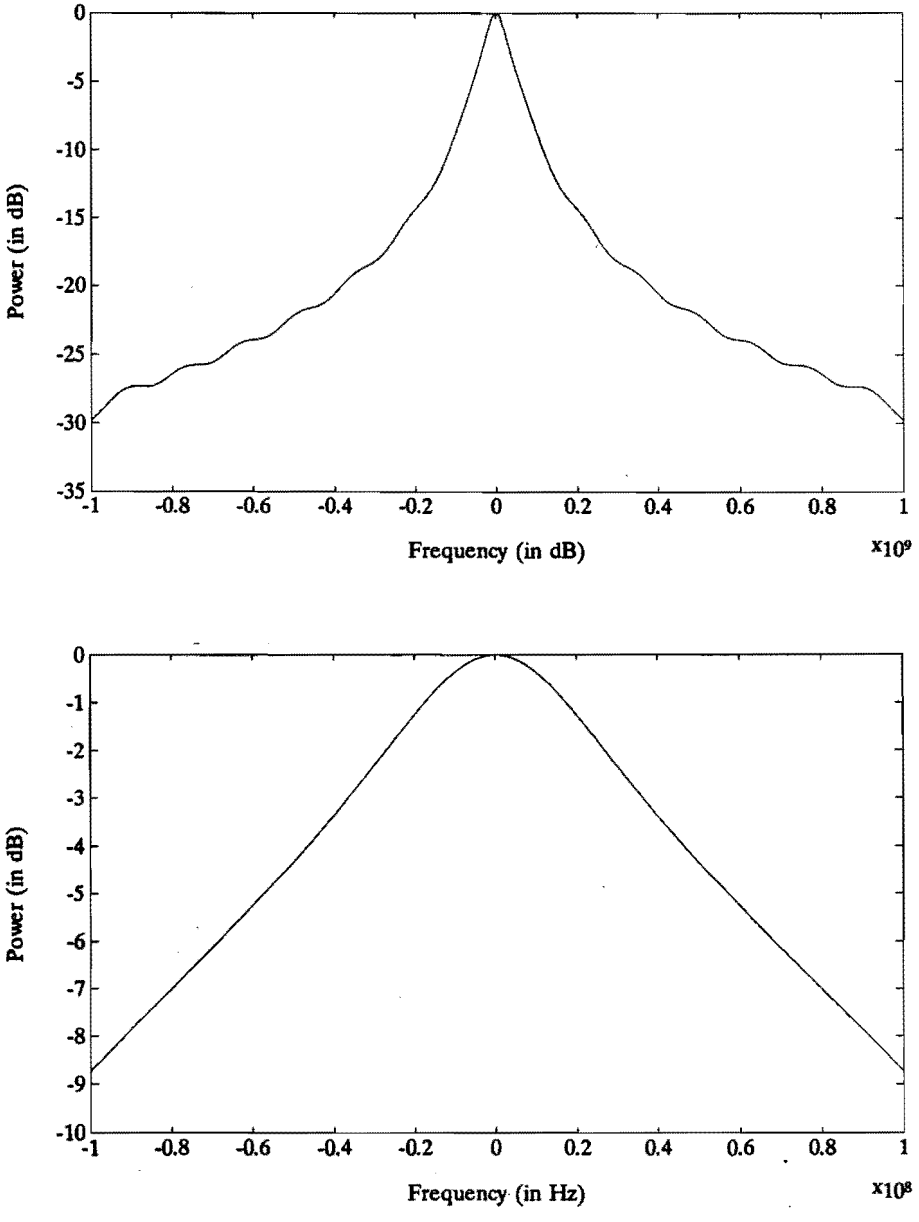

Figure 6.11 *The computed equivalent baseband ASK modulated power spectrum for a PRBS of 140 Mbit/s, an extinction ratio of 1/8, and FWHM laser linewidths of 30 MHz each.*

A comparison of the computed power spectrum of Figure 6.11 with the measured power spectrum of Figure 6.8 reveals, that the FWHM bandwidth of both spectra matches very well. For an increasing value of the ER, the FWHM bandwidth decreases. This can easily be explained, since the power spectrum $S_m(f)$ is the convolution of the modulation spectrum and the laser spectrum, the spectrum $S_m(f)$ is broader than both power spectra separately. However, for values of the ER approaching towards one, M(f) becomes a delta function. The convolution of $S_m(f)$ and M(f) then results in the unmodulated laser spectrum, with a FWHM bandwidth equal to the sum of the FWHM laser linewidths.

6.6 Conclusions

For the {2x2} and {3x3} phase diversity ASK receiver, the sensitivity degradation, due to the use of an external amplitude modulator with a nonzero ER, has been calculated. The sensitivity degradation highly depends on the position of the threshold level. By optimization of the threshold parameter k, the sensitivity penalty can be significantly reduced. For an optimized threshold level and a BER = 10^{-9}, the {3x3} receiver is less sensitive to a nonzero value of the ER than the {2x2} receiver. For a typical value of the ER of 1/8 and a BER = 10^{-9}, the sensitivity degradation for the {2x2} and {3x3} phase diversity ASK receiver has been calculated to be 2.25 dB, and 2.13 dB, respectively. For optimal threshold levels, the threshold parameter (k) of the {2x2} receiver merges with the threshold parameter of the {3x3} receiver for increasing values of the ER.

For ASK modulation, the FWHM bandwidth of the IF power spectrum is broadened in comparison with the FWHM bandwidth of the unmodulated laser spectrum. Increasing the value of the ER leads to a smaller modulation depth (=index), and therefore, to a smaller value of the FWHM bandwidth.

Appendix 6A

The conditional error probability P_0 is found from the PDF of the sum of two independent squared Gaussian variables with nonzero means ηs_0, and ηs_1, respectively. Hence, the conditional error probability P_0 reads

$$P_0 = \frac{1}{2\pi} \iint_V \exp[-((x-\eta s_0)^2 + (y-\eta s_1)^2)/2]\, dx.dy \ , \qquad \text{(A6.1)}$$

where $V = x^2 + y^2 > 2k^2SNR = T$, the integration region. Using Equation (6.4), changing the coordinates to polar ones, and using the integral representation of the modified Bessel function, of the first kind and zero order, $I_0[.]$, we can derive the following equation for the conditional error probability P_0

$$P_0 = 2.\exp[-\eta^2 SNR] \int_{\sqrt{T/2}}^{\infty} r.\exp[-r^2].I_0[2\eta\sqrt{SNR}.r]\, dr \ . \qquad \text{(A6.2)}$$

Appendix 6B

The conditional error probability P_1 is found from the PDF of the sum of two independent squared Gaussian variables with nonzero means s_0, and s_1, the signal values. Hence the conditional error probability P_1 reads

$$P_1 = \frac{1}{2\pi} \iint_V \exp[-((x-s_0)^2 + (y-s_1)^2)/2]\, dx.dy \ , \qquad \text{(B6.1)}$$

where $V = x^2 + y^2 \le 2k^2SNR = T$, the integration region. Following the same procedure as in Appendix 6A, the twofold integral of Equation (B6.1) can, after some mathematical manipulation, be reduced to

$$P_1 = 2.\exp[-SNR] \int_0^{\sqrt{T/2}} s.\exp[-s^2].I_0[2\sqrt{SNR}.s]\, ds \ . \qquad \text{(B6.2)}$$

Approximating the modified Bessel function of the first kind and zero order by its asymptotic expansion $I_0[z] = \exp[z]/\sqrt{2\pi z}$ [6.7], the conditional error probability P_1 can be calculated to give

$$P_1 = \frac{1}{\sqrt{\pi}(SNR)^{-1/4}} \int_0^{\sqrt{T/2}} \sqrt{s}.\exp[-(s-\sqrt{SNR})^2]\, ds \ . \qquad \text{(B6.3)}$$

Appendix 6C

The conditional error probability P_0 is found from the PDF of the sum of three independent squared Gaussian variables with nonzero means ηs_0, ηs_1, and ηs_2, respectively. Hence, the conditional error probability P_0 reads

$$P_0 = \frac{1}{(2\pi)^{3/2}} \iiint_V \exp[-\{(x-\eta s_0)^2 + (y-\eta s_1)^2 + (z-\eta s_2)^2\}/2]\, dx.dy.dz \ , \qquad (C6.1)$$

where the integration region V is given by $V = x^2 + y^2 + z^2 \geq T\ (= 2k^2SNR)$. Making use of the fact that the integral of Equation (C6.1) over x, y and z is spherical-symmetrical, rotation of the coordinates, according to the same procedure as in Appendix 4C, results in the following equation

$$P_0 = \frac{1}{(2\pi)^{3/2}} \iiint_V \exp[-\{x^2 + y^2 + (z-\eta\sqrt{2SNR})^2\}/2]\, dx.dy.dz \ . \qquad (C6.2)$$

A reduction of the number of variables can be obtained by using the following spherical coordinates instead of cartesian

$$\begin{aligned} x &= r.\sin\theta\sin\varphi \ , & 0 \leq \theta \leq \pi \\ y &= r.\sin\theta\cos\varphi \ , & 0 \leq \varphi \leq 2\pi \\ z &= r.\cos\theta \ , & r \geq 0 \end{aligned} \qquad (C6.3)$$

which leads to the following equation

$$P_0 = \frac{1}{\sqrt{2\pi}}.\exp[-\eta^2 SNR] \int_{k\sqrt{2SNR}}^{\infty} r^2.\exp[-r^2/2].\int_0^{\pi} \exp[\eta\sqrt{2SNR}.r.\cos\theta].\sin\theta \ d\theta.dr \ . \qquad (C6.4)$$

Substitution of $s \triangleq r/\sqrt{2}$ finally leads to the following equation for the conditional error probability P_0

$$P_0 = \frac{2}{\sqrt{\pi}}.\exp[-\eta^2 SNR] \int_{\sqrt{T/2}}^{\infty} s^2.\exp[-s^2].\int_0^{\pi} \exp[2\eta\sqrt{SNR}.s.\cos\theta].\sin\theta \; d\theta.ds \; .$$

(C6.5)

References

[6.1] L. Thylén, "Integrated optics in $LiNbO_3$: recent developments in devices for telecommunications",
J. Lightwave Technol., vol. 6, no. 6, pp. 847-861, June 1988.

[6.2] J. Siuzdak and W. van Etten, "BER evaluation for phase and polarization diversity optical receivers using noncoherent ASK and DPSK demodulation",
J. Lightwave Technol., vol. 7, no. 4, pp. 584-599, April 1989.

[6.3] W. van Etten and J. van der Plaats, "Fundamentals of Optical Fiber Communications",
Prentice Hall, New York, 1991.

[6.4] A. Papoulis, "Probability, random variables, and stochastic processes",
McGraw-Hill, New York, 1965.

[6.5] T. Okoshi, "Novel method for high resolution measurement of laser output spectrum",
Electron. Lett., vol. 16, no. 16, pp. 630-631, 1980.

[6.6] J.F.L. Tol, "Meten aan en met 1550 nm lasers",
Graduation Report Eindhoven University of Technology, Aug. 1989.

[6.7] M. Abramowitz and I.A. Stegun, "Handbook of mathematical functions",
Dover Publications, New York, 1965.

CHAPTER 7.

CONCLUSIONS

For the optical coherent phase (and polarization) diversity receivers analyzed it is assumed that, at the IF stages, the shot noise, the thermal noise, the local oscillator Relative Intensity Noise (RIN), and the phase difference $\Delta\Phi \triangleq \phi(t) - \phi(t-T)$ due to the phase noise of both lasers, have Gaussian statistics. The subsequent demodulation is a non-linear operation which results in a non-Gaussian probability density function for the stochastic process at the input of the threshold comparator. The probability density function of this process has been derived analytically. However, the form of this function was usually rather complicated, and for this reason, numerical integration was necessary in order to determine the BER values.

The impact of nonzero laser linewidths on the performance of a {3x3} phase and polarization diversity DPSK receiver has been analyzed. With respect to the ideal heterodyne DPSK receiver, the sensitivity penalty introduced for the {3x3} phase and polarization diversity DPSK receiver is approximately 0.7 dB. This for a Bit Error Rate (BER) of 10^{-9}, and comprising shot noise only.

For typical values of the polarization overcoupling of less than 2% in non-ideal polarization beamsplitters, the sensitivity penalty introduced for a phase and polarization diversity receiver as depicted in Figure 3.2 is about 0.18 dB, and therefore, almost negligible in practical systems.

In comparison with optical coherent heterodyne DPSK reception, phase diversity reception of optical DPSK signals does not increase the tolerance to laser phase noise. The value of the BER floor only depends on the normalized laser linewidth and the demodulation scheme, and not on the receiver structure. Due to the existence of this BER floor, the {3x3} phase (and polarization) diversity DPSK receiver approaches the performance of the heterodyne DPSK receiver for nonzero laser linewidths and a consistently large value of the Signal-to-Noise Ratio (SNR).

For a sensitivity penalty of 1.0 dB, the maximum allowable normalized laser linewidth for the {3x3} phase and polarization diversity DPSK receiver

analyzed, has been calculated to be approximately 0.46% for an IF filter matched to the data signal. Therefore, a relaxation of the laser linewidth requirements by broader IF filtering and matched post-detection filtering, as is possible in case of ASK and CPFSK modulation, can not be obtained for DPSK modulation.

The influence of shot noise, thermal noise, and local oscillator Relative Intensity Noise (RIN) on the performance of a {2x2} and {3x3} phase diversity ASK receiver has been analyzed. For both ASK receivers, an optimum value for the local oscillator power (P_L) is found, for which the sensitivity penalty is minimal. This value of P_L highly depends on the position of the threshold level and the to the local oscillator related RIN. For an optimum threshold level, the {3x3} phase diversity ASK receiver outperforms the {2x2} phase diversity receiver for values of P_L larger than this optimum value. The reverse is true for values of P_L smaller than this optimum.
The BER of the {3x3} phase diversity ASK receiver is constant for a given value of the SNR. This is in contrary to the BER of the {2x2} phase diversity receiver, which shows a time varying character with a frequency equal to twice the IF. In comparison with the {3x3} phase diversity DPSK receiver, the equivalent phase diversity ASK receiver performs very similar, except for an excess sensitivity penalty of approximately 0.3 dB.

All phase diversity receivers are sensitive to an IF gain imbalance and an aberration of the phase relations at the output of the optical hybrid. These imperfections lead to a time varying character of the BER with a frequency of two times the IF. Due to these imperfections, the signal value at the input of the threshold comparator is a function of the IF. Without these imperfections, the signal value is constant.
Calculations for a {2x2} and {3x3} phase diversity ASK receiver revealed that the sensitivity penalty highly depends on the position of the threshold level, and that by optimization of this level, the sensitivity penalty for typical values of the IF gain imbalance (< 10%) and phase mismatch (< 5°) could be reduced to allowable values (< 0.5 dB).

The impact of an external amplitude modulator with a nonzero Extinction (or

Off/On) Ratio (ER) on the performance of a {2x2} and {3x3} phase diversity ASK receiver has been analyzed. The sensitivity penalty highly depends on the position of the threshold level, and therefore, optimization is required for optimal performance. The {3x3} phase diversity ASK receiver is slightly less sensitive to nonzero values of the ER than the {2x2} phase diversity ASK receiver. For a typical value of 1/8 for the ER and a BER = 10^{-9}, the sensitivity penalty is 2.25 dB for the {2x2} receiver, and 2.13 dB for the {3x3} receiver and an optimal threshold level.

In comparison to the unmodulated laser spectrum, optimal ASK modulation of the optical carrier (ER = 0), implying a modulation index of 1, results in a broadening of the IF power spectrum. However, increasing the value of the ER leads to a smaller modulation index, and therefore, to a smaller value of the FWHM bandwidth.

LIST OF ABBREVIATIONS

ASK	Amplitude Shift Keying
BER	Bit Error Rate
BISDN	Broadband Integrated Service Digital Network
BP	BandPass
CPFSK	Continuous Phase Frequency Shift Keying
DBR	Distributed Bragg Reflector
DFB	Distributed FeedBack
DPSK	Differential Phase Shift Keying
EHP	Electron Hole Pairs
ER	Extinction Ratio
FEL	Fysisch en Elektronisch Laboratorium
FLL	Frequency-Locked-Loop
FSK	Frequency Shift Keying
FWHM	Full-Width-Half-Maximum
IBCN	Integrated Broadband Communication Network
IF	Intermediate Frequency
IM/DD	Intensity-Modulation/Direct-Detection
IOP	Innovatief Onderzoek Programma
LAN	Local Area Network
LC	Liquid Crystal
LP	Low-Pass
OEIC	Opto-Electronic Integrated Circuit
OOK	On-Off Keying
PBS	Polarizing BeamSplitter
PDF	Probability Density Function
PMF	Polarization Maintaining Fiber
PRBS	Pseudo Random Bit Sequence
PTT	Post Telegraaf Telefoon
RF	Radio Frequency
RIN	Relative Intensity Noise
SAP	Stress-Applying-Parts
SNR	Signal-to-Noise Ratio
SOP	State-Of-Polarization
TNO	Nederlandse Organisatie voor Toegepast Natuurwetenschappelijk Onderzoek
TUD	Technische Universiteit Delft
TUE	Technische Universiteit Eindhoven
UT	Universiteit Twente
WDM	Wavelength Division Multiplexing

SAMENVATTING

Dit proefschrift behandelt de invloed en specificatie van verschillende systeemparameters, -toleranties en -componenten, die van belang zijn voor de realisatie van optisch coherente "phase diversity"-ASK- en DPSK-ontvangers. Om een beter inzicht te krijgen in deze systeemaspecten en de invloed ervan op de kwaliteit van de ontvangers zijn er diverse theorieën, mathematische hulpmiddelen en modellen ontwikkeld. Voor zover noodzakelijk zijn reeds bestaande theorieën aangepast of verder uitgewerkt. Gestreefd is naar een model dat de experimentele systemen zo goed mogelijk benadert. De ontwikkelde modellen en de bijbehorende computerprogrammatuur zijn gebruikt om de invloed van diverse systeemdegradaties zoals faseruis, intensiteitsruis en niet ideale systeemconfiguraties te kunnen analyseren.

De invloed van faseruis in een {3x3} "phase and polarization diversity"-DPSK-ontvanger is bestudeerd. Exacte analytische uitdrukkingen zijn verkregen voor de foutenkans als een functie van de signaal-ruis-verhouding en de Full-Width-Half-Maximum (FWHM) laserlijnbreedten.
Speciale aandacht is geschonken aan de combinatie van het "polarization diversity"- en het "phase diversity"-concept en de invloed van polarisatieoverkoppeling in de polarisatiesplitsers. Aangetoond is dat de invloed van deze polarisatieoverkoppeling op de kwaliteit van de "polarization diversity"-ontvanger doorgaans kan worden verwaarloosd.
De voor de {3x3} "phase and polarization diversity"-ontvanger verkregen resultaten zijn vergeleken met resultaten uit de literatuur voor optisch coherente "phase (and polarization)"-diversity ASK- en CPFSK-ontvangers.

Voor een {2x2} en {3x3} "phase diversity"-ASK-ontvanger zijn de ontwikkelde mathematische modellen en computerprogrammatuur ook toegepast ter bepaling van de systeemdegradatie als gevolg van intensiteitsruis, veroorzaakt door de lokale oscillator-laser (LO). De voor de foutenkans verkregen analytische oplossing is exact. De resultaten tonen aan dat er een optimale waarde voor het lokaal oscillator vermogen, P_L, bestaat, waarvoor de systeemdegradatie minimaal is. Deze optimale waarde voor P_L hangt af van het drempelniveau en de LO-intensiteitsruis. Voor waarden van P_L groter dan deze optimale waarde

is de kwaliteit van de {3x3} "phase diversity"-ASK-ontvanger beter dan van de {2x2} ontvanger. Dit in tegentelling tot waarden van P_L kleiner dan dit optimum, waarvoor de {2x2} ontvanger beter presteert.
Aangetoond is dat intensiteitsruis in een {2x2} "phase diversity"-ontvanger leidt tot een periodiek verloop van de foutenkans met een frequentie gelijk aan tweemaal de midden-frequentie (MF). Daarentegen is de foutenkans van de {3x3} "phase diversity"-ontvanger onder gelijke voorwaarden constant.
Vergelijking van de resultaten met literatuur tonen aan dat de {3x3} "phase diversity"-DPSK-ontvanger, in een vergelijkbare situatie, minder gevoelig is voor LO-intensiteitsruis dan de {2x2} "phase diversity"-ASK-ontvanger.

De invloed van MF versterkingsonbalans en een afwijking in de faserelaties aan de uitgang van de optische hybride is bestudeerd voor de {2x2} en {3x3} "phase diversity"-ASK-ontvanger. Een analytische uitdrukking is afgeleid voor de foutenkans en tolerantiewaarden voor de faseafwijking en versterkingsonbalans zijn gegeven voor een systeemdegradatie van 0.5 dB. Voor beide ontvangers geldt dat de foutenkans in sterke mate afhangt van de keuze van de drempelwaarde en bovendien een periodiek verloop heeft met een frequentie gelijk aan tweemaal de midden-frequentie.

Het gebruik van een externe amplitude modulator met niet-ideale (uit/aan verhouding) Extinction Ratio (ER) in optisch coherente ASK-systemen leidt tot een systeemdegradatie. Voor de foutenkans van een {2x2} en {3x3} "phase diversity"-ASK-ontvanger zijn exacte uitdrukkingen verkregen. Aan de hand van deze uitdrukkingen is de systeemdegradatie berekend voor diverse waarden van de ER. Gezien het feit dat de syteemdegradatie afhankelijk is van de keuze van het drempelniveau, moet dit in relatie met de ER worden gekozen. Aangetoond is dat de geïntroduceerde systeemdegradatie voor de {3x3} "phase diversity"-ASK-ontvanger geringer is dan voor de {2x2} "phase diversity"-ASK-ontvanger.
Voor ASK-modulatie van de optische draaggolf is de FWHM-bandbreedte van het MF-vermogensspectrum maximaal voor een ER gelijk aan nul. Voor waarden groter dan nul (en < 1) wordt de modulatie-index kleiner, hetgeen resulteert in een kleinere waarde voor de FWHM-bandbreedte.

ACKNOWLEDGEMENTS

The completion of this thesis has only been possible thanks to the close cooperation of colleagues, students, and relatives. I would like to thank some people in particular.

I am grateful to my supervisor and thesis advisor, Dr. W.C. van Etten, who provided me with the opportunity and the support necessary for me to complete my thesis. He has made many suggestions, raised many mind-boggling questions, and helped me with daily problems.

I thank in particular my promoter, Prof. G.D. Khoe, very sincerely for his guidance and stimulating support.

I am much indebted to my parents, whom I thank for my education and their support in all daily matters. They have encouraged me in my studies and have always provided me the necessary moral and financial support.

Last, but not least, I am very grateful to my fiancee, Anne Velthuyse, for devotedly proofreading the manuscript, and her indispensable patience and understanding in the period during which I worked on this thesis.

BIOGRAPHY

Wilbert de Krom was born in Tilburg, the Netherlands, on November 20, 1964. In 1983 he started studying Electrical Engineering at the Eindhoven University of Technology, the Netherlands, from where he graduated in 1988. His master's thesis work concerned the design and implementation of a 4-level Soft-Decision Viterbi decoder at a data rate of 2048 Mbit/s. In 1989 he started to work on his thesis on optical coherent phase diversity receivers at the Department of Electrical Engineering, Eindhoven University of Technology, the Netherlands.

STELLINGEN

behorende bij het proefschrift

Optical coherent phase diversity systems

van

W.H.C. de Krom

Eindhoven, 12 mei 1992

I

Eenduidigheid omtrent het gebruik van de term "coherent" in technisch-wetenschappelijke artikelen handelend over optische communicatiesystemen is doorgaans ver te zoeken.

II

Als gevolg van de intensiteitsruis van de lokale oscillator laser vertoont de Bit Error Rate (BER) van een {2x2} phase diversity-ASK-ontvanger een periodiek verloop met een frequentie gelijk aan tweemaal de Midden Frequentie (MF). Dit in tegenstelling tot de BER van een {3x3} phase diversity-ASK-ontvanger die in een gelijke situatie constant is.
(Hoofdstuk 4)

III

De in dit proefschrift gepresenteerde berekeningen omtrent de invloed van intensiteitsruis in een {2x2}/{3x3} phase diversity-ASK-ontvanger rechtvaardigen twijfel aan de bruikbaarheid van de door A.F. Elrefaie et al. gebruikte methode, waarin de kans-dichtheidsfunctie van het ruisproces aan de ingang van de drempel-detector Gaussisch wordt verondersteld.
(Hoofdstuk 4)

A.F. Elrefaie, D.A. Atlas, L.G. Kazovsky, R.E. Wagner,
"Intensity noise in ASK coherent lightwave receivers",
Electron. Lett., vol. 24, no. 3, pp. 158-159, 1988.

IV

Al daalt het vertrouwen in een minister nog zo snel, de carrière-ladder bestijgt hij vaak wel.

V

Voor een {2x2} en {3x3} phase diversity-ASK-ontvangers mag de invloed van MF versterkingsonbalans voor waarden kleiner dan 5% worden verwaarloosd (=penalty < 0.5 dB), indien de afwijking in het faseverschil tussen de diverse takken van de ontvanger kleiner is dan 5°.
(Hoofdstuk 5)

VI

De systeemdegradatie voor een {2x2}/{3x3} phase diversity-ASK-ontvanger bij gebruik van een externe amplitude modulator met een niet ideale aan/uit verhouding, kan aanmerkelijk worden verminderd door aanpassing van het drempelniveau.
(Hoofdstuk 6)

VII

De zeer snelle vooruitgang in de ontwikkeling en fabricage van Erbium-Doped Fiber Amplifiers (EDFA's), kan de noodzaak tot het gebruik, en de daarmee samenhangende behoefte tot een monolithische integratie, van optisch coherente phase diversity-systemen vertragen.

VIII

In het kantoor van de toekomst werken de meeste mensen thuis.

IX

Reflecties in optisch coherente systemen leiden tot een verhoogd ruisspectrum rond 0 MHz. Dit verschijnsel wordt hoofdzakelijk veroorzaakt door self-homodyning van lokaal oscillator laserlicht en gereflecteerd lokaal oscillator laserlicht.

X

Bij de fabricage van fused-fiber couplers voor gebruik in optisch coherente phase diversity-ontvangers, is het beter om de faserelaties tussen de diverse uitgangstakken als procesparameters te gebruiken dan de verdeling van het uitgangsvermogen.